The Astrophysical Journal Supplement Series, 244:14 (47pp), 2019 September https://doi.org/10.3847/1538-4365/ab3799

Cassini Composite Infrared Spectrometer (CIRS) Observations of Titan 2004–2017

Conor A. Nixon[1], Todd M. Ansty[2], Nicholas A. Lombardo[1,3], Gordon L. Bjoraker[1], Richard K. Achterberg[1,4], Andrew M. Annex[5,11], Malena Rice[6,11], Paul N. Romani[1], Donald E. Jennings[7], Robert E. Samuelson[1,4], Carrie M. Anderson[8], Athena Coustenis[9], Bruno Bézard[9], Sandrine Vinatier[9], Emmanuel Lellouch[9], Regis Courtin[9], Nicholas A. Teanby[10], Valeria Cottini[1,4], and F. Michael Flasar[1]

[1] Planetary Systems Laboratory, NASA Goddard Space Flight Center, Greenbelt, MD 20771, USA; conor.a.nixon@nasa.gov
[2] Department of Space Science, Cornell University, Ithaca, NY 14853, USA
[3] Center for Space Science and Technology, University of Maryland, Baltimore County, 1000 Hilltop Circle, Baltimore, MD, USA
[4] Department of Astronomy, University of Maryland College Park, College Park, MD, USA
[5] Department of Earth and Planetary Sciences, Johns Hopkins University, Baltimore, MD 21218, USA
[6] Department of Astronomy, Yale University, New Haven, CT 06511, USA
[7] Detector Systems Branch, NASA Goddard Space Flight Center, Greenbelt, MD 20771, USA
[8] Astrochemistry Laboratory, NASA Goddard Space Flight Center, Greenbelt, MD 20771, USA
[9] LESIA, Observatoire de Paris, Université PSL, CNRS, Sorbonne Université, Université de Paris, 5 place Jules Janssen, F-92195 Meudon, France
[10] School of Earth Sciences, University of Bristol, Wills Memorial Building, Queens Road, Bristol BS8 1RJ, UK
Received 2019 April 26; revised 2019 July 6; accepted 2019 July 24; published 2019 September 11

Abstract

From 2004 to 2017, the *Cassini* spacecraft orbited Saturn, completing 127 close flybys of its largest moon, Titan. *Cassini*'s Composite Infrared Spectrometer (CIRS), one of 12 instruments carried on board, profiled Titan in the thermal infrared (7–1000 μm) throughout the entire 13 yr mission. CIRS observed on both targeted encounters (flybys) and more distant opportunities, collecting 8.4 million spectra from 837 individual Titan observations over 3633 hr. Observations of multiple types were made throughout the mission, building up a vast mosaic picture of Titan's atmospheric state across spatial and temporal domains. This paper provides a guide to these observations, describing each type and chronicling its occurrences and global-seasonal coverage. The purpose is to provide a resource for future users of the CIRS data set, as well as those seeking to put existing CIRS publications into the overall context of the mission, and to facilitate future intercomparison of CIRS results with those of other *Cassini* instruments and ground-based observations.

Key words: infrared: planetary systems – instrumentation: interferometers – planets and satellites: atmospheres – planets and satellites: individual (Titan) – space vehicles: instruments – techniques: spectroscopic

Supporting material: machine-readable tables

1. Introduction

Titan is the largest moon of Saturn—5150 km in diameter—and the only moon in the solar system to possess a substantial atmosphere. Titan was discovered by Christiaan Huygens in 1655, and proof of its atmosphere was provided by Kuiper (1944) through observations of methane absorption in its spectrum. The first up-close encounter was made by the *Voyager 1* spacecraft on 1980 November 12 (Stone & Miner 1981), which used the technique of radio occultation to penetrate the atmosphere and determine the surface radius (Tyler et al. 1981), hitherto unknown. *Voyager 1* made many important findings about Titan using its onboard suite of instruments, but was unable to penetrate the thick haze to observe the surface (Smith et al. 1981).

In 2004, the *Cassini* spacecraft arrived at the Saturn system, beginning a planned 4 yr investigation of the planet, its rings, and its moons (Matson 2002). Ultimately the mission was extended twice, and the spacecraft was retired only in 2017 September after all fuel reserves had been expended, at which time it was plunged into Saturn's atmosphere, making a final set of unique measurements. Titan was a major focus of the mission, and during its 13 yr in orbit, *Cassini* made 127 targeted encounters with Titan at ranges <100,000 km, as well as numerous additional observations from greater distances. During its third flyby, *Cassini* released the *Huygens* probe built by the European Space Agency (ESA), which descended to Titan's surface under parachute (Lebreton et al. 2005). *Huygens* delivered the first close-up pictures of Titan's surface (Tomasko et al. 2005) and made the first in situ measurements of the local atmospheric conditions (Bird et al. 2005; Fulchignoni et al. 2005; Israël et al. 2005; Niemann et al. 2005; Zarnecki et al. 2005).

Each Titan encounter was different, occurring with a unique combination of approach and departure direction, velocity, minimum approach distance, local time, Kronian season, and other characteristics. Every flyby was also therefore different in science potential, and a unique emphasis was developed for each one: RADAR versus mass spectrometry at closest approach, inbound mapping in reflected light (daylit inbound encounters) versus thermal infrared (nighttime inbound encounters), spacecraft orientation optimized for remote sensing platform versus particles and fields, and so on.

Cassini's TOST group (Titan Orbiter Science Team; Steadman et al. 2010), with representation from each of the 12 instrument teams plus major spacecraft subsystems, was tasked with developing the exact science timeline for each Titan encounter. TOST worked by dividing the 24–48 hr encounter segment into

[11] Contributions to the project during internship at NASA GSFC.

smaller periods, each assigned to a "prime" instrument that would dictate spacecraft pointing, as well as any number of "rider" instruments that would passively collect data without determining their direction of pointing.[12] This strategy was effective because similar instruments were typically "co-boresighted," i.e., pointing in the same direction. In particular, this was the case for the "ORS group" (Optical Remote Sensing), which consisted of four remote sensing spectrometers and cameras: the Ultraviolet Imaging Spectrometer (UVIS; Esposito et al. 2004), the Imaging Science Subsystem (ISS; Porco et al. 2004), the Visual and Infrared Mapping Spectrometer (VIMS; Brown et al. 2004), and the Composite Infrared Spectrometer (CIRS) described hereafter.

CIRS (Kunde et al. 1996; Flasar et al. 2004; Jennings et al. 2017) was designed and built by NASA's Goddard Space Flight Center (GSFC) in partnership with more than a dozen other institutions, including hardware contributions from the UK, France, and Germany. CIRS was the successor to *Voyager*'s IRIS instrument (Infrared Radiometer and Spectrometer; Hanel et al. 1980), built on the same principle of Fourier Transform Spectroscopy (FTS) in the mid- and far-infrared but with significant upgrades to its spectral range, spectral resolution, sensitivity, and number of detector pixels. CIRS continued to operate at full capacity during the entire 13 yr mission and was ultimately allocated the most Titan observation time as the "prime" instrument of any *Cassini* instrument, by virtue of its ability to observe both Titan's day and night sides, and to conduct high-value science over the entire range of spacecraft distances.

This paper covers two main topics: (i) the main types of CIRS observations of Titan and (ii) the spatial and temporal coverage of Titan achieved for each type. The objective is to provide a complete and comprehensive description of the CIRS observations of Titan—the science goals, observation implementation, and spatial and temporal coverage. This is anticipated to be of value to multiple groups: members of other *Cassini* instrument teams in their ongoing data analysis efforts, future users of CIRS data accessible through the Planetary Data System (PDS; McMahon 1996; see Appendix A), ground-based observers analyzing complementary data sets such as the ALMA archive (Stoehr et al. 2014), and perhaps also science planners of future Titan instruments and missions. Concluding remarks are given in Section 8.

2. *Cassini* Mission and CIRS Instrument Overview

2.1. Cassini *Mission Implications for Titan Science*

Saturn has an obliquity of 26°.7 and an orbital period of 29.5 Earth yr, so it has seasons that are approximately 7.4 terrestrial yr in length. Titan orbits in Saturn's equatorial plane with a negligible axial tilt relative to its orbit, so has seasons of the same length as Saturn. When *Cassini* arrived at Saturn in 2004 July, the season was northern winter. *Cassini* was originally planned to have a prime mission (PM) from 2004–2008; eventually, this was extended to 2010, which encompassed Saturn's equinox in 2009. A second and final extension then continued the mission through 2017, thereby reaching Saturn's northern summer solstice that year (Figure 1). Finally, on 2017 September 15, the spacecraft exhausted all its fuel and was destroyed by a planned entry into Saturn to prevent the possibility of a later, uncontrolled impact with a moon. The long duration of this 13 yr mission thus enabled *Cassini* to experience almost two full seasons on Saturn and Titan, which has proved crucial for understanding the seasonal and even interannual change (by comparison to other data sets such as *Voyager*) in their atmospheres (Lockwood & Thompson 2009; Coustenis et al. 2013).

During the mission, the spacecraft changed its orbital inclination relative to the Saturn ring plane (equatorial plane) continuously (Figure 2), so as to have equal opportunities to rendezvous with the moons (requiring low inclination) and to view the rings (requiring high inclination). Flybys of Titan were used as gravity-assist maneuvers, changing the spacecraft inclination while minimizing fuel expenditure. The effect on Titan observations was twofold: (i) frequent flyby opportunities and (ii) almost every flyby geometry was different, in terms of encounter range at closest approach and trajectory (subspacecraft track on Titan). This implied that each flyby had to be individually designed for unique science observations/instrument operations, and that the possible atmospheric and surface coverage was dictated by the particular orbital geometry.

Flybys of Titan are divided into two categories: "targeted" encounters ($r < 100{,}000$ km) and "untargeted" or distant encounters ($r > 100{,}000$ km). All of these encounters may be identified by a *Cassini* orbit number; in addition, the targeted encounters are also given a flyby number in the format T*n*—see data table in Appendix B. For example, the T6 flyby occurred on orbit 13 at a range of 3660 km, while the last encounter of the mission on orbit 292 was at a range of 119,733 km and therefore does not have a "T" number. Several exceptions to the naming convention must be noted. The very first, untargeted Titan encounter at a range of 339,123 km immediately following Saturn orbit insertion (SOI) is given the special designation "T0," on orbit 0. Immediately following T0, the first several orbits, originally containing T1 and T2, were redesigned to accommodate a more distant flyby for the *Huygens* probe data relay. This entailed adding an additional orbit; therefore, encounters T1 and T2 became TA, TB and TC, with the rest of the planned tour continuing using the already designated numbers from T3 onward.

Figure 3 shows a histogram of flyby ranges; approximately one-third of targeted flybys (41/127) were at ranges <1000 km, and a further one-third (39/127) occurred at ranges 1000–1500 km, still inside the atmosphere defined by the exobase at 1500 km (Yelle et al. 2008; Vuitton et al. 2019). Therefore, on 63% of Titan targeted flybys (those where $r < 100{,}000$ km) in situ measurements of the atmosphere were possible, as well as remote sensing on approach and departure. The remaining approximately one-third (47/127) of targeted flybys were at ranges 1500–100,000 km, along with 14 more distant encounters.

2.2. CIRS Instrument Overview

A detailed description of the instrument is given in Jennings et al. (2017), while some key facts are given here that are most relevant to the Titan observation planning. The CIRS instrument was a dual spectrometer, which used a field-splitting beam splitter to direct the incoming light from a 50 cm diameter telescope into mid- and far-infrared spectrometers. These functioned in tandem, sharing a common mirror carriage mechanism that defined the spectral resolution through its distance of travel, from a lowest apodized resolution of 15.5 cm^{-1} to a highest apodized resolution of 0.5 cm^{-1}. The

[12] Mostly: some riders were listed as "collaborative" between several instruments, meaning that the prime instrument was required to develop pointing that would also fulfill science goals for important rider observations.

(a)

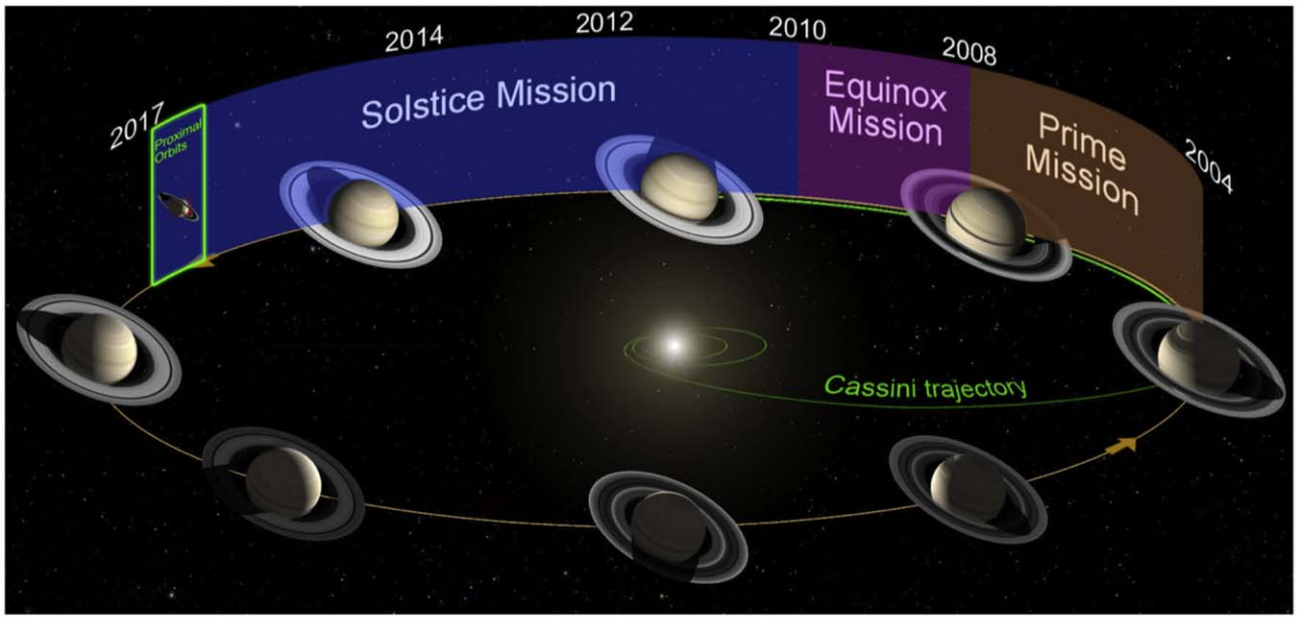

(b)

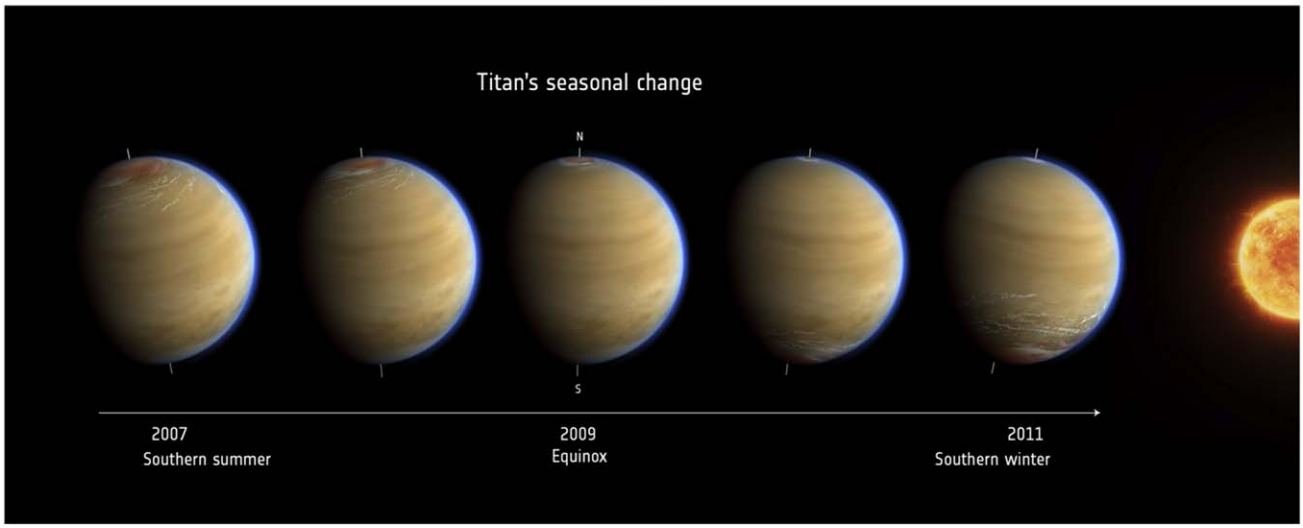

Figure 1. (a) Changing seasons on Saturn during the *Cassini* mission timeframe. (JPL/NASA) (b) Seasons on Titan around equinox in 2009. (ESA/AOES).

lowest resolutions required the shortest movements (4.5 s), while the highest resolutions required the longest movements (52 s). Intermediate resolutions were possible, with the most common medium resolution being 2.75 cm^{-1} (12 s). This created a trade-off: acquiring many low-resolution spectra was desirable in some circumstances—for example during observations of strong gas emissions such as methane—and enabled rapid repositioning for mapping purposes. High-resolution spectra required longer acquisition times, and therefore a substantial dwell time on source to build up significant a signal-to-noise ratio (S/N). This was desirable when measuring weaker gas emissions of less abundant species that required a higher resolution to isolate.

A second important consideration was the number and configuration of the pixels, as shown in Figure 4. The far-infrared focal plane, known as FP1, was a single large pixel similar to *Voyager* IRIS that was optimized for sensitivity to light from 10 to 600 cm^{-1} (1000-17 μm).[13] The mid-infrared reception was very different from that of *Voyager* IRIS and used twin 1 × 10 mercury–cadmium–telluride arrays sensitive to 600–1100 cm^{-1} (FP3, photoconductive-type detectors, 17–9 μm) and 1100–1400 cm^{-1} (FP4, photovoltaic-type detectors, 9–7 μm). The optical boresights were closely aligned with the spacecraft $-Y$ direction, while the mid-infrared arrays were aligned along the Z axis, and FP1, FP3, and FP4 were offset in the X direction (Nixon et al. 2009b). The implication was that the $-Y$ direction was pointed at Titan for optical measurements, while rotating the spacecraft about the Z axis swept the mid-infrared arrays across the sky to perform "pushbroom" mapping. Subsequent offsetting in X permitted multiple, parallel sweeps.

[13] A second detector in the far-infrared, FP2, was descoped before launch.

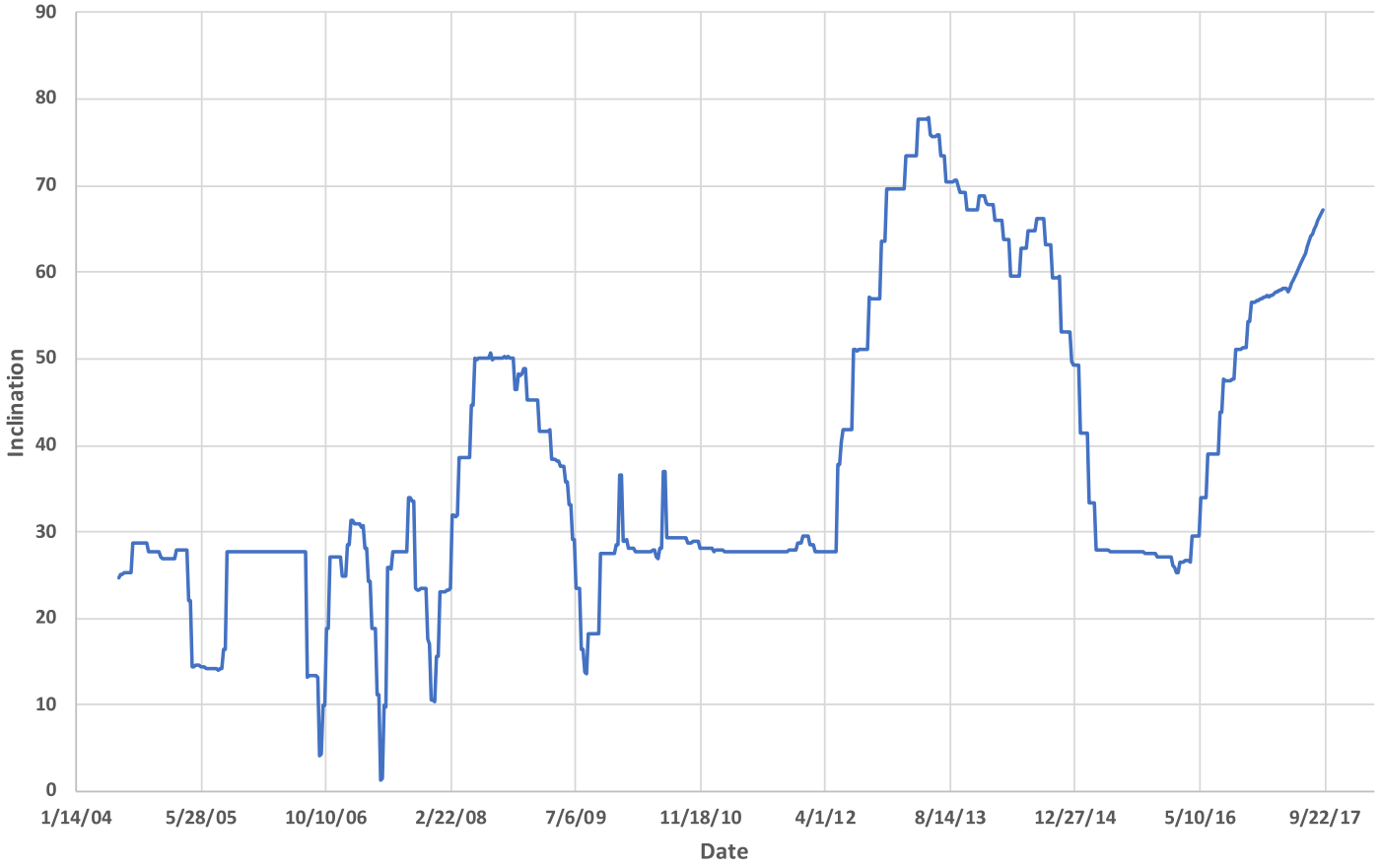

Figure 2. Magnitude of inclination of *Cassini*'s orbit over time relative to the Saturn ring plane.

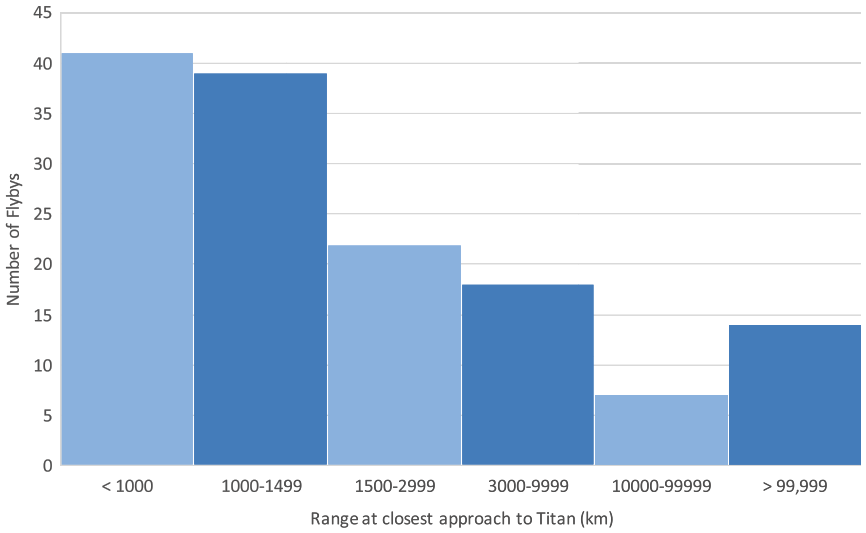

Figure 3. Frequency of Titan flybys at different closest approach distances. Close flybys at $r < 1500$ constituted the majority of targeted flybys ($r < 100{,}000$ km), while flybys at 100,000 km and farther were considered untargeted distant encounters.

A further factor in observation design was detector readout. CIRS had 11 simultaneous readout channels: one for FP1, and five each for FP3 and FP4. This meant that typically only half of the mid-infrared detectors could be used at a time. Readout modes for the mid-infrared included odd detectors only (1, 3, 5, 7, 9 on each of FP3 and FP4), even detectors only (2, 4, 6, 8, 10 on each array), or center mode (4–8 on FP3 and 3–7 on FP4). A typical observation alternated back and forth between the even and odd readout modes on successive scans to allow for the fullest spatial sampling, known as "blink" mode. However, a "pair" mode was also available that utilized all 10 detectors on each array by reading them out in five pairs ($1+2$, $3+4$, $5+6$, $7+8$, $9+10$). Pair mode effectively created double-size detector pixels that may be harder to model in certain

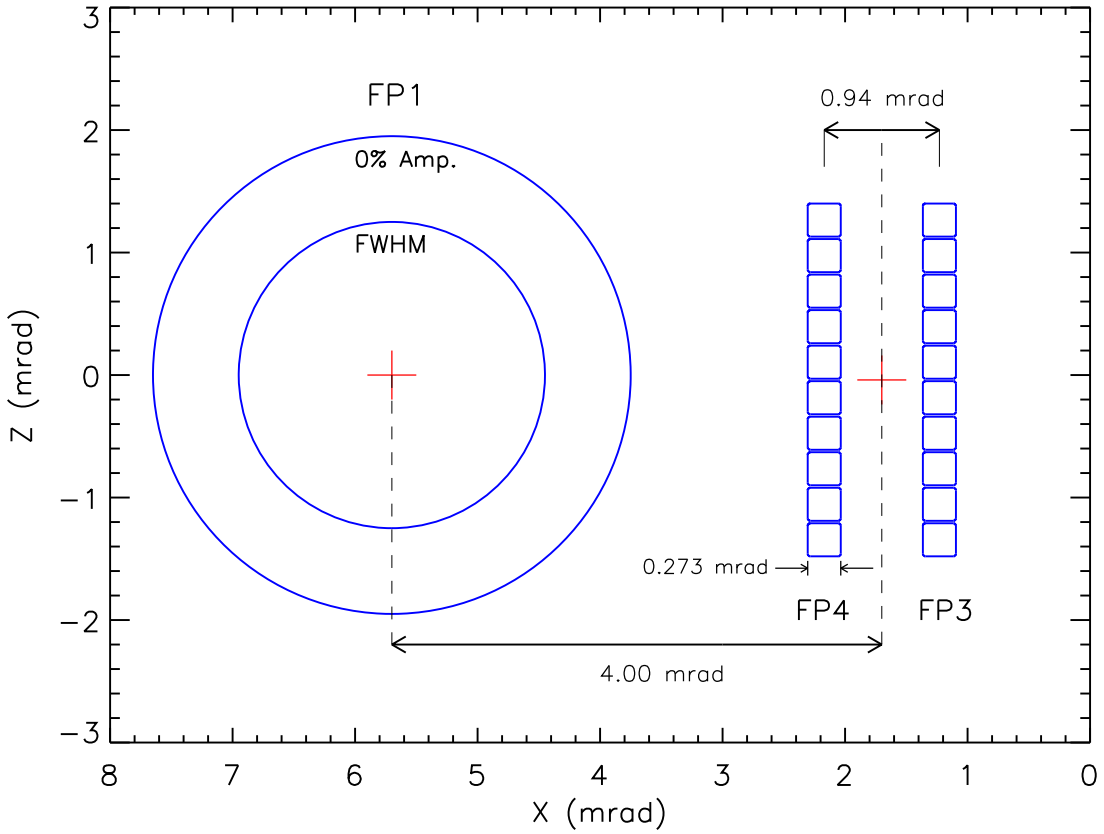

Figure 4. CIRS field of view showing relative sizes and orientations of detectors.

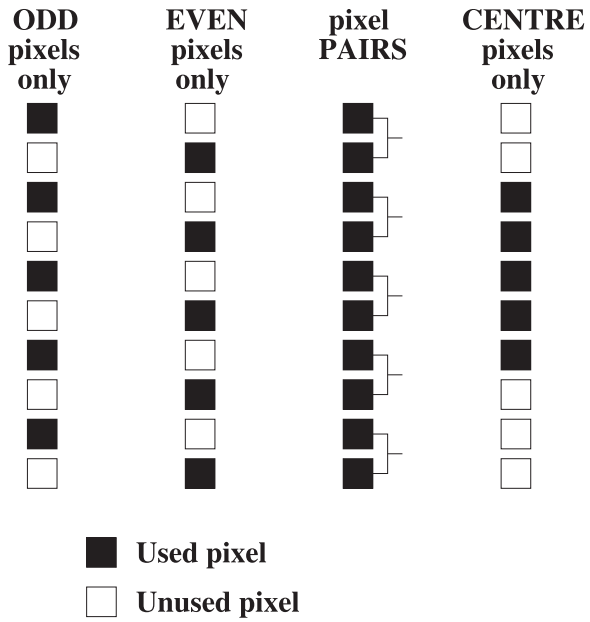

Figure 5. CIRS detector readout modes for the mid-infrared arrays: FP3 and FP4.

circumstances, but had the advantage of using the maximum possible amount of incoming flux—a $\sqrt{2}$ advantage over the other modes that was used to improve the S/N. A graphical summary is shown in Figure 5.

A final note regarding the instrument is that frequent calibration data were required in addition to science observations. Only radiometric (flux) calibration was taken in flight, to enable the conversion from detector counts to physical radiance units, and comprised two types. The first was "dark sky" or "deep space" observations of the 2.73 K background (sky background avoiding planets, moons, the Sun, IR-bright stars, etc.), equivalent to zero radiance for the purpose of CIRS, and the second was a warm internal target (shutter) that was periodically emplaced into the beam path for the mid-infrared only (FP3 and FP4).[14] These flux calibration observations were made sometimes before, sometimes after, or occasionally interspersed within longer science observations; and sometimes while slewing the spacecraft to reach a target point. Later in the mission, the normal practice became to concentrate the calibration observations in dedicated blocks of time (normally 6–8 hr) during downlink of spacecraft data to Earth when the instrument was usually pointing at empty space, and previous practice of taking calibration data during science observations diminished. This new paradigm created longer, more homogeneous blocks of calibration data, at the expense of the calibration data being slightly more remote in time from the science observations that they would later be used to calibrate. When using CIRS data, care must be taken to sift out calibration observations from science data. For further details, see Jennings et al. (2017).

3. Overview of CIRS Titan Observations

We define two common terms used to distinguish major types of CIRS observations: nadir and limb. A nadir observation was one where the detector field of view intersects

[14] FP1 did not require a shutter, as the detector was thermostated to the temperature of the rest of the instrument optics, providing a virtual reference point.

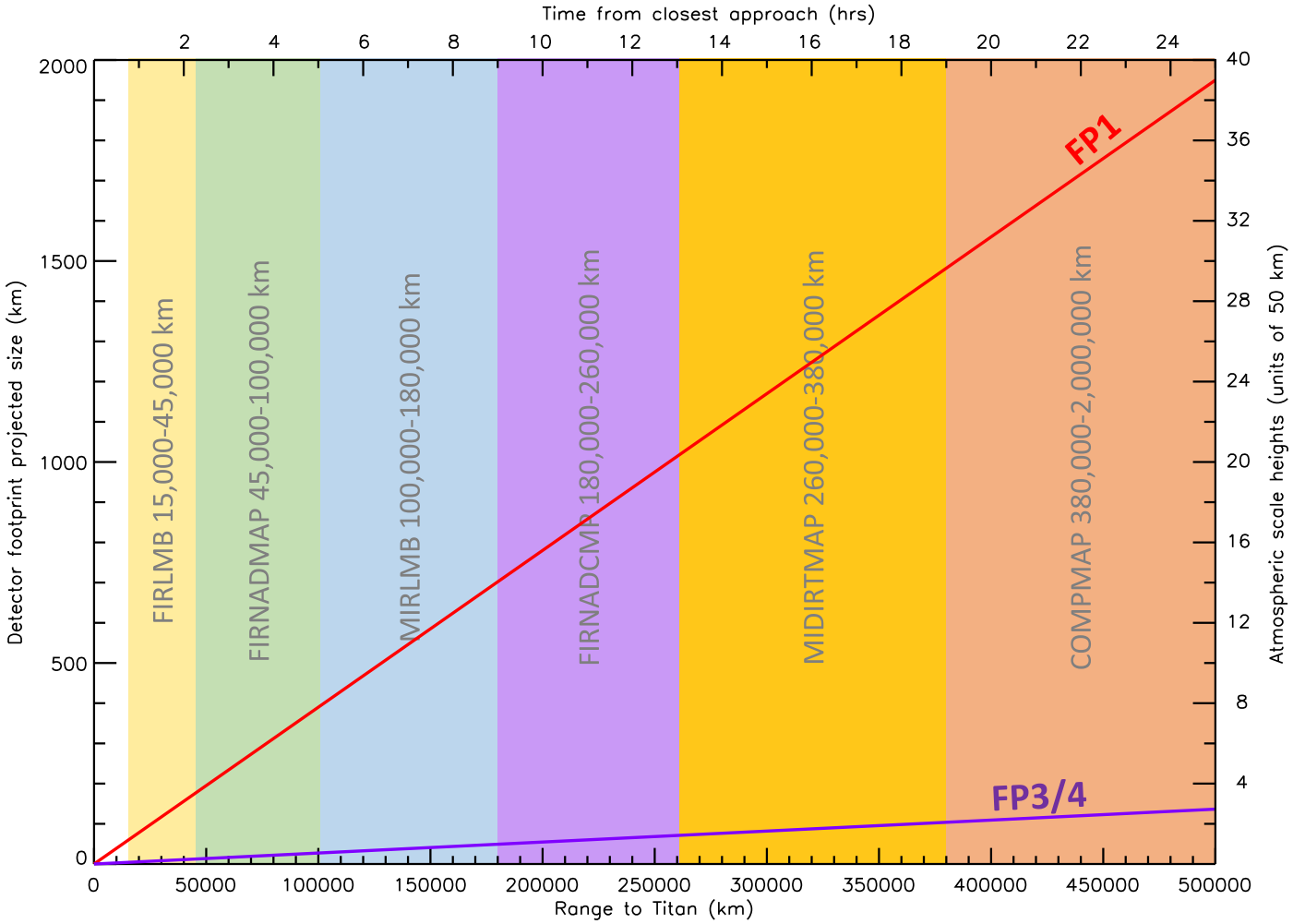

Figure 6. Projected footprint size of the CIRS far-infrared (FP1) and mid-infrared (FP3/4) detectors as a function of range from Titan. Different observation types were performed at different ranges.

Titan's surface (not necessarily normal to the surface), whereas a limb observations pointed the detector(s) just outside the disk of Titan's solid body and measured the atmosphere only, between the surface and the exobase at around 1500 km. To obtain a nadir map in the far- or mid- infrared, the detector(s) was (were) swept up and down in parallel tracks in the Z direction, with offsets in X. A limb profile (vertical cross-section) could be obtained with FP1 by moving the detector in a radial direction, from the surface outward. In the mid-infrared, scanning was not needed as the detectors formed a linear array: a vertical profile could be obtained by placing the arrays perpendicular to the limb and moving upward to a second higher position if required.

The CIRS team developed a suite of different observation types customized for each distance range from Titan. These were divided into two wavelength categories: mid or far-infrared led, and three articulation types: integration, 1D map, or 2D map. The distinction between "far-infrared" and "mid-infrared" observations may initially appear confusing: after all, during all Titan observations, both the far-infrared pixel (FP1) and some subset of the mid-infrared pixels (FP3/4) were read out, as shown in Figure 5. The reason for the dichotomy was due to the vast difference in pixel sizes: 3.9 mrad FWHM for FP1 versus 0.273 mrad for FP3/4, a factor of 14 different. This required that position-step sizes, slewing rates, and other spacecraft-pointing maneuvers were customized not only according to distance from Titan, but also by detector type (mid-/far-infrared), both of which combined to determine the projected size of the footprint in kilometers, according to the formula $s = r\Delta\theta$, where s is the footprint size, r is the distance, and $\Delta\theta$ is the angular size of the detector (Figure 6).

"Integrations," otherwise known as "sit-and-stare" type observations, consisted of a long dwell at a single target point, either on the disk or "limb" (atmosphere visible on the horizon), often punctuated by periods of offset pointing onto space ("dark sky") for calibration purposes. One-dimensional maps occurred in several flavors: latitudinal, longitudinal, or vertical. Latitudinal or longitudinal scans consisted of a slow "slew" (spacecraft turning about one inertial axis) so as to move the detectors slowly across Titan's disk in the north–south (N–S) or east–west (E–W) direction. Vertical scans, on the other hand, were designed to move the arrays in a radial direction—usually away from Titan's center—to measure a vertical section (or profile) of the atmosphere. Radial scans usually began on Titan's disk, moving upward (away from center) over the limb and stopping when the atmosphere became too tenuous (optically thin) for any further signal to be recorded.

Because articulating the spacecraft in two dimensions was more difficult and demanding on the spacecraft reaction wheels

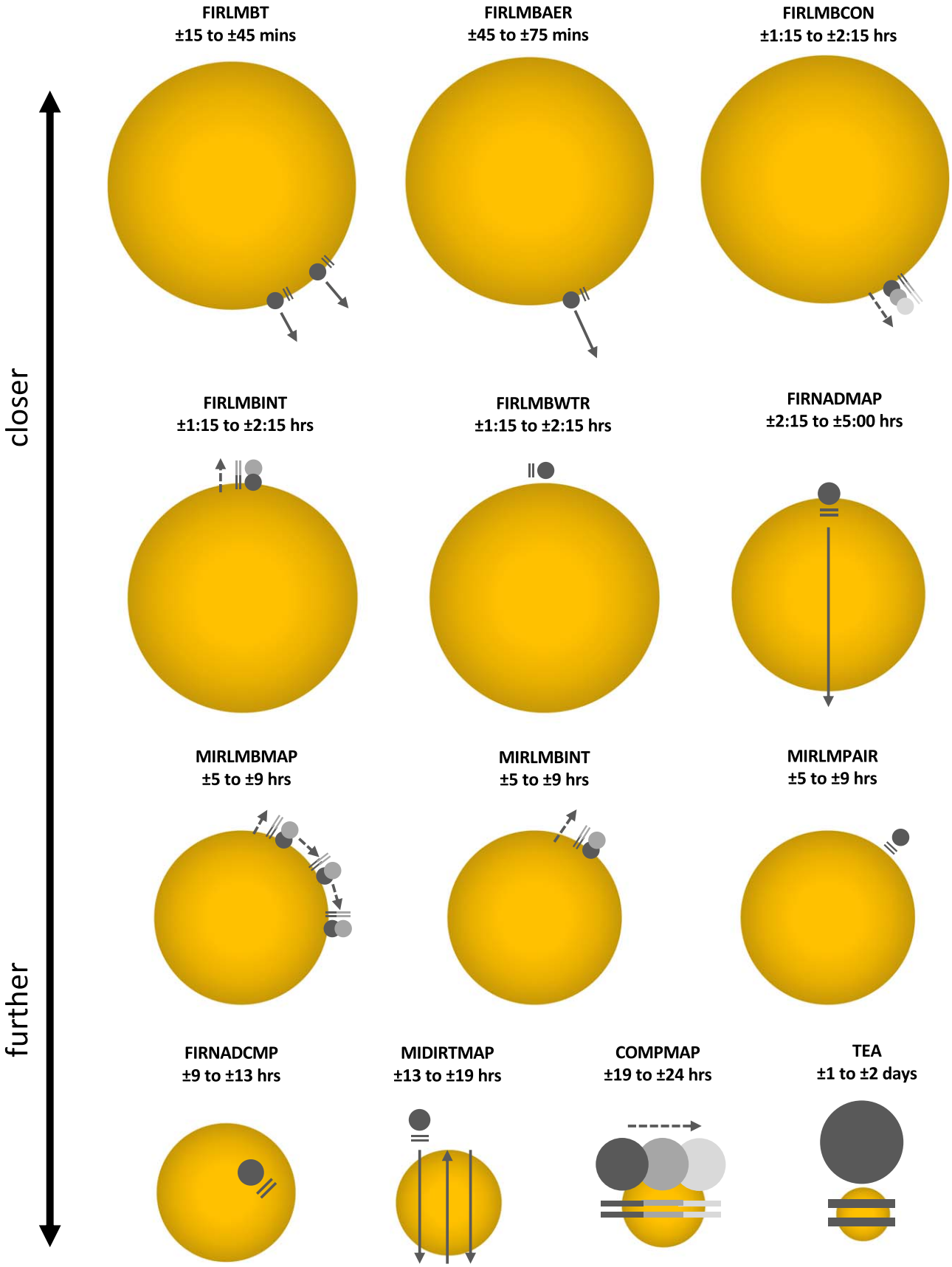

Figure 7. Schematic showing the types of CIRS Titan observations performed at various times from closest approach. Arrows with solid lines indicate continuous slewing, while arrows with broken lines indicate repositioning. Projected detector footprints are approximate only, because these change with distance.

Table 1
Types of CIRS Titan Observations

Observation Name	Time Relative to C/A (HH:MM)		Range (10^3 km)		Spectral Resol. (cm^{-1})	Type	Maximum Scan Rate (μrad s^{-1})	Maximum Num. of Positions
	Start	End	Min	Max				
Standard Far-infrared Types								
FIRLMBT	±00:15	±00:45	5	15	15.0	radial scan	43	⋯
FIRLMBAER	±00:45	±01:15	15	25	15.0	radial scan	55	⋯
FIRLMBINT	±01:15	±02:15	25	45	0.5	integration	⋯	2
FIRNADMAP	±02:15	±05:00	45	100	15.0	1D map	7	⋯
Standard Mid-infrared Types								
MIRLMBINT	±05:00	±09:00	100	180	0.5	integration	⋯	2
MIRLMBMAP	±05:00	±09:00	100	180	15.0	integration	⋯	2 × 18
FIRNADCMP	±09:00	±13:00	180	260	0.5	integration	⋯	1
MIDIRTMAP	±13:00	±19:00	260	380	3.0	2D scan	4	⋯
COMPMAP	±19:00	±24:00	380	2000	0.5	integration	⋯	2–5
Evolved Late-mission Types								
FIRLMBCON	±01:15	±02:15	25	40	3.0	integration	⋯	3
FIRLMBWTR	±01:15	±02:15	25	40	0.5	integration	⋯	1
MIRLMPAIR	±05:00	±09:00	100	180	0.5	integration	⋯	2
TEA	±40:00	±100:00	800	2000	0.5	integration	⋯	variable

and thrusters than a single axis articulation, 1D scans of any type were usually preceded by a turn about the $-Y$ direction (optical boresight direction). This would set up the secondary axes (X and Z) in a N–S, E–W, or appropriate direction perpendicular to the limb, so that the 1D scan could then be performed by turning about a single axis only. For example, an N–S scan might be set up by first turning about $-Y$ so that the $+X$ axis was aligned with Titan's north pole; the N–S scan would then proceed by turning about the Z axis to "comb" the mid-infrared detector arrays downward in an N–S direction. Similarly, a radial scan at 45°N latitude might be set up by pointing $+X$ perpendicular to the limb at 45°N (i.e., Z parallel or tangent to the edge of Titan's disk) and then rotating the spacecraft about the Z axis to scan the detectors upward (radially away from Titan's center).

Two-dimensional maps were performed by slewing in two directions, X and Z. Typically, the map might proceed by imaging a square box on the sky enclosing Titan; the initial pointing would then be moved to one "corner" of the box and a turn performed around the Z axis to comb the array down the first side of the box (see Figure 7, MIDIRTMAP). The arrays would then be offset in X, and the scan repeated in the opposite direction. The amount of X offset would typically be set to just under one array length of the FP3 detectors to allow for positional overlap (which could be used later for calibration purposes to compensate for any instrument temperature drifts). The angular size of the scan in Z would be reduced or increased at every iteration to compensate for the changing distance to Titan and its changing angular size on the sky.

With these major goals and categories in mind, nine initial CIRS Titan observation types were constructed prior to SOI in 2004, when planning the PM (2004–2008), as described in Flasar et al. (2004). Experience during the PM led to four new observation types being introduced in the Equinox (2008–2010) and Solstice (2010–2017) Missions; see also Nixon et al. (2012a). A summary of all final observation types is given in Table 1 and shown in Figure 7. Final observation specifications are described with examples in the following subsections, grouped by observation type.

4. Far-infrared Limb Observations

Far-infrared limb observations constituted the closest observations to Titan, in the window from 15 to 135 minutes from closest approach, or a range of approximately (5–45) × 10^3 km. At this close range, the large FP1 detector achieved the best possible resolution on Titan's limb to obtain vertical profiles of temperature, aerosol opacity, and gas abundances. At ∼45 minutes from closest approach, FP1 could resolve about 1 pressure scale height on Titan's limb; by 2 hr from closest approach, the resolution was ∼3 scale heights (see Figure 6).

During a flyby, and especially at close range, the horizon circle was constantly changing, either in longitude, latitude, or both. However, there were two points on the horizon, roughly perpendicular to the subspacecraft track projected onto Titan's surface, where multiple horizon circles (as a function of time) intersected, as seen in Figure 8. These were considered to be "horizon nodes," or "limb stationary points," and targeting limb observations at or close to these points was desirable because a more homogeneous atmospheric sample could thus be obtained (see Nixon et al. 2010a for a more detailed discussion of this topic). Figure 9 shows the limb horizon nodes for all flybys in the mission, which were used as a guide when choosing pointing for positioning scans/integrations; additional factors included a preference for covering a wide range of latitudes and not repeating latitudes close together in time.

Descriptions of types of far-infrared limb observations are given below, and a full listing of the far-infrared limb observation dates, times, and pointing locations is given in Appendix C.

4.1. FIRLMBT

Science overview: The far-infrared limb temperature scan (FIRLMBT) observation was the closest observation to Titan,

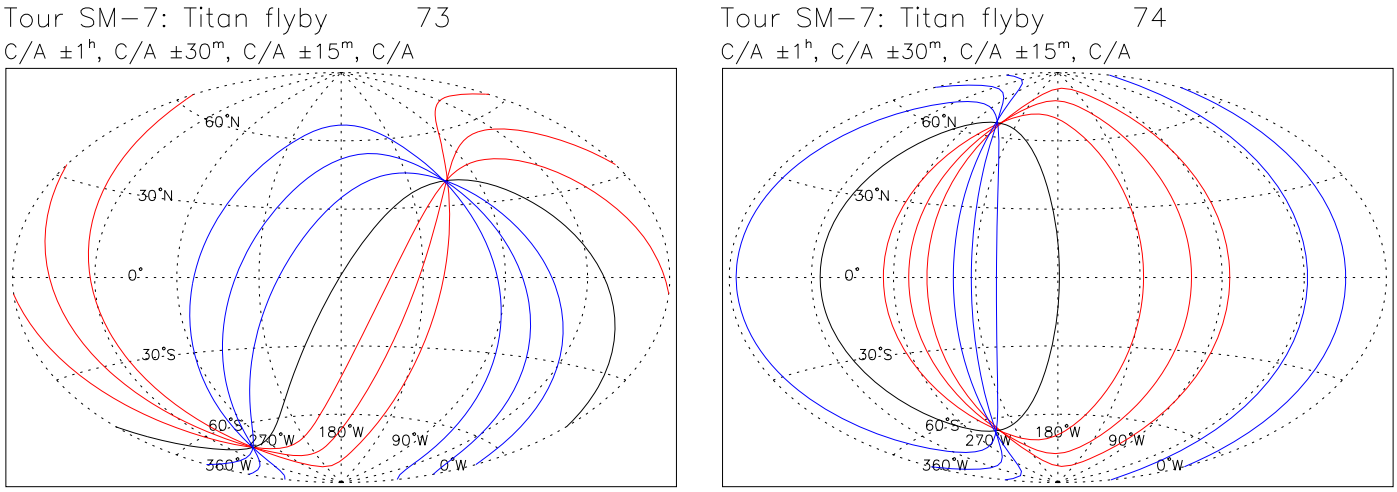

Figure 8. Example horizon circles at 0, ±15, ±30, ±60 minutes for T73 and T74. Red = approaching, Blue = receding, Black = closest approach. Horizon "nodes" were two locations where all circles intersected, indicating limb-viewing locations that were continuously visible and ideal for limb sounding.

occurring at (5–15) × 10^3 km (15–45 minutes from closest approach). At 30 minutes from closest approach, FP1 resolved ∼40 km on Titan's limb, or about 80% of an atmospheric scale height (∼50 km). The observation was designed to allow for several vertical profiles of temperature to be obtained via measurement of N_2–N_2 collision-induced absorption (CIA) or opacity at 50–150 cm^{-1}, focusing on pressure levels of 8–100 mbar in the lower stratosphere and upper troposphere (Flasar et al. 2004; Sylvestre et al. 2018)—see Figure 10.

Implementation: The lowest spectral resolution of CIRS was used (15.5 cm^{-1}), which enabled a rapid spectrum acquisition time (5 s). A turn rate of ∼40 $\mu rad\ s^{-1}$ meant that the FOV moved by only 0.2 mrad, or 1/20 of a pixel, during a single spectrum. Therefore, at least 10 spectra can be coadded (2 mrad) without loss of spatial resolution, typically considered to be one-half of the detector size (i.e., Nyquist sampling). Each limb scan covered ∼28 mrad, taking about 11 minutes. Allowing for repositioning at the start and end of the scan, two scans were typically achieved in the nominal 30 minute window. The two scans were notionally positioned 10° apart in latitude, although this was not achievable if the flyby was at high inclination. Due to the customization of each Titan flyby through negotiation with other *Cassini* teams, the FIRLMBT observation was sometimes shorter or longer than 30 minutes, in which case the scan rate was adjusted accordingly (up or down). If the required scan rate exceeded 50 $\mu rad\ s^{-1}$, only one scan was implemented, and/or the observation was merged with the adjacent FIRLMBAER observation.

4.2. FIRLMBAER

Science overview: The far-infrared aerosol scan (FIRLMBAER) was the second-closest observation to Titan, occurring at (15–25) × 10^3 km (45–75 minutes from closest approach). Like FIRLMBT, this was also a limb scan observation designed to measure vertical profiles of aerosol opacity in the range 250–600 cm^{-1}. Due to the differing spectral dependence of CIA, aerosols, and clouds (condensates), the vertical profile can be isolated and measured (Teanby et al. 2009a; de Kok et al. 2010; Anderson & Samuelson 2011; Anderson et al. 2018). By considering multiple flybys, latitudinal and temporal variations of aerosol and condensates may be inferred (Jennings et al. 2012a, 2012b, 2015). FIRLMBAER data also provide important constraints for modeling nadir-viewing observations, where vertical information is more ambiguous.

Implementation: From 2004 to 2010, two scans separated by 5° on the horizon were implemented in the 30 minute window, covering a radial distance of 51 mrad, or about 1000 km from −100 to +900 km relative to the surface. The scan required was consequently rapid: ∼55 $\mu rad\ s^{-1}$. From 2010, the observation was redesigned to focus on altitudes −100 to +600 km, because the signal became too weak for detection at higher altitudes. A slower scan rate was also employed (∼28 $\mu rad\ s^{-1}$) to increase the S/N. Also, the number of scans was reduced from two to one (Figure 11), as it was found that similar aerosol information could be obtained from the FIRLMBT observations, and therefore, it became desirable to focus on high fidelity rather than greater spatial coverage.

4.3. FIRLMBINT

Science overview: The far-infrared limb integration constituted the third type of the original FIRLMB observation group, designed prior to orbit insertion. This observation type was implemented from 75 to 135 minutes from closest approach, or at a range of (25–45) × 10^3 km. In contrast to FIRLMBT and FIRLMBAER, the FIRLMBINT was not a scan (slew), but rather a sit-and-stare observation (or integration) at a series of fixed pointings relative to Titan. The objective was to obtain measurements of trace gas concentrations at two altitudes to obtain a basic vertical gradient. In particular, measurements of the gases CO (30–70 cm^{-1}), C_2N_2 (233 cm^{-1}), and H_2O (∼150–250 cm^{-1}; de Kok et al. 2007b; Cottini et al. 2012b; Lellouch et al. 2014) were of interest, because they do not have spectral bands detectable by CIRS in the mid-infrared. However, C_3H_4 (328 cm^{-1}) and C_4H_2 (228 cm^{-1}) were also measured (Sylvestre et al. 2018), as well as a weak band of HC_3N at 499 cm^{-1}. FIRLMBINTs have also been used to characterize aerosols and condensates (ices; de Kok et al. 2007a, 2010; Samuelson et al. 2007; Anderson et al. 2010, 2014, 2016, 2018; Anderson & Samuelson 2011; Jolly et al. 2015).

Implementation: The FIRLMBINT was implemented as two fixed integrations at 125 and 225 km above the limb (later, a third, intermediate point at 175 km was added as a separate observation: see FIRLMBWTR). The highest spectral resolution of CIRS was used, 0.5 cm^{-1}, requiring 52 s acquisition

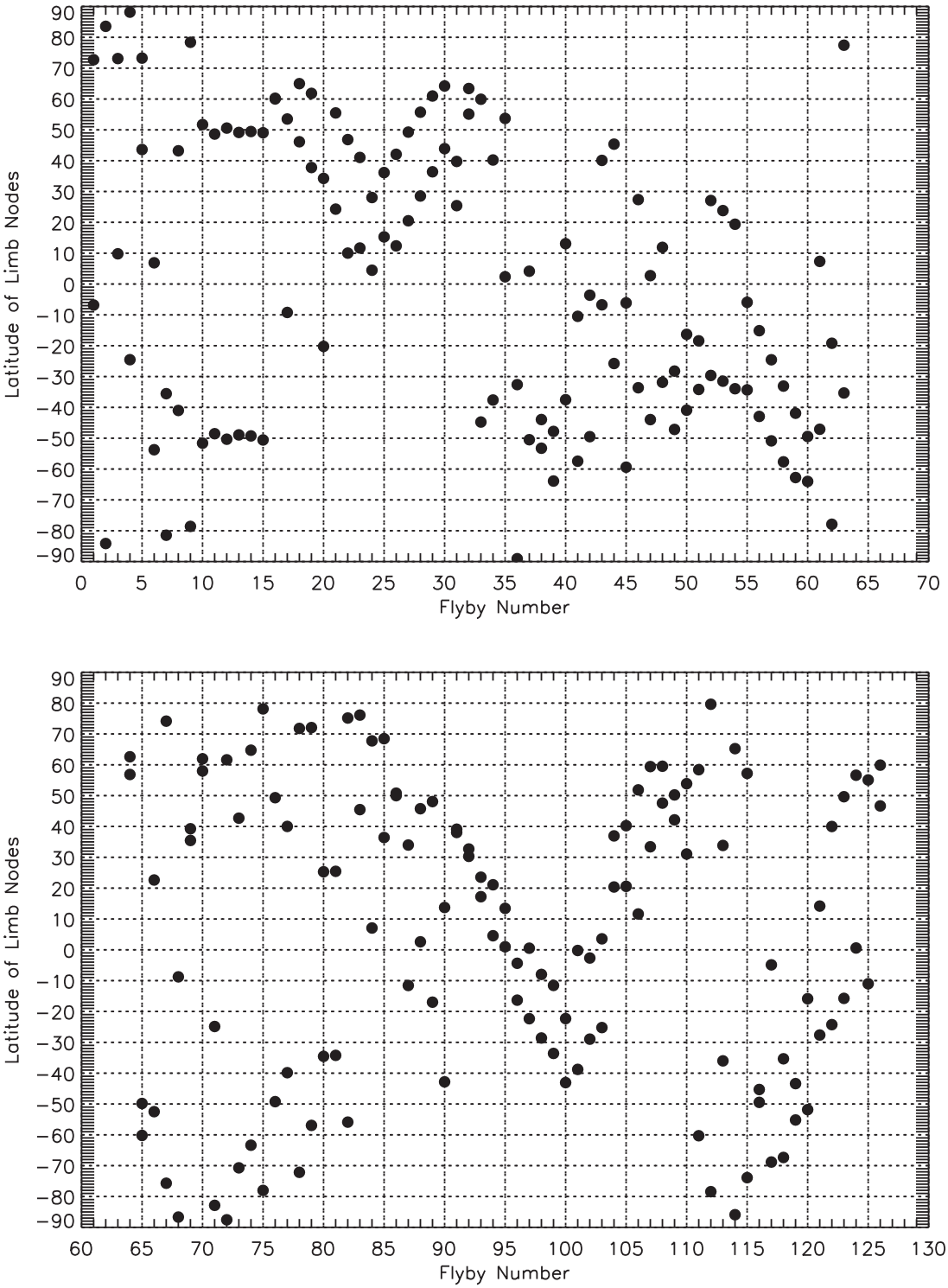

Figure 9. Horizon nodes for Titan flybys during the *Cassini* mission. Flybys "1" and "2" are TB and TC, respectively. These indicated desirable pointing positions for far-infrared limb observations (close to Titan) and were used to guide observation design.

times for a single spectrum. The observation proceeded by pointing for nominally 13 minutes (15 spectra) at 125 km, then 13 minutes at 225 km, followed by a repeat of the two positions. Due to the changing range from Titan, two shorter visits at each altitude (Figure 12) were preferred instead of one longer visit, ensuring that the spatial footprint at each altitude was not too dissimilar.

4.4. FIRLMBCON

Science overview: The far-infrared limb condensate integration (FIRLMBCON) was designed to address the gap in resolution between the high spectral resolution integrations (FIRLMBINT, 0.5 cm^{-1}), and the low-resolution scans (FIRLMBT and FIRLMBAER, 15 cm^{-1}). The lower resolution of the aerosol scans was insufficient to resolve condensate (ice)

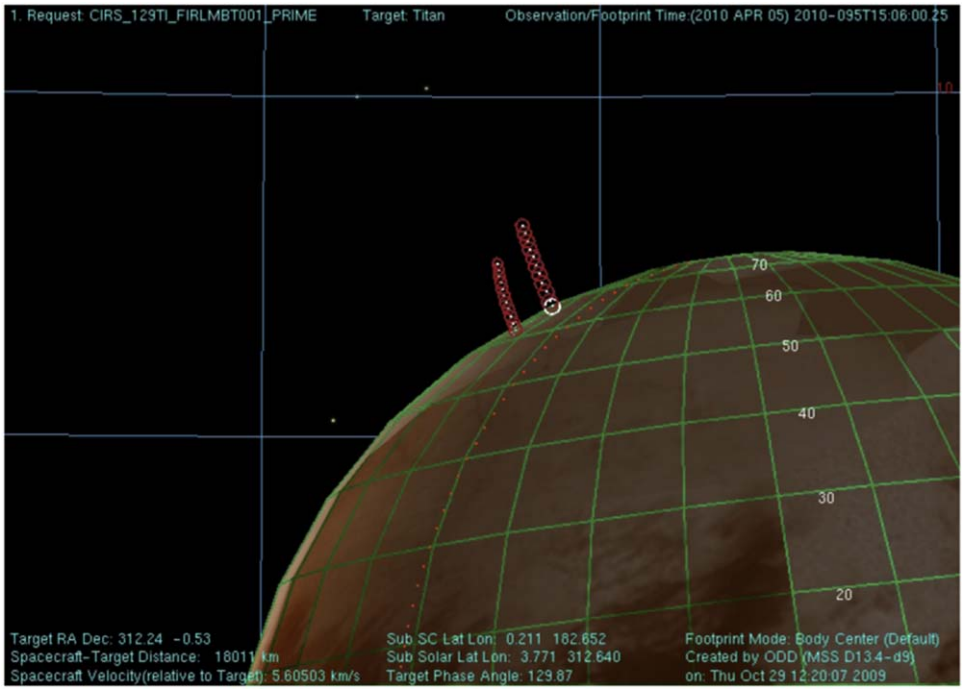

Figure 10. Example of a CIRS far-infrared limb temperature observation (CIRS_129TI_FIRLMBT001_PRIME, 2010 April 5, T67) showing two parallel limb scan tracks with FP1 at around 70° N to measure lower atmosphere temperatures. FP1 FOV projected size ∼70 km at time of snapshot.

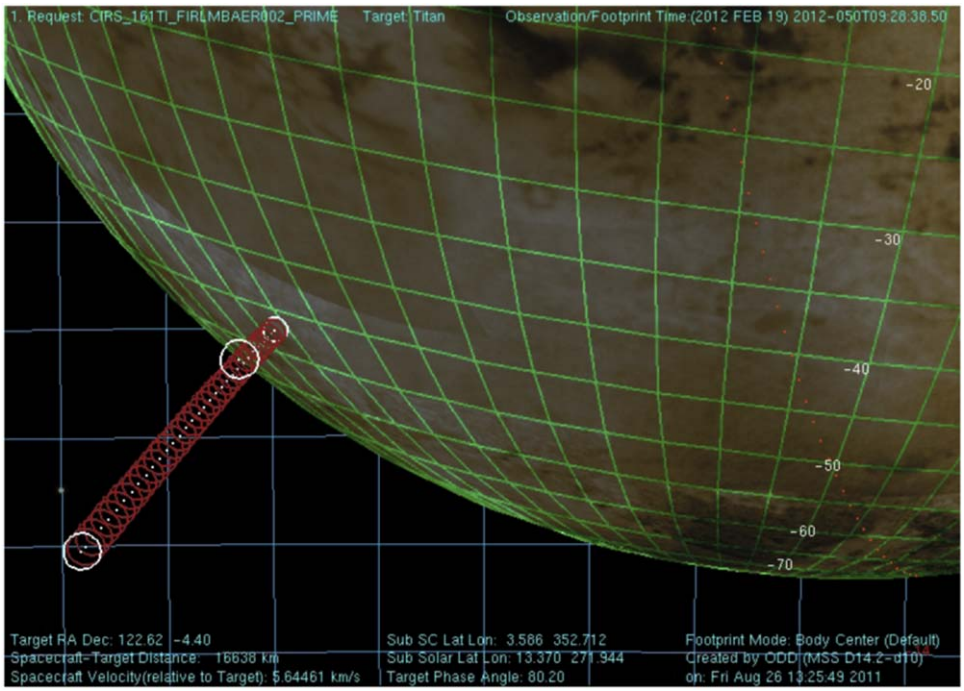

Figure 11. Example of a CIRS far-infrared limb aerosol scan (CIRS_161TI_FIRLMBAER002_PRIME, 2012 February 19, T82) showing a single slow limb scan with CIRS FP1 to measure aerosols. FP1 FOV projected size ∼65 km at time of snapshot.

features in the spectrum, such as HC_3N at 506 cm^{-1}, while the high-resolution integrations had sufficient spectral resolution but an insufficient S/N and altitude information. Data from the FIRLMBCON observation has been used to infer the presence of C_4N_2 ice at 478 cm^1 (Anderson et al. 2016, 2018).

Implementation: The observation was implemented twice, on T67 and T118 (see Table 5), as a modified FIRLMBINT from 135 to 75 minutes from closest approach on the inbound approach of the flyby. The spectral resolution was set to 3.0 cm^{-1}, with three dwells at 125, 175, and 225 km. See Figure 13.

4.5. FIRLMBWTR

Science overview: Water had previously been detected on Titan by the *Infrared Space Observatory* (Coustenis et al. 1998),

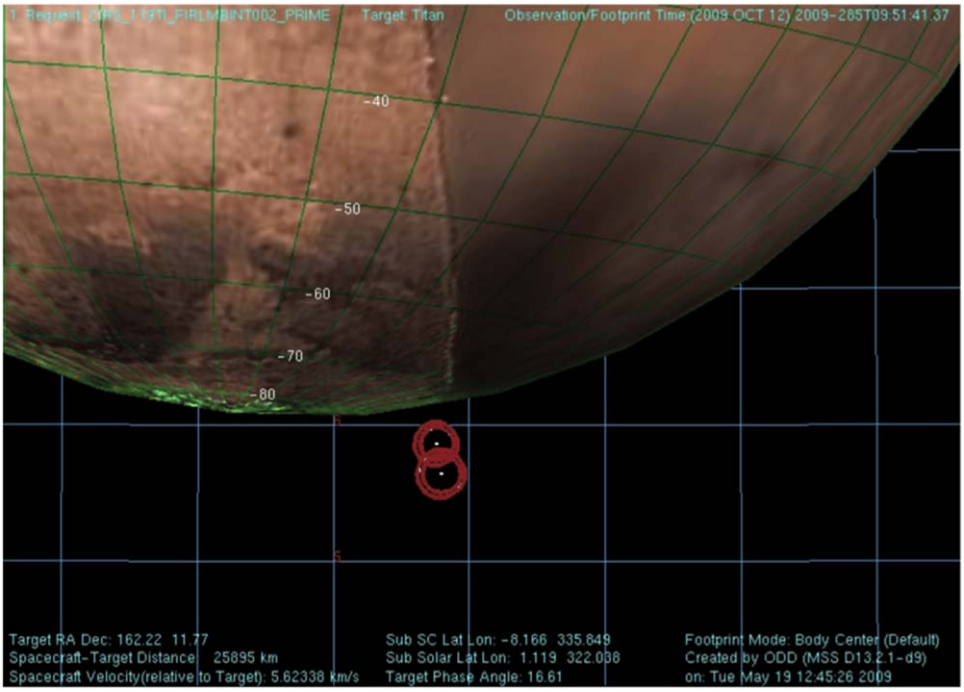

Figure 12. Example of a CIRS far-infrared limb integration (CIRS_119TI_FIRLMBINT002_PRIME, 2009 October 12, T62) showing integration at two altitudes with CIRS FP1 to measure the vertical gradient of trace gases including C_2N_2, C_3H_4 and C_4H_2. Each altitude was visited twice during a one-hour observation to reduce the difference in size of the projected FOV. FP1 FOV projected size ~100 km at time of snapshot.

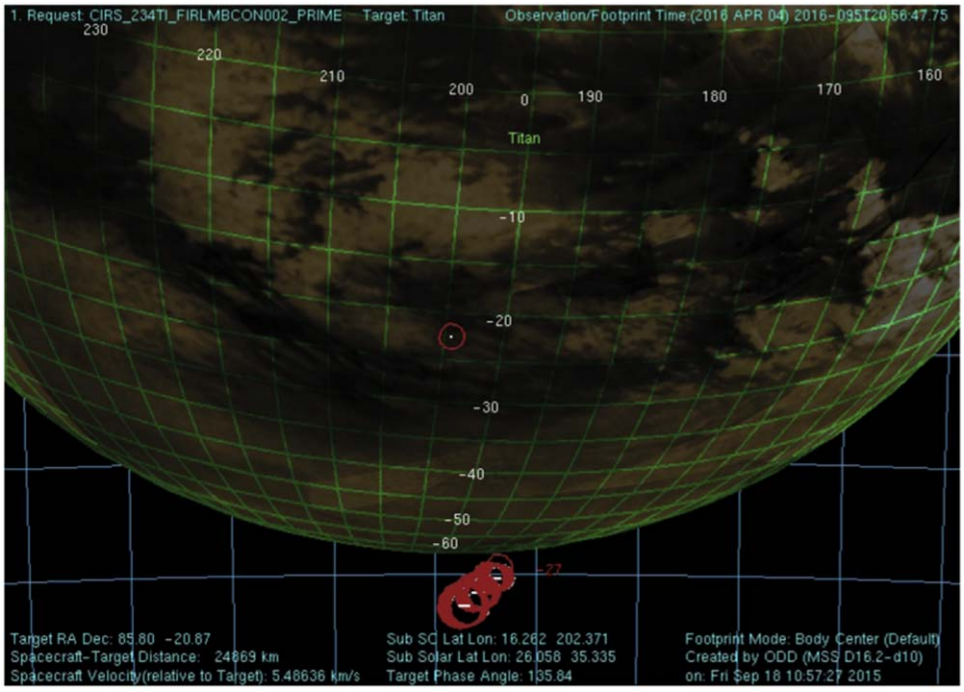

Figure 13. Example of a CIRS far-infrared limb condensate observation (CIRS_234TI_FIRLMBCON002_PRIME, 2016 April 4, T118) showing integration at three vertical positions (100, 150, 200 km altitude) to measure concentrations of condensed gas species. FP1 footprints on the disk were due to spacecraft slewing at the start of the observation to arrive at the limb pointing. FP1 FOV projected size ~97 km at time of snapshot.

which determined a disk-average abundance. The use of CIRS data, which averaged over multiple FIRLMBINTs to provide a simple vertical profile from abundances retrieved at 125 and 225 km, permitted the first measurement of water on Titan's limb (Cottini et al. 2012b). It was later suggested (S. Hörst 2012, private communication) that a third, intermediate data point at 175 km would help to better distinguish between photochemical model profiles.

Implementation: As with the FIRLMBCON, the FIRLMBWTR was performed as a modified FIRLMBINT in the same time/distance window of 75–135 minutes from closest approach. In this case, however, the entire 1 hr period was spent integrating at a

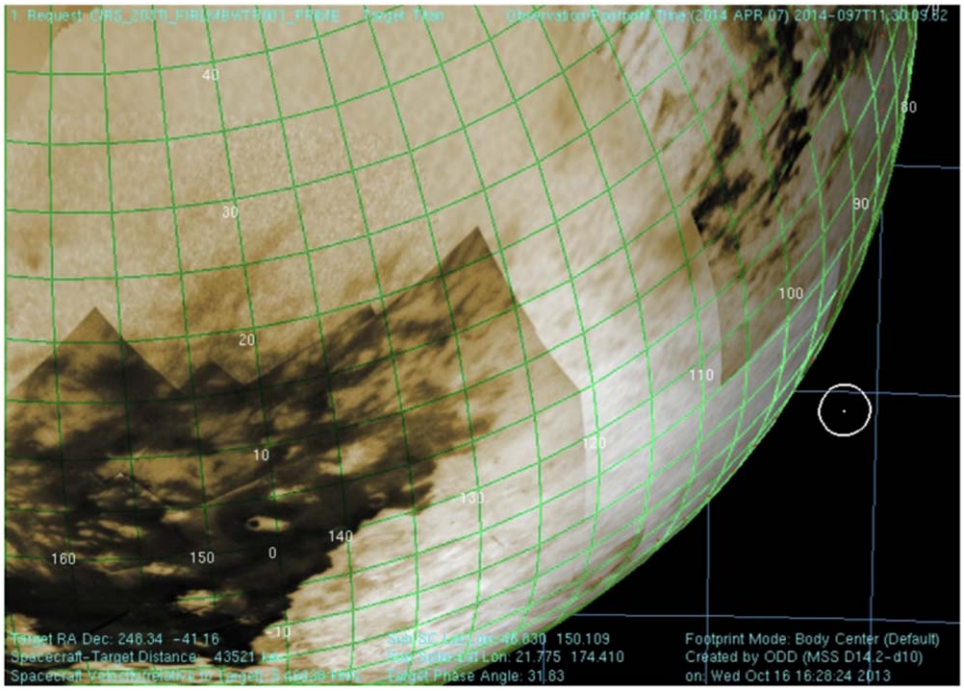

Figure 14. Example of a CIRS far-infrared limb water observation (CIRS_203TI_FIRLMBWTR001_PRIME, 2014 April 7, T100) showing a single integration at 175 km with CIRS FP1 to fill in between the 125 and 225 km positions of the FIRLMBINT. FP1 FOV projected size ~170 km at time of snapshot.

single altitude of 175 km, intermediate to the usual two FIRLMBINT altitudes, at 0.5 cm^{-1} resolution. Due to the very weak water emission, three 1 hr observations at low latitudes were scheduled on T100, T123, and T125 with the intention that these would later be combined to provide a single measurement at 175 km. See Figure 14.

4.6. Spatial and Temporal Coverage of Far-infrared Limb Observations

The coverage of CIRS far-infrared limb observations is shown in Figure 15. Observations (symbols) largely track the limb stationary nodes (points). These provide a huge improvement over the previous limb observations by *Voyager 1* (Coustenis et al. 1991) both in latitude coverage and in time. While the latitude sampling over the entire mission is excellent, different latitudes are mostly sampled at different times, preventing a true global snapshot from being obtained at any one epoch. It is clear from the pattern where the inclined orbits occur (2008–2010 and 2013–2015), where limb viewing is restricted to low latitudes as the flybys took the spacecraft over the polar regions. The consequence is that there are some gaps in spatial and temporal coverage that hinder our attempts to understand the formation and breakup of the polar vortices.

5. Mid-infrared Limb Observations

Mid-infrared limb observations were made from 5 to 9 hr from closest approach, or a distance of approximately (100–180) × 10^3 km. At the start of the mission, there were two principal types —MIRLMBINT and MIRLMBMAP, which were alternated throughout the mission. Later, an additional type, MIRLMPAIR, was added. Note that unlike FP1, where the single detector was circular and rotations around the detector (approximately equivalent to the $-Y$ direction of the spacecraft) were unimportant, for CIRS FP3 and FP4 the arrays were linear, and therefore the array direction (spacecraft secondary axis pointing) was also important. A complete listing of the mid-infrared limb observations is given in Appendix D. Note that the horizon nodes, so crucial for the far-infrared limb observations, were not an important consideration for the mid-infrared limb measurements, as the distance was much greater and therefore the horizon was changing much more slowly.

5.1. MIRLMBMAP

Science overview: The mid-infrared limb map (MIRLMBMAP) observation was designed to measure vertical profiles of temperature in Titan's stratosphere from ~120–500 km, or 5.0 to 0.005 mbar, primarily by modeling/inversion of the ν_4 band emissions of CH_4 centered at 1304 cm^{-1} (Achterberg et al. 2008a, 2008b, 2011; Teanby et al. 2012, 2017). MIRLMBMAPs have also been used to measure the vertical profile of the most abundant trace gases, such as HCN, C_2H_2, and HC_3N (Teanby et al. 2007), and to observe dynamical redistribution over Titan's changing seasons (Teanby et al. 2012; Vinatier et al. 2015).

Implementation: At 140,000 km range, the mid-infrared arrays 3 mrad in length had a projected size of ~420 km. The arrays were positioned perpendicular to Titan's limb ($+/-Z$ direction perpendicular to the edge of the disk). Two successive and overlapping pointing altitudes were used with the array centers at 100 km and then 350 km, which also allowed for pointing error by the spacecraft of up to 1 mrad (although in practice pointing accuracy was always better than 0.5 mrad.) If pointing was exact, the arrays covered altitudes −120 to +570 km over both positions. Dwells were performed at each altitude for ~4 minutes using the fast acquisition, low spectral resolution mode (15 cm^{-1}), with the FP3/4 arrays "blinking" between odd and even detector readout on alternate spectra to allow for maximum possible vertical information. The arrays

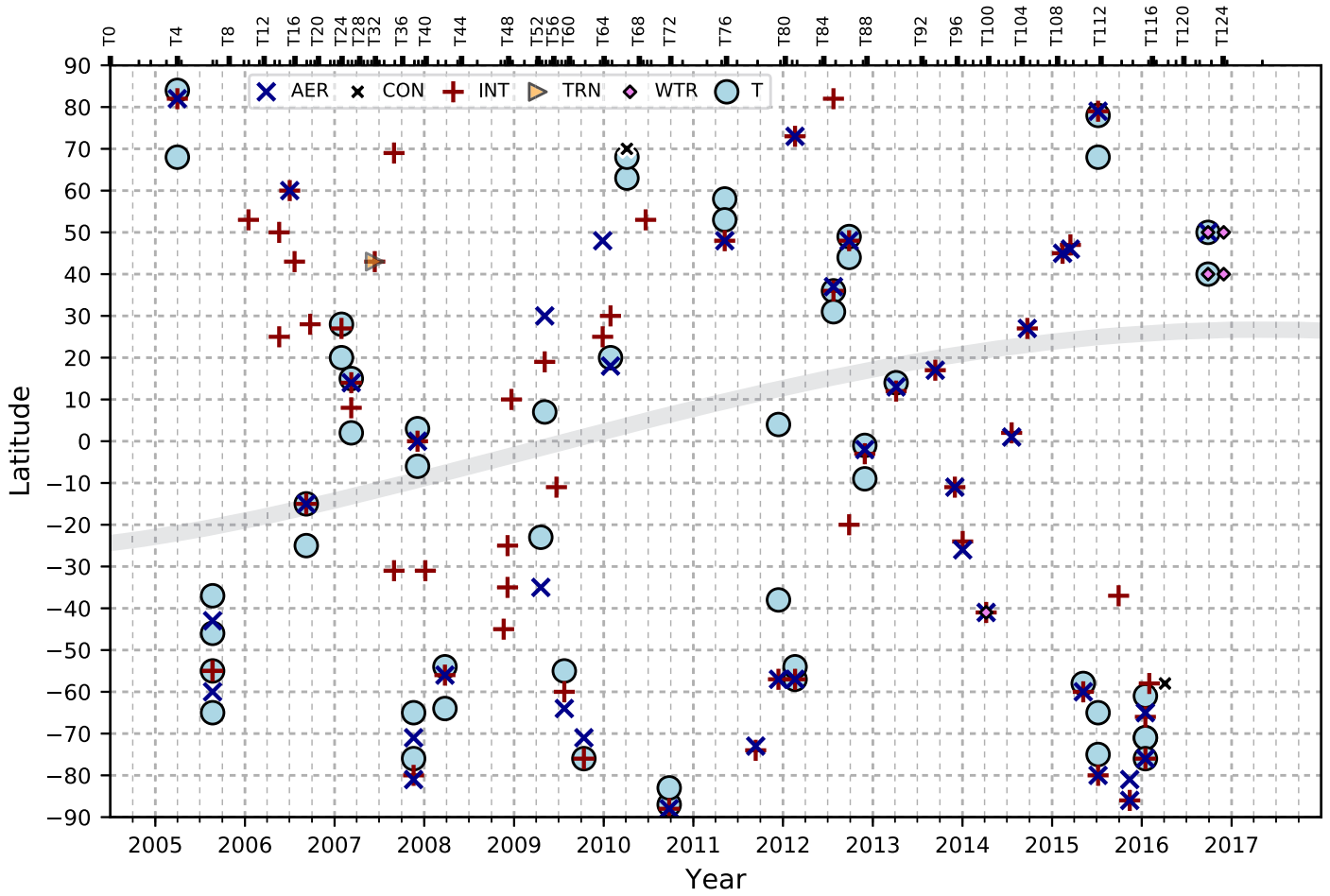

Figure 15. Latitudes and times of CIRS far-infrared limb observations throughout the mission. Different symbols denote different observation types, and the small black points denote horizon-viewing nodes. See text for details. The gray line indicates the subsolar latitude.

were then repositioned to a different limb location. This was notionally an increment of 5° in latitude, although as flyby inclination increased, the horizon circle unavoidably transitioned from latitude (most useful) to longitude (less useful). This may be understood by considering that when viewing Titan from the equatorial plane, the horizon circle includes all latitudes, while from a vantage point above either pole, the horizon circle is the equator, permitting only limb viewing of a single latitude (but multiple longitudes). Altogether, some 15–18 vertical profiles were typically obtained in a 4 hr observation window (see Figure 16).

5.2. MIRLMBINT

Science overview: The mid-infrared limb integrations were designed to measure a single vertical profile of trace gases from ∼100–500 km, including hydrocarbons, nitriles, CO_2, and other species using high spectral resolution (0.5 cm^{-1}). Many of these were detected on CIRS FP3 (600–1100 cm^{-1}). FP4 provided vertical temperature information at approximately the same location (although the two arrays were actually side by side, so the locations were not identical). MIRLMBINT data have resulted in numerous publications describing vertical and temporal mapping of trace gases (Teanby et al. 2007, 2008a, 2012, 2017; Vinatier et al. 2007a, 2010b, 2015, 2018; Nixon et al. 2009a; Lombardo et al. 2019b), aerosols (Vinatier et al. 2010a, 2012) and benzene ice (Vinatier et al. 2018). In addition, these data proved invaluable for new detections such as propene (Nixon et al. 2013a; Lombardo et al. 2019a) and many isotopologues of previously known gas species including $H^{13}CN$ and $HC^{15}N$ (Vinatier et al. 2007b), $^{13}CH_4$ and $^{13}CH_3D$ (Bézard et al. 2007; Nixon et al. 2008a, 2012b), $H^{13}CCH$ and C_2HD (Coustenis et al. 2008; Nixon et al. 2008a), $^{13}CH_3^{12}CH_3$ (Nixon et al. 2008a), $H^{13}CCCN$ (Jennings et al. 2008), $^{13}CO_2$ and $CO^{18}O$ (Nixon et al. 2008b), and $H^{13}CCCCH$ and $HC^{13}CCCH$ (Jolly et al. 2010).

Implementation: MIRLMBINT was similar to the MIRLMBMAP; however, only a single limb location (latitude) was observed, again at two altitudes together covering approximately −100 to +600 km. As with the complementary far-infrared limb integration (FIRLMBINT), the two positions were observed twice for ∼1 hr each to reduce the difference in projected array size at the two altitudes that would otherwise be incurred due to the spacecraft approaching/receding from Titan. See Figure 17.

5.3. MIRLMPAIR

Science overview: While the mid-infrared limb integrations were successful in measuring vertical profiles of many known trace gases, CIRS scientists later wished to search more intensively for new, undetected gases and isotopes that may have even weaker signals undetectable in the MIRLMBINTs. As it was impossible to increase spectral resolution beyond the maximum (0.5 cm^{-1}), the other option was to increase the S/N by acquiring more spectra, including the use of the pair mode (see Section 2.2). Results from modeling of MIRLMBPAIR

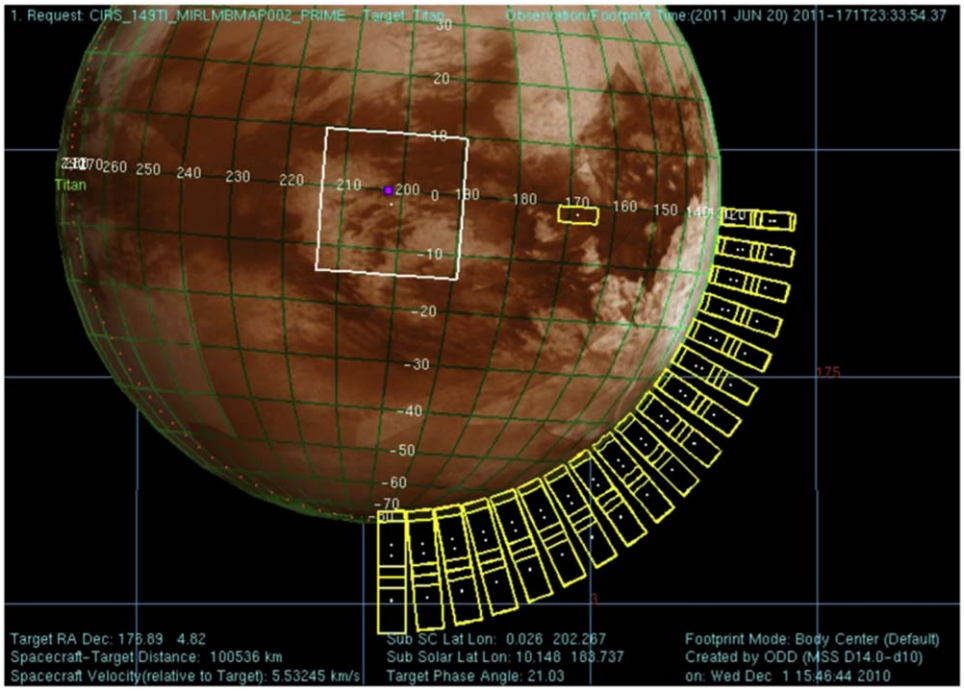

Figure 16. Example of a CIRS mid-infrared limb temperature map (CIRS_149TI_MIRLMBMAP002_PRIME, 2011 June 20, T77) showing the progressive "stepping" of the mid-infrared detectors around the limb while maintaining a "vertical" (radial) orientation of the arrays. Each yellow rectangle encompasses both FP3 and FP4. Two altitude positions were used at each latitude, with slight vertical overlap to allow for pointing uncertainties. Mid-IR projected array length ~290 km at time of snapshot.

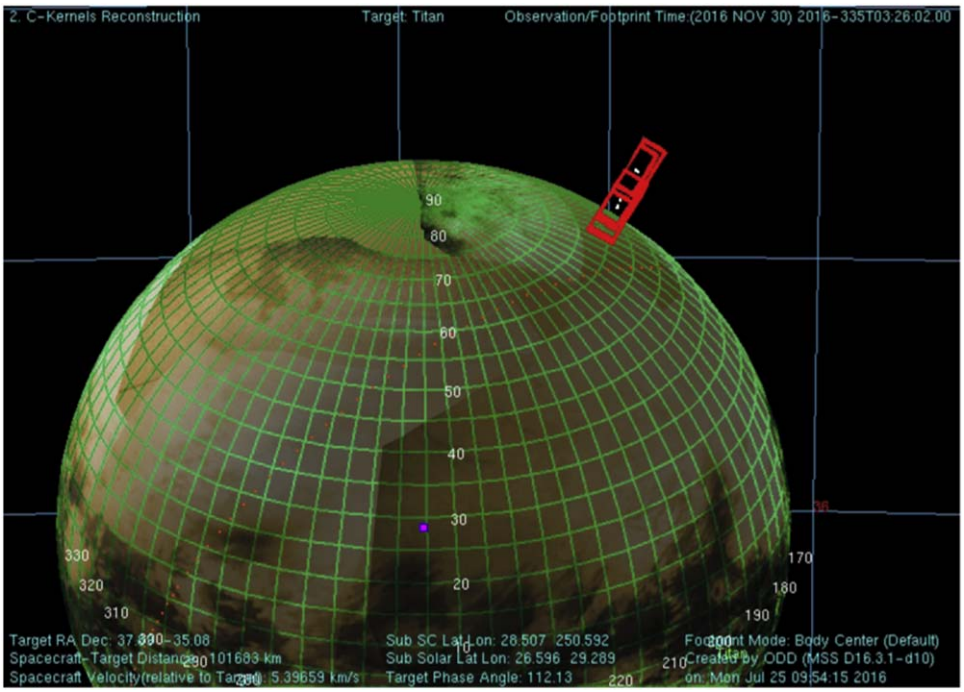

Figure 17. Example of a CIRS mid-infrared limb integration (CIRS_250TI_MIRLMBINT002_PRIME, 2016 November 30, T125) showing a limb integration with CIRS FP3/4 to measure the vertical profile of trace gases at a single latitude. Red rectangles indicate the FP3/4 combined footprint, two footprints at lower altitude position, and two at higher altitude position with some overlap. Projected array length ~295 km at time of snapshot.

data to search for trace gases and measure isotopes are described in Nixon et al. (2010b, 2012b, 2013b)

Implementation: The solution adopted to increase the S/N was to position the arrays parallel to the disk edge, so that all pixels were close to the same altitude (actually, there was a small difference between the pixels at the array ends, which are farther from the horizon, and those at the center). Then all pixels from either FP3 or FP4 could be coadded into a single spectrum. The spectra were acquired at 0.5 cm^{-1} resolution (52 s scans), and the pixels were read out in pair mode, doubling the effective number of spectra compared to the usual odd/even modes that only read out half the pixels at a time. The arrays were maintained at a single position throughout the observation, with the lower array (either FP3 or FP4) at a fixed

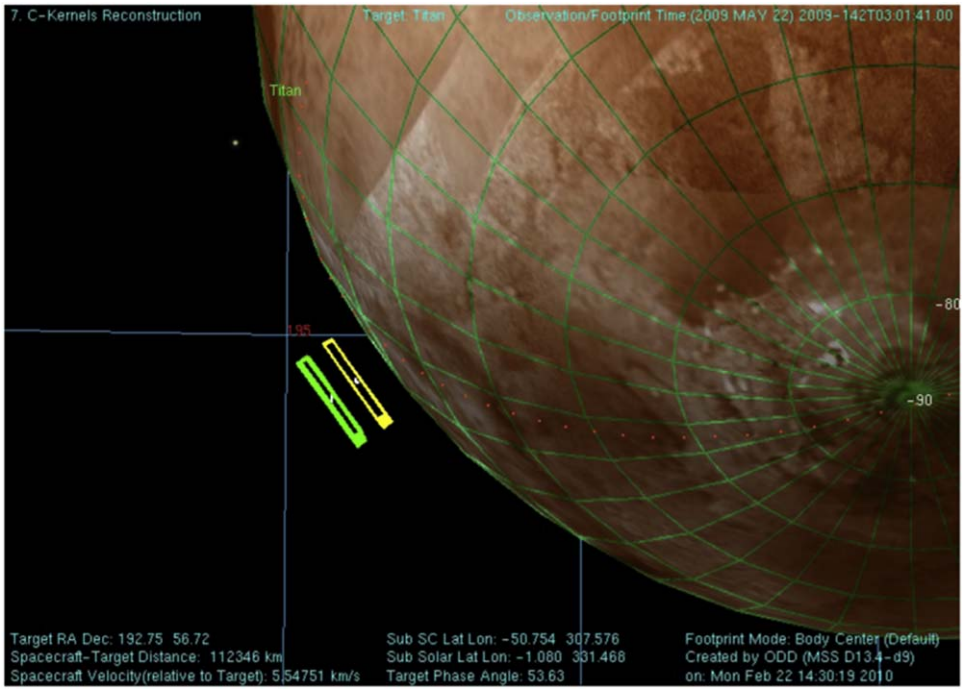

Figure 18. Example of a CIRS mid-infrared limb "pair" observation (CIRS_111TI_MIRLMPAIR002_PRIME, 2009 May 22, T55) showing integration with the arrays parallel to the limb to allow for coadding of all pixels on each array, used in pair mode. Yellow (lower altitude) array is FP3, and green (upper altitude) array is FP4. Each array spans ~325 km in length at the time of the snapshot.

Table 2
MIRLMPAIR Observations

	Latitude	
Altitude	Low	High
FP3 Low/FP4 High	T55	T64
FP3 High/FP4 Low	T95	T72

altitude; see Figure 18. The observation was repeated on four occasions: twice at low latitude and twice at high latitude. At each latitude, there were two observations: one with FP3 at low altitude ("bottom") and FP4 above, and a second observation with the reverse configuration (summarized in Table 2).

5.4. Spatial and Temporal Coverage of Mid-infrared Limb Observations

Figure 19 shows the spatial and temporal coverage of the mid-infrared limb observations during the mission. Of principal note is that the limb maps (MIRLMBMAP, blue bars) have a relatively complete coverage in latitude and season. However, as with the far-infrared limb observations, there are some gaps (e.g., late 2008 to early 2009, late 2010, mid 2014) where the highest northern and southern latitudes are not sampled due to the inclined spacecraft orbits. Limb integrations (MIRLMBINT) also exhibit this pattern, although overall there is repeat coverage of low, medium, and high latitudes in each hemisphere during the mission, providing an excellent reference data set for understanding atmospheric circulation and composition.

6. Far-infrared Nadir Observations

Far-infrared nadir observations, like the limb observations, are divided into two types: integrations and scans/maps.

6.1. FIRNADMAP (UVIS EUVFUV)

Science overview: The far-infrared nadir map observation was designed primarily to measure the temperature of Titan's surface using a spectral window at ~530 cm^{-1} (19 μm) where the opacity of both aerosols and collision-induced gas absorption is low (Jennings et al. 2009, 2011, 2016; Cottini et al. 2012a). However, these observations have also been used to measure the spatial variation of condensates (Jennings et al. 2012a, 2015; see also FIRLMBAER). Tropospheric temperatures may also be obtained from the N_2–N_2 CIA region at 50–150 cm^{-1} (Lellouch et al. 2014), and the N_2–H_2 CIA regions around 350 and 600 cm^{-1} have been used by Bézard & Vinatier (2019) to infer the H_2 mole fraction and ortho-to-para ratio in the troposphere.

Implementation: The observation nominally takes place in the period 02:15 to 05:00 (HH:MM) from closest approach, when the spatial footprint of FP1 is about 200–400 km (see Figure 6). The FP1 detector was typically scanned slowly in a north–south or east–west direction across a diameter of the disk, starting from a position off the limb on dark sky and ending on a dark sky position situated off the disk on the opposite side. The spectral resolution was 15.0 cm^{-1}, and the scan speed was ~7 μrad s^{-1}. See Figure 20.

Variations: the 2–5 hr time window from Titan closest approach was often requested by other instruments, including RADAR, VIMS, and ISS, resulting in changes to the default template, whereby CIRS might have a shorter time than the nominal 2 hr 45 minutes. In these cases, the scans may have been shortened to cover half a diameter only or to cover a specific part of the visible hemisphere such as Xanadu. Therefore, extracting the exact pointing for the observations from the CIRS archive in the PDS is important.

The FIRNADMAP observation was very similar to a UVIS-designed slow scan observation (EUVFUV scan) that took

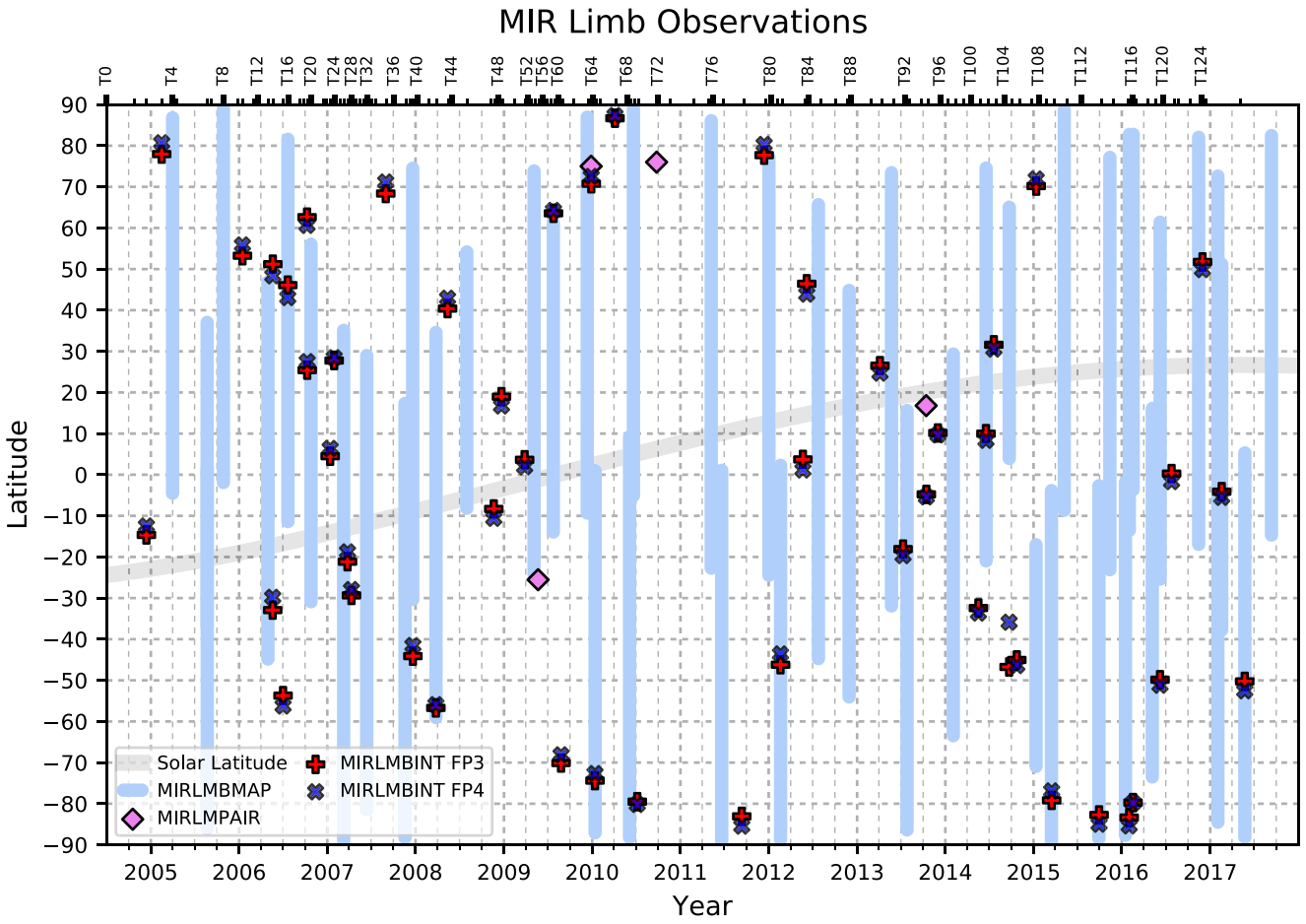

Figure 19. Latitudes and times of CIRS mid-infrared limb observations throughout the mission. Different symbols denote different observation types as described in the text—points are high spectral resolution integrations, while blue bars are low spectral resolution maps. The thick gray line shows the subsolar latitude, indicating advancing seasons.

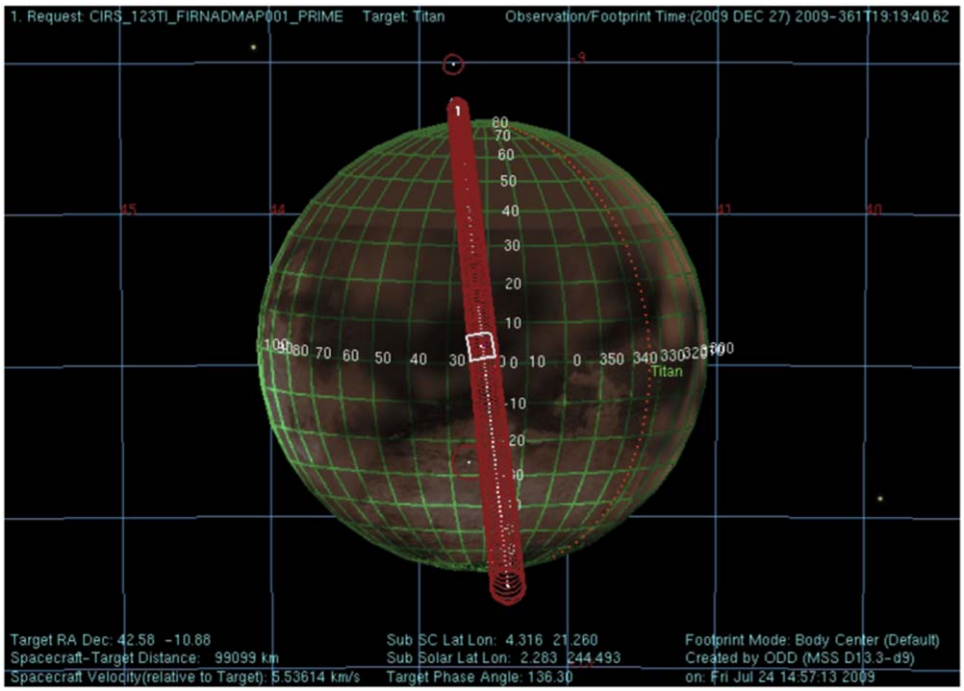

Figure 20. Example of a CIRS far-infrared nadir map (CIRS_123TI_FIRNADMAP001_PRIME, 2009 December 27, T64) showing a single slow scan across Titan's disk to measure latitude variation of temperatures of the lower atmosphere and surface. The largest footprint circle (off the south pole) is 386 km in diameter. The white box is the ISS Narrow Angle Camera (NAC) footprint.

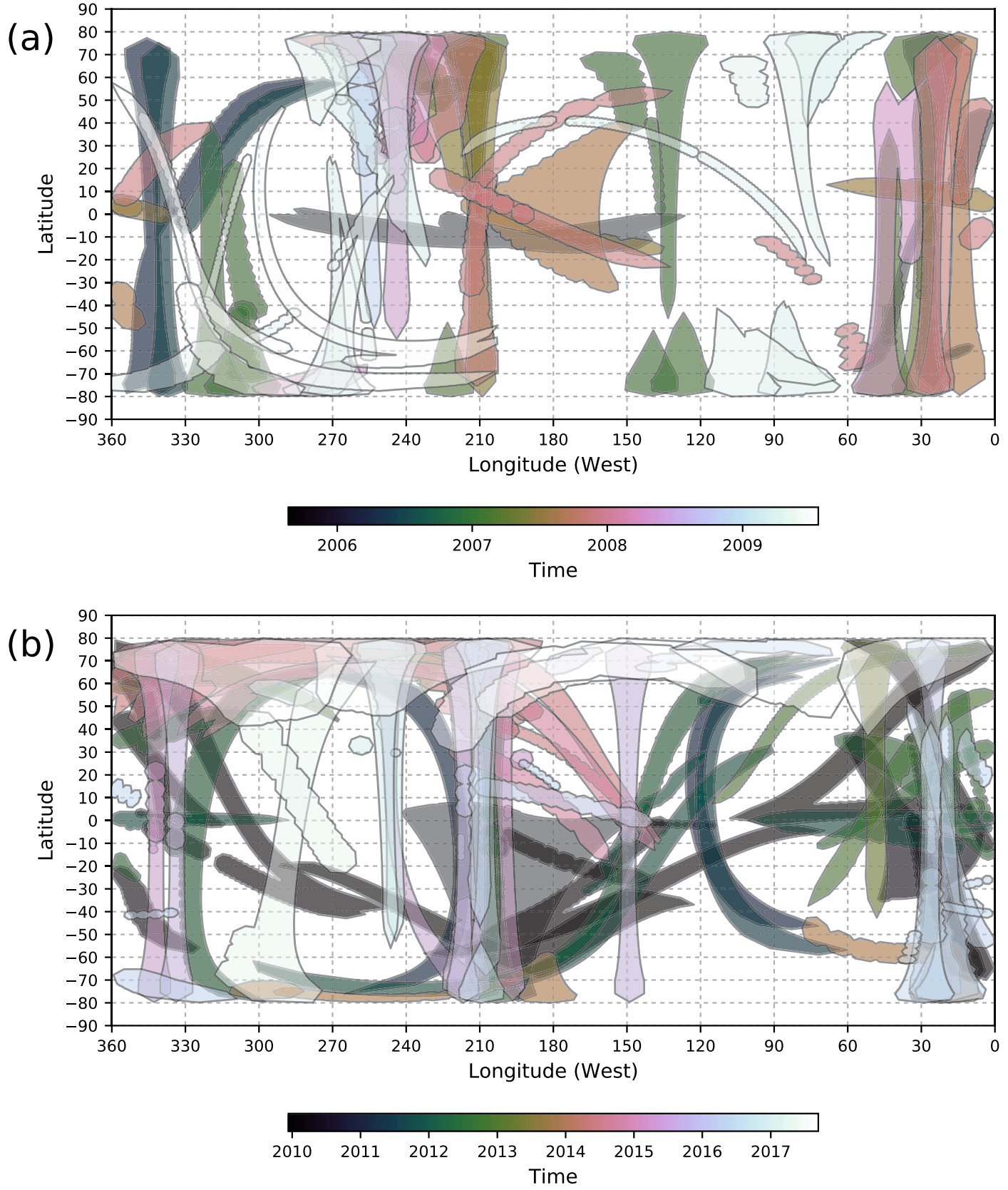

Figure 21. Coverage maps of CIRS far-infrared nadir-mapping observations (FIRNADMAP) in cylindrical projection for (a) the early mission, 2004–2010, and (b) the late mission, 2010–2017.

place typically 2–7 hr from closest approach to map airglow across an entire hemisphere by sweeping a linear detector array. CIRS acted as a "rider" taking data on these observations, and they are considered equivalent to the FIRNADMAP for CIRS data analysis purposes. The CIRS ride-along observations with EUVFUV were initially labeled in the form

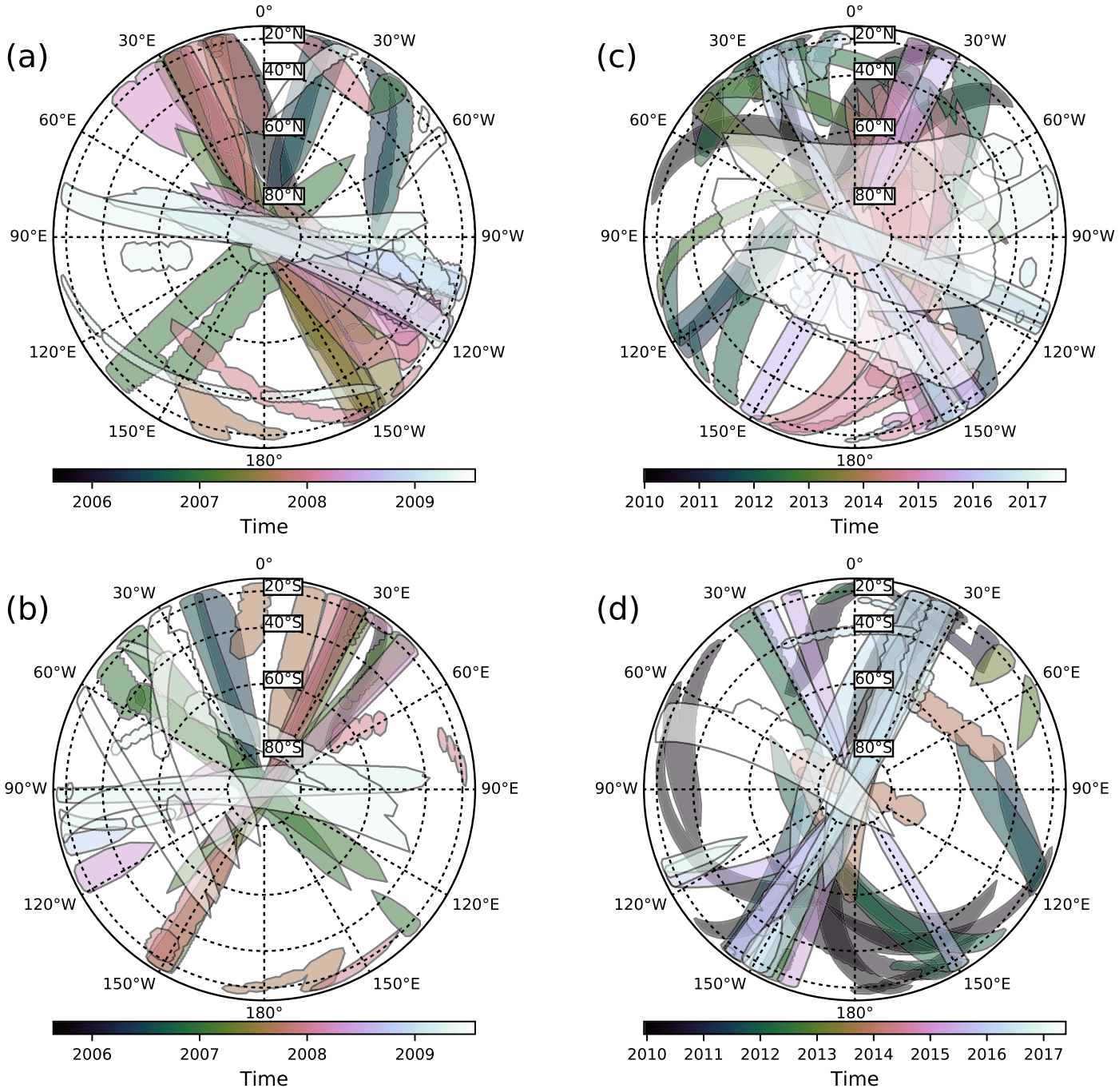

Figure 22. Coverage maps of CIRS far-infrared nadir-mapping observations (FIRNADMAP) in polar projection for the early mission, 2004–2010, northern (a) and southern (b) hemispheres, and the late mission, 2010–2017, northern (c) and southern (d) hemispheres.

CIRS_nnnFIRNADMAPnnn_UVIS (where "nnn" are numbers) but later switched to CIRS_nnnEUVFUVnnn_UVIS to further distinguish these from the CIRS-designed FIRNADMAPs (see Appendix E).

6.2. FIRNADMAP: Coverage

Coverage of CIRS FIRNADMAP observations in cylindrical projection is shown in Figure 21, divided into early (2004–2010) and late (2010–2017) mission phases for clarity of viewing. Due in part to the map projection, and also the typically equatorial viewing geometry from the spacecraft, there is substantial "stretching" of the FOV footprint near the poles. Figure 22 shows the same information but plotted in polar projection, producing less distortion, although the stretching of the FOV footprint at high latitudes is still evident where the spacecraft was viewing from low latitudes. Finally, Figure 23 shows the coverage of the complementary UVIS EUVFUV maps in both rectangular and polar projection for the entire mission.

6.3. FIRNADCMP

Science overview: The far-infrared nadir composition integrations (FIRNADCMP) were designed to complement the far-infrared limb integrations (FIRLMBINT) by providing

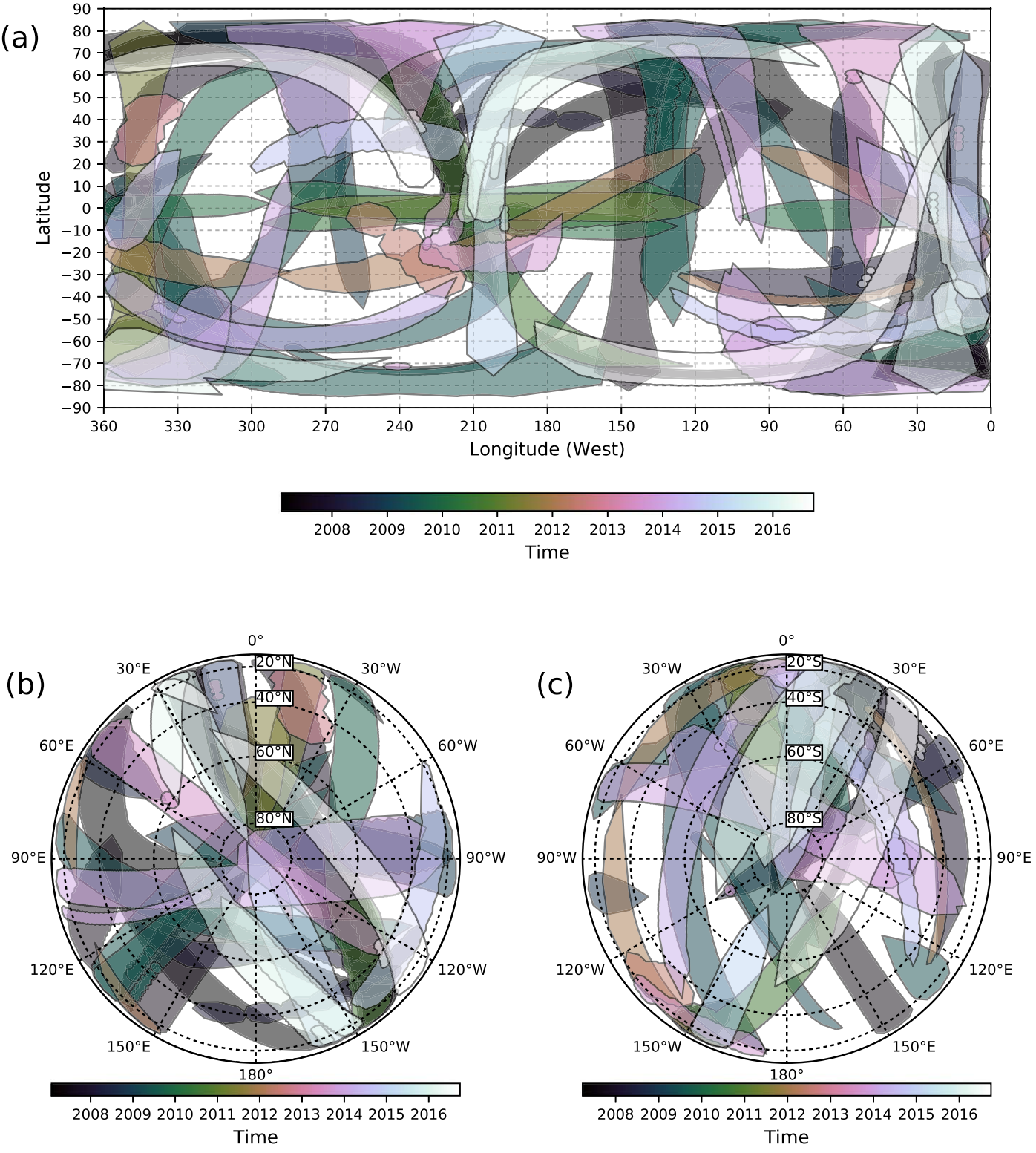

Figure 23. Coverage maps of UVIS EUVFUV observations, equivalent to CIRS FIRNADMAP in cylindrical (a) and polar (b), (c) projections.

latitude–longitude spatial coverage with high spectral resolution and S/N, although without vertical resolution. The principal science goals were to measure the abundances of HCN, CO, H_2O, and CH_4 through their far-infrared rotational lines (de Kok et al. 2007b; Lellouch et al. 2014); hydrocarbons (C_3H_4, C_4H_2) and nitriles (C_2N_2, HC_3N) can also be measured (de Kok et al. 2008; Teanby et al. 2009b; Sylvestre et al. 2018). Due to the time and distance from closest approach (nominally 9–13 hr, or (180–260) $\times$ 10^3 km), these became the most frequent and numerous of all CIRS Titan observations. In addition to the desired FP1 science, large amounts of FP3 and FP4 data were acquired in nadir mode at 0.5 cm^{-1} resolution. These FP3 and FP4 data were used for many purposes: to map latitude variations of trace gases (e.g., Coustenis et al. 2007, 2010;

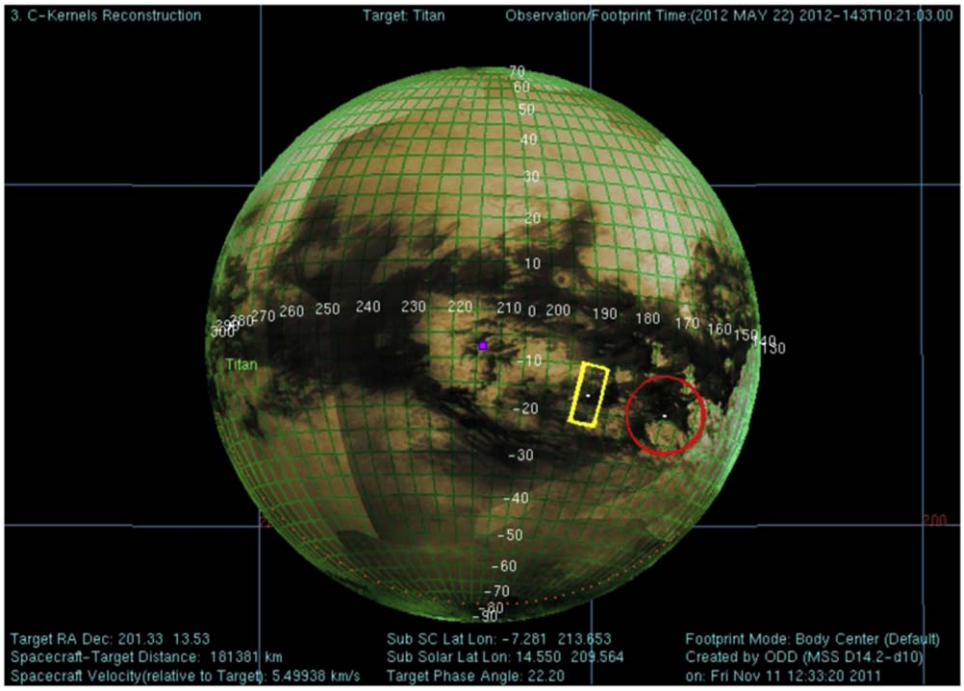

Figure 24. Example of a CIRS far-infrared nadir composition integration (CIRS_166TI_FIRNADCMP001_PRIME, 2012 May 22, T83) showing a long-duration integration with CIRS FP1 (red circle) on Titan's disk to measure the abundances of trace gases in the far-infrared. FP1 spans 705 km diameter at the time of the snapshot, while FP3/4 (yellow rectangle) is 525 km in length.

Teanby et al. 2010a; Bampasidis et al. 2012; Coustenis et al. 2013, 2016, 2018; see also MIDIRTMAP), to measure isotopic ratios of hydrocarbons (Nixon et al. 2008a), and to search for new species (Jolly et al. 2015).

Implementation: The FP1 detector was positioned at approximately 45°–60° emission angle, or about two-thirds of the way between the disk center and the disk edge. Where possible, the detector was rotated so that FP3 and FP4 were also on the disk. The instrument then dwelled for typically ∼90 minutes, bracketed on either side by shorter integrations on deep space, about 1000 km above the limb. Observations of more than 3–4 hr were broken up with an additional one, or in some circumstances by two deep space calibration observations of about 30 minutes between the science time blocks on Titan's disk. See Figure 24.

6.4. FIRNADCMP: Coverage

Figures 25 and 26 show mission coverage of the far-infrared nadir composition integrations in cylindrical and polar projections, respectively. It is evident that these numerous observations achieved excellent spatial and temporal coverage. See also Appendix F for a complete listing of FIRNADCMP observations.

7. Mid-infrared Nadir Observations

Mid-infrared nadir observations were the least constrained by detector footprint, because FP3/4 have the smallest projected pixel size. This meant that even at significant distances (300–500) × 10^3 km or more from Titan—outside the range in which the limb could be resolved—there was still significant science that could be achieved by mapping the visible disk in nadir mode. Indeed, these proved to be invaluable for monitoring the temperatures and dynamics at a "planetary" scale as the seasons progressed.

7.1. MIDIRTMAP and TEMPMAP

Science overview: The mid-infrared temperature map observation was designed as a map of the visible hemisphere at medium spectral resolution (3 cm^{-1}) primarily to allow temperature retrievals from the ν_4 band of methane at 1305 cm^{-1}. Subsequently, the temperatures retrieved could be converted into wind fields via the thermal wind equation, allowing for Titan's changing global circulation to be tracked. MIDIRTMAP observations have proved essential for mapping of Titan's global stratospheric temperature and wind fields; see, for example, Flasar et al. (2005) and Achterberg et al. (2008b, 2011). Due to the excellent spatial coverage and medium spectral resolution, MIDIRTMAP observations have been widely used for not only temperature retrievals, but also for mapping the more abundant trace gases such as C_2H_2, HCN, and C_2H_6 (Teanby et al. 2006, 2008b, 2009c, 2010b, 2017, 2019; Coustenis et al. 2007, 2013; Bampasidis et al. 2012), and for measuring Titan's total emitted power (Li et al. 2011; Li 2015). The combined latitudinal and longitudinal coverage has been used to determine a tilt in the atmospheric rotation axis relative to Titan's solid body from the temperature field (Achterberg et al. 2008a) and trace gases (Teanby et al. 2010c). In addition, medium spectral resolution FP1 data from the MIDIRTMAPs have been used for retrievals of Titan's H_2 abundance from the H_2–N_2 dimer at ∼360 cm^{-1} (Courtin et al. 2012).

Implementation: MIDRTMAP was a "workhorse" observation for CIRS that was performed on almost every flyby on either the inbound leg of the flyby, the outbound leg, or both. This observation was commonly used because the range at 13–19 hr from C/A ((260–480) × 10^3 km) was not in high demand for measurements by other instruments, with the exception of cloud monitoring by ISS. The observation was performed using the "pushbroom mapping" method, where the

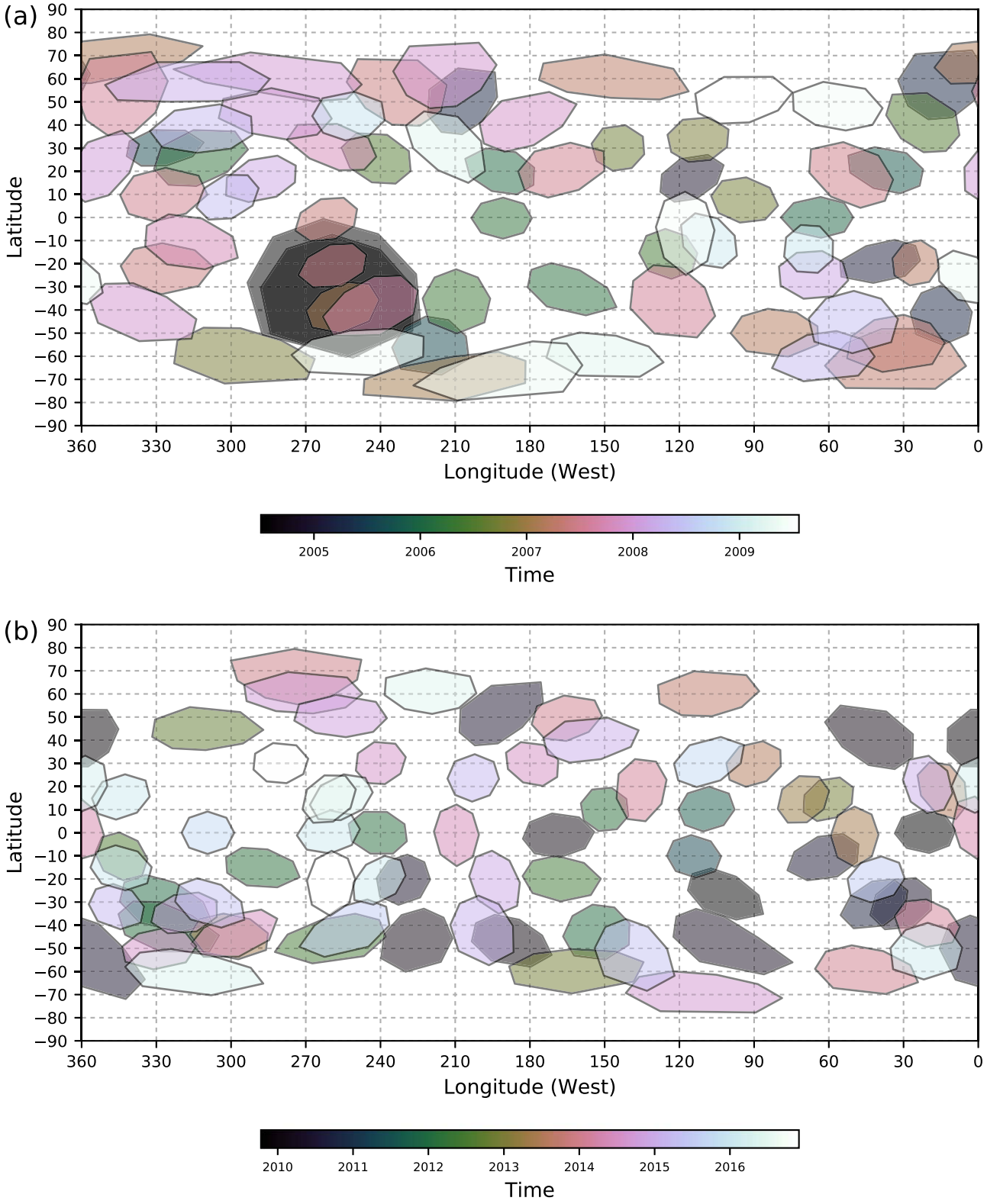

Figure 25. Coverage maps of CIRS far-infrared nadir composition integrations (FIRNADCMP) in cylindrical projection for (a) the early mission, 2004–2010, and (b) the late mission, 2010–2017. Note that the circular FP1 detector is plotted as an octagon, because pointing information is stored for the detector center and eight evenly spaced points around the circumference.

FP3 and 4 arrays were slowly scanned across the visible disk in several (typically four to seven) parallel tracks to map the entire disk. The scan rate was $\sim$4 μrad s^{-1} and tracks overlapped slightly ($\sim$20%) to prevent any gaps in coverage. In the early part of the mission, the observations were usually preceded and followed by a "stare" (integration) on deep space significantly away from the atmosphere. Later, this function was performed instead by dedicated deep space calibration observations ("DSCAL") by CIRS made during spacecraft downlinks (data relay to Earth), so the "embedded" deep space calibration

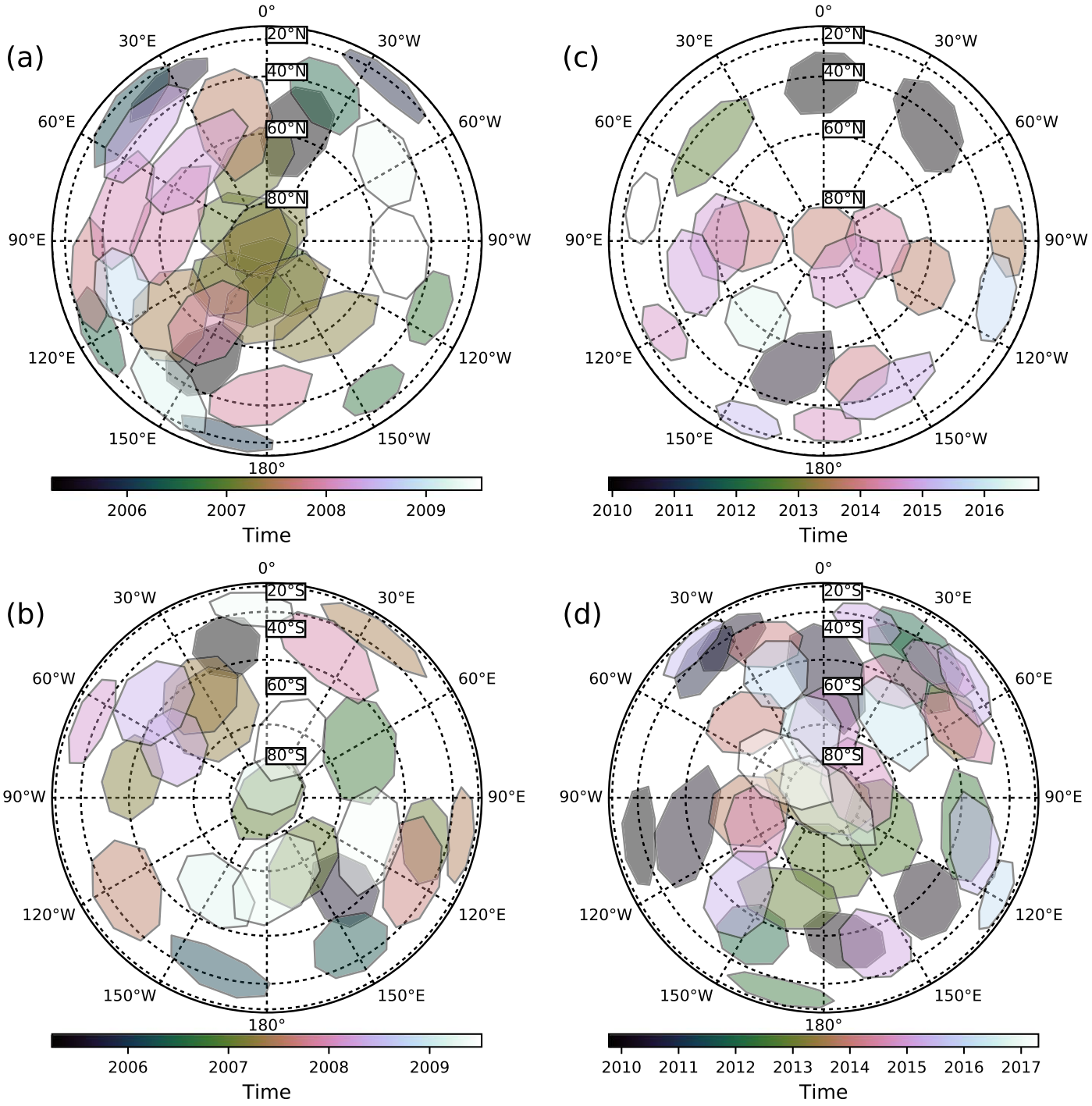

Figure 26. Coverage maps of CIRS far-infrared nadir composition integrations (FIRNADCMP) in polar projection for the early mission, 2004–2010, northern (a) and southern (b) hemispheres, and the late mission, 2010–2017, northern (c) and southern (d) hemispheres. Note that the circular FP1 detector is plotted as an octagon, because pointing information is stored for the detector center and eight evenly spaced points around the circumference.

blocks within observations gradually disappeared from usage. See Figure 27.

Variations: The label "TEMPMAP" was used early in the mission for more distant MIDIRTMAP observations that fell outside of a canonical TOST period—a segment of the *Cassini* timeline designated as a Titan encounter time block. These typically have lower spatial resolution (i.e., larger detector footprints on Titan) than normal MIDIRTMAPs, and correspondingly fewer and shorter angular scans of the arrays to cover the disk, but otherwise accomplish the same mid-infrared nadir-mapping goal. After the end of the PM, from 2008 onward, the TEMPMAP designation was deprecated, and all observations of this type became MIDIRTMAPs, or the time was used for integrations instead.

In the late mission, many MIDIRTMAPs were cut short by downlinks that increasingly were moved inward in time, shortening the Titan observation block (a.k.a. the "TOST segment," after the TOST working group) especially on the unlit (night) side, whether inbound or outbound. In these cases, MIDIRTMAPs that were notionally 6 hr in length were

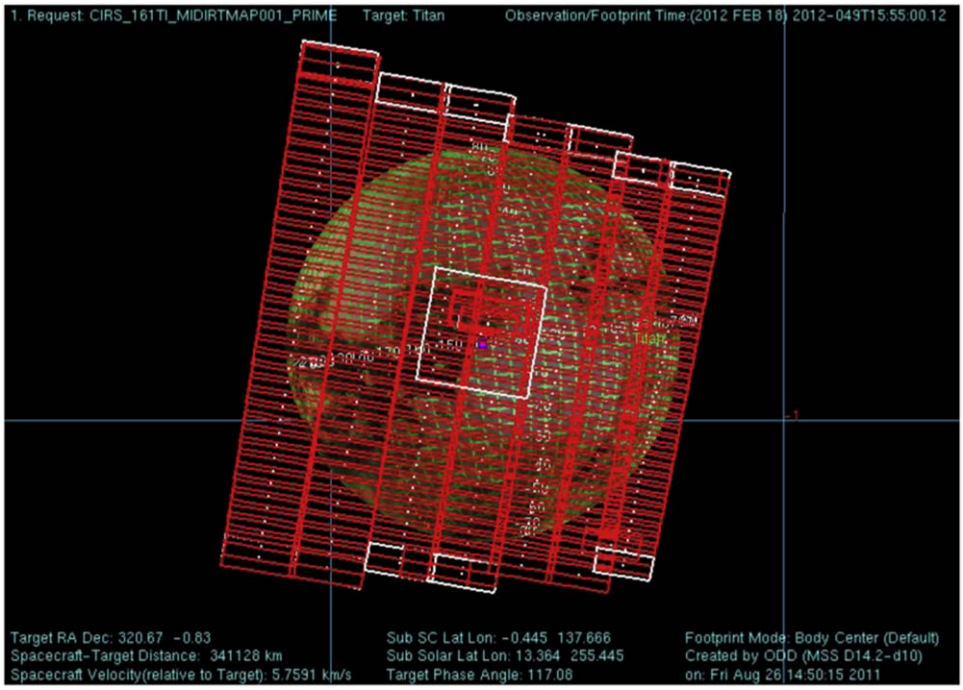

Figure 27. Example of a CIRS mid-infrared temperature map (CIRS_161TI_MIDIRTMAP001_PRIME, 2012 February 18, T82) showing a disk-mapping observation with FP3/4 in "pushbroom" format to measure stratospheric temperatures across the visible disk. Each rectangle is a combined FP3/4 footprint, with the final (largest) footprint spanning 990 km in length. The white box is the ISS Narrow Angle Camera (NAC) footprint.

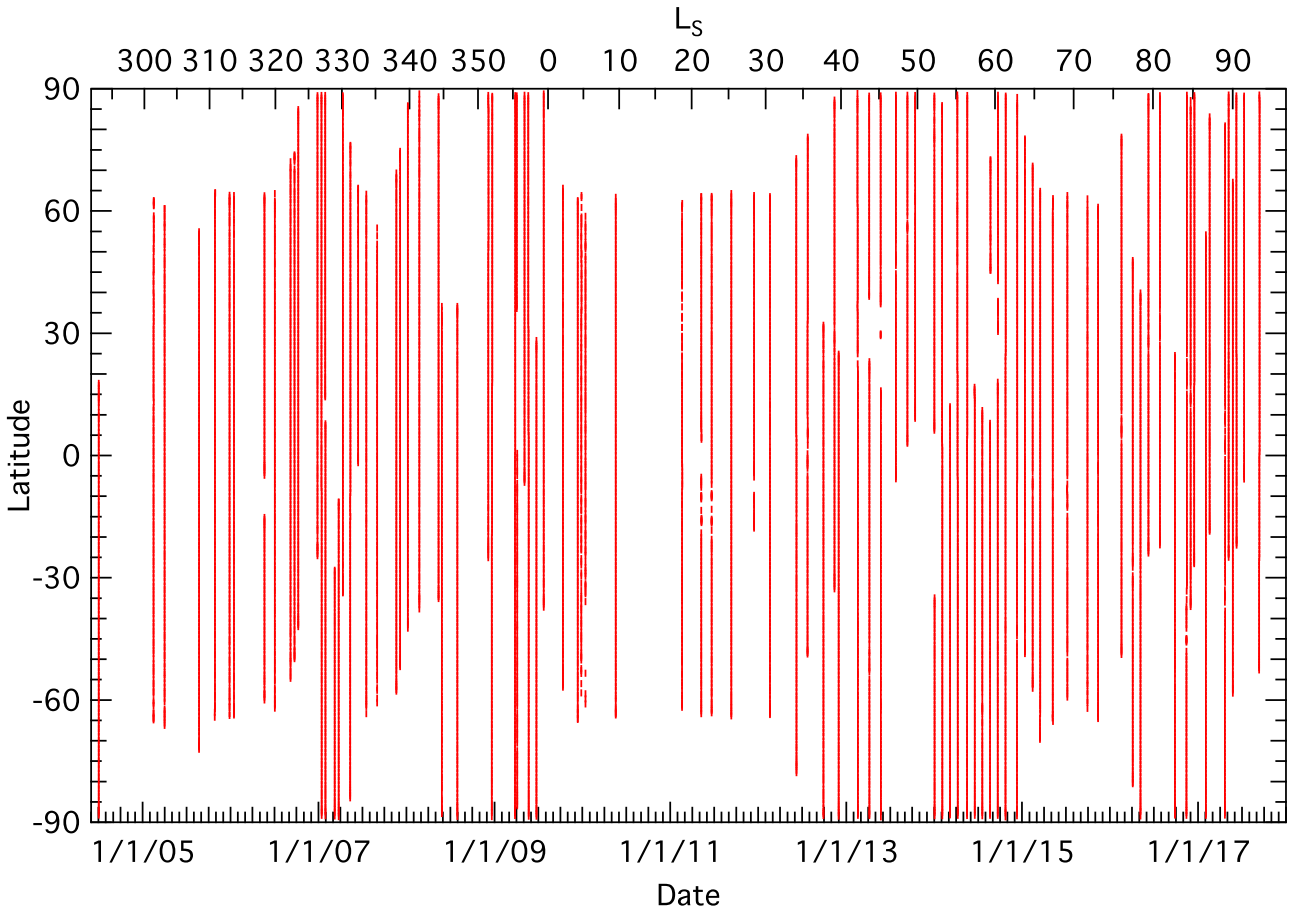

Figure 28. Coverage of CIRS mid-infrared temperature maps in latitude and time during the mission. L_s indicates the solar longitude, the position angle of the planetary rotation axis relative to the Sun, where 0° is by convention the vernal equinox at the start of northern spring.

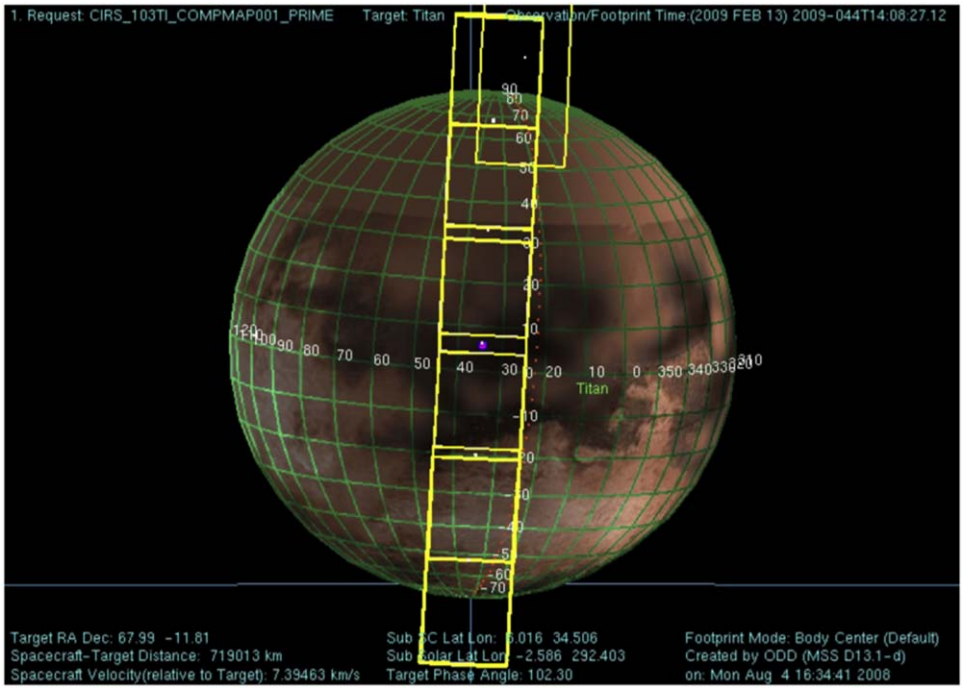

Figure 29. Example of a CIRS distant composition integration (CIRS_103TI_COMPMAP001_PRIME, 2009 February 13) showing the mid-infrared detector arrays repositioned at several locations to straddle Titan's disk to obtain a 1D profile of trace gases. Each yellow rectangle is the combined FP3/4 footprint, spanning about 2085 km at time of snapshot.

sometimes cut down to 3–4 hr, resulting in only partial disk maps. In the final months of the mission, during the "F-ring" and "proximal" orbits at high inclination with repeated distant Titan encounters, MIDIRTMAPs were often performed as multiple short blocks, interspersed with ISS "mosaic" observations designed to search for clouds.

7.2. MIDIRTMAP: Coverage

Coverage of mid-infrared temperature maps in latitude and time is shown in Figure 28. Aside from a loss of high latitude coverage from 2010 to 2012 due to spacecraft-viewing geometry, overall coverage during the mission is excellent, permitting a wide-ranging survey of Titan's atmospheric dynamics (winds and circulation). For a full list of these observations, see Appendix G.

7.3. COMPMAP and TEA

Overview: These were the most distant Titan observations performed by CIRS, occurring at distances (0.5–2.0) $\times$ 10^6 km. They were very distant integrations at high spectral resolution (0.5 cm^{-1}), usually designed to measure a single section (either N–S or E–W) of trace gas abundances across the disk (Teanby et al. 2006, 2008b, 2010b). The COMPMAP (composition map) name was used when the observation occurred in a regular TOST segment, while in the later mission phases the name TEA was used instead (Titan Exploration at Apoapse) when the observation took place in a non-TOST observation block, and usually at greater range than COMPMAP. See also the observation listing in Appendix H.

Implementation: The FP3/4 arrays were positioned to span Titan's disk in one to five positions, with long dwells at each position to build up the S/N. COMPMAP varieties tended to be at somewhat closer distances than TEAs and typically had two or more pointings (Figure 29), whereas the TEAs had only one (Figure 30).

Variations: Several very distant TEA observations were specially designed to place Titan entirely within the FP1 pixel for comparison with far-infrared unresolved observations made with *ISO* (Coustenis et al. 1998) and *Herschel* (Moreno et al. 2012), as published in Bauduin et al. (2018; see Figure 31).

8. Summary and Conclusions

Table 3 summarizes the number of each type of observation performed, the observation times, numbers of spectra, and data volumes, showing that substantial amounts of data were taken across all observation types. One striking conclusion is that the original nine types of observations (Table 1), planned long before orbit insertion, remained in use throughout the entire 17 yr mission with only minor modifications, a strong testament to the thoughtful forward planning that was put into constructing the standard observation templates. In this process, the *Cassini* CIRS team benefited from many personnel having previous experience with *Voyager* IRIS observations of Titan. The use of these standard observation-type formats greatly facilitated the planning of CIRS observations during 127 flybys of Titan. There is no doubt that designing new and different observations for each flyby would not only have put a much larger burden on the science planning and instrument commanding, but would also have made the data much less useful by complicating the intercomparison of data from observations on different flybys. Though the evolved observation types were used to a much lesser extent, they provided valuable data for some specific science cases and filled in some key gaps left by the standard observation templates. The conclusion is that flexibility and adaptation is important, alongside standardization.

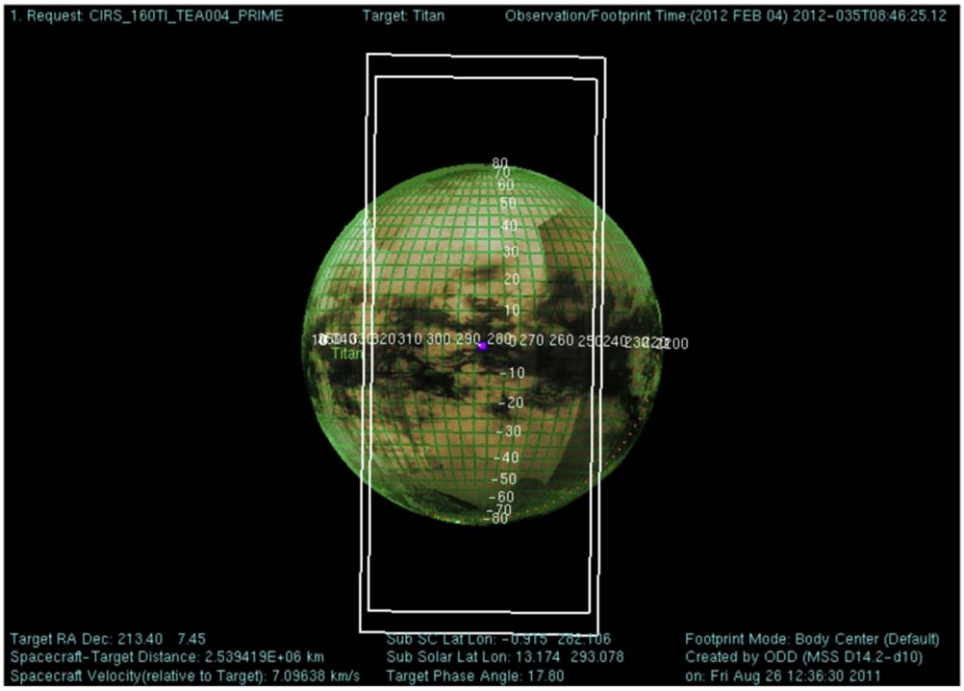

Figure 30. Example of a CIRS TEA ("Titan Exploration at Apoapse") observation (CIRS_160TI_TEA004_PRIME, 2012 February 4) showing the mid-infrared arrays centered across Titan's disk to obtain a 1D profile of trace gases. The white rectangle shows the combined FP3/4 footprint, about 7340 km in length for the larger footprint.

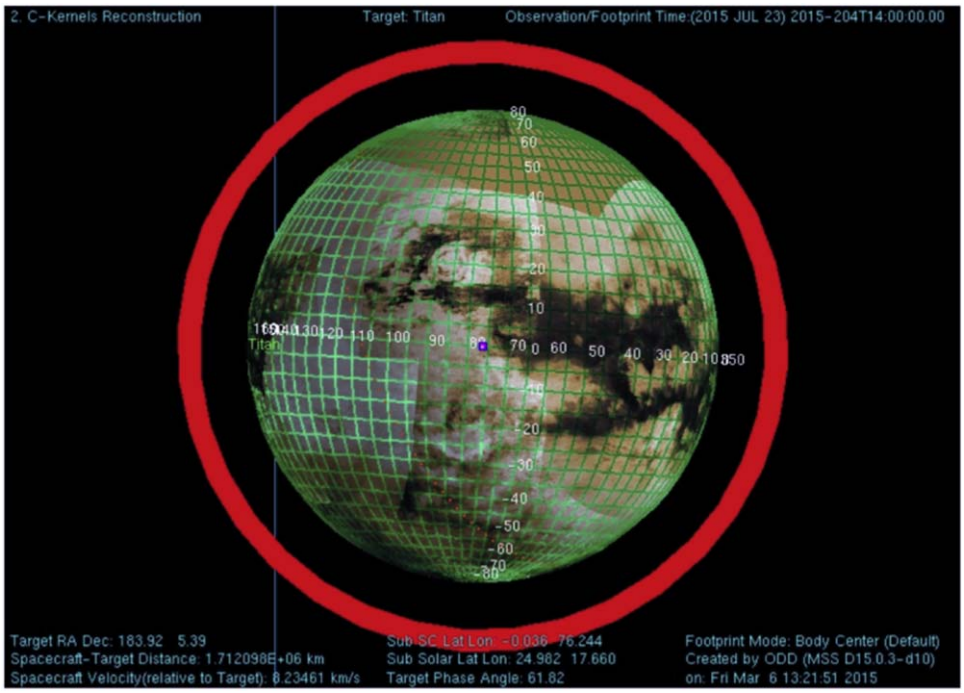

Figure 31. Distant TEA observation CIRS_219TI_TEA001_PRIME (2015 July 23) at a range of 1.7m km designed to place Titan entirely within the FP1 FOV to measure a far-infrared disk-average spectrum for comparison to *ISO* and *Herschel* data. The largest footprint depicted here is 6670 km, about 1500 km larger than Titan's solid body.

Although the CIRS Titan observing campaign was highly successful, going beyond the expectations and requirements of the mission and instrument design, there were nevertheless restrictions on the science that were imposed by the mission and instrument characteristics. For the purpose of planning successor missions, it is important therefore to consider the limitations of the current data set:

1. *Coverage: Cassini* averaged 10 flybys of Titan per Earth calendar year, or about 25 per Titan "month" (1/12 of a Titan year, or 2.5 Earth years). However, due to the different orbital inclinations, flyby distances, and divisions of time between *Cassini* instruments on each flyby, both spatial and temporal coverage remains incomplete. Coverage is more complete for the more distant

Table 3
Summary of Acquired CIRS Titan Data

Observation Type	PRIME MISSION				EQUINOX MISSION				SOLSTICE MISSION			
	#	Total Time	Num. Spectra	Data (MB)	#	Total Time	Num. Spectra	Data (MB)	#	Total Time	Num. Spectra	Data (MB)
FIRLMBT	9	05:21:00	43212	74	6	03:31:20	27648	50	18	11:39:00	81996	163
FIRLMBAER	9	05:23:00	42765	75	8	04:56:40	39735	71	30	18:12:00	134807	259
FIRLMBINT	20	17:39:00	13638	254	11	11:42:00	9581	168	30	29:27:00	24193	410
FIRLMBCON	0	00:00:00	0	0	1	01:00:00	3279	14	1	01:10:00	3763	15
FIRLMBWTR	0	00:00:00	0	0	0	00:00:00	0	0	3	02:53:00	2291	40
FIRNADMAP	25	49:52:00	342800	599	15	34:35:48	230653	368	35	94:46:00	625336	1095
EUVFUV	27	111:09:24	642448	1086	15	91:41:55	383166	809	26	158:35:01	840383	1620
MIRLMBINT	19	59:55:00	45779	834	9	33:20:00	23511	422	25	99:25:40	78609	1302
MIRLMBMAP	15	48:19:00	312133	645	6	24:08:00	179270	318	26	102:15:00	774009	1345
MIRLMPAIR	0	00:00:00	0	0	2	08:00:00	6404	115	2	07:00:00	5579	100
FIRNADCMP	68	251:35:00	186369	3524	30	111:22:33	74083	1573	74	286:25:06	222175	3916
MIDIRTMAP	41	226:33:03	494729	2227	23	110:06:03	228900	987	88	471:10:23	1324522	5447
COMPMAP	34	257:51:09	193514	3656	6	39:11:00	27836	451	28	163:07:00	111984	2237
TEMPMAP	18	72:09:00	216905	945	0	00:00:00	0	0	0	00:00:00	0	0
TEA	0	00:00:00	0	0	0	00:00:00	0	0	34	601:27:00	406303	7601

observations (e.g., MIDIRTMAP) and much more sparse for close-in observations (e.g., FIRLMBINT). Far-infrared limb observations in general fell into a high-demand observation period near closest approach and were therefore more sparsely observed, with the least complete spatial and temporal coverage.

2. *Spatial resolution:* For the far-infrared in particular, observations were frequently limited by the large footprint size of the detector. This meant that observations needed to be made very close to Titan for limb viewing, and even these had a rather large footprint on the limb, never resolving better than a scale height. Similarly, the nadir measurements such as FIRNADMAP were limited to large footprints and were consequently unable to search for phenomena such as temperature anomalies at sub 100 km scales that could be due to differing thermal inertias of lakes, craters, mountains, or any geothermal activity.
3. *S/N:* The FP1 bolometer detector was limited by a lower S/N compared to the mid-infrared detectors, which used a more sensitive technology (photoconductive and photovoltaic band-gap semiconductor for FP3 and FP4 respectively). This became a limiting factor in searching for new gas species and condensates the far-infrared.
4. *Spectral Resolution:* The CIRS highest spectral resolution of 0.5 cm^{-1} was a large improvement over *Voyager* IRIS (4.3 cm^{-1}), but nevertheless the resolution proved limiting in some cases. This was especially true when trying to detect new trace gases with emissions that may be blended with stronger overlying gas bands from molecules such as CH_4, C_2H_6, and C_2H_2. Higher spectral resolution on future instruments may help to tease apart the emission of trace gases and isotopes currently blended with other emissions.

If a future Saturn system mission includes a touring spacecraft (like *Cassini*), with multiple Titan flybys, then low-inclination flybys are clearly preferable scientifically for a CIRS-like instrument. This is because arguably the most important information provided by CIRS is the vertical atmospheric (limb) profiles of temperature and abundance, which can be mapped across all latitudes only during low-inclination flybys where the horizon circle encompasses all latitudes. On high-inclination flybys, on the other hand, the horizon circle is near-equatorial, limiting the latitudinal information that can be obtained. High-inclination flybys do provide the opportunity for surface temperature mapping of polar regions, although in practice no variation with topography or lakes has yet been measured and only a slow variation with latitude, due to Titan's long days and seasons, and high atmospheric thermal inertia. The closest flyby range implied by CIRS would be set by the FP1 detector resolving one atmospheric scale height (~50 km), which occurs at a surface-relative altitude of 8600 km, or 3000 km for half scale height resolution (25 km)—similar constraints may apply to other missions.

It is clearly desirable for one type of future mission to Titan to be an orbiter that could have long-term, high-repeat global coverage at uniform spatial resolution. Several have been proposed (e.g., Coustenis et al. 2009; Tobie et al. 2014). A Titan orbiter equipped with a thermal infrared spectrometer (as in the 2007 Titan Explorer mission concept; Lorenz & Waite 2008) and other instruments would permit frequent global "snapshot" measurements of the entire atmospheric state, including temperature, winds, and composition. These, in turn, would enable much tighter constraints to be placed on atmospheric models, such as coupled chemistry and climate 3D Titan global circulation models (GCMs) now under development (Lebonnois et al. 2009, 2012). Future observations and models will both be necessary to fully understand the complex time-dependent interactions between chemistry, dynamics, and meteorology that CIRS and the other *Cassini* instruments have unveiled (Nixon et al. 2018).

The planning, scheduling, execution, and downlink of CIRS Titan observations required the efforts of a large number of people, including the entire *Cassini* mission team at the Jet Propulsion Laboratory (JPL) and international staff at NASA's Deep Space Network (DSN), who uplinked instrument commands and downlinked the science data. Special thanks are due to the *Cassini* Titan Orbiter Science Team (TOST), comprising JPL Science Planning Engineers and representatives from all 12 *Cassini* instrument teams, for collaborative

working to schedule observations. At NASA Goddard Space Flight Center, CIRS instrument operations were supported by a local CIRS Operations Team. Funding for US coauthors was provided by NASA's *Cassini* Project. N.A.T. received support from the UK Science and Technology Facilities Council (STFC). French coauthors were supported by the Centre National d'Études Spatial (CNES).

Appendix A
CIRS Data in the PDS

The following information is correct at the time of writing; however, the PDS is an evolving internet archive and hence tools and data accessibility may have changed since publication. *Cassini* CIRS data is distributed via two sites: the Atmospheres Node and the Rings Node.

A.1. Atmospheres Node

The PDS Atmospheres node is the primary delivery point for CIRS data, which can be found here:
https://pds-atmospheres.nmsu.edu/data_and_services/atmospheres_data/Cassini/inst-cirs.html.

Data search tools include the `Event Calendar` and `Master Schedule`. Image cubes showing coverage of individual observations are contained in the `EXTRAS/CUBE_OVERVIEW` subdirectory of individual data volumes, which are labeled by year and month: e.g., "`cocirs_0401`" is the volume for "*Cassini* Orbiter, CIRS, 2004 January." Data are stored in the `DATA/TSDR` area of the volumes, while documentation, including a detailed User Guide to the CIRS data set, is included in the `DOCUMENT` area.

Note: CIRS data at the Rings node is stored in a space-minimizing binary format, with fixed-length records for most ancillary and pointing information, and variable length records for interferogram and spectra. A different format is used at the Rings Node.

A.2. Rings Node

CIRS data is also stored at the Rings Node:
https://pds-rings.seti.org/cassini/cirs/

It is important to note that the data are reformatted by the Rings Node compared to the Atmospheres Node, offering some advantages in readability at the cost of more storage space in bytes. Ancillary data records are stored in ASCII rather than binary format, while the interferograms and spectra are provided as fixed-length (as opposed to variable length) binary records. The remainder of the archive volumes—directories other than `DATA`—is the same as that at the Atmospheres Node, as delivered by the CIRS team. The data may be browsed, and is also searchable using the OPUS tool: https://tools.pds-rings.seti.org/opus/#/.

Appendix B
Ephemerides of *Cassini* Titan Flybys

The dates, times, distances, and other details of *Cassini* targeted and untargeted flybys of Titan are given in Table 4. Note that there are officially 127 targeted flybys: TA, TB, TC (replacing original T1 and T2), and T4-T126. T0 is categorized as untargeted, occurring at a range >100,000 km.

Table 4
Titan Flyby Data

Flyby	Orbit # (Rev)	Date	DOY	C/A Time	Alt (km)	Illum. Inb. or Outb.	Appr. dir. wrt. Saturn	Local Sol. Time (Dec-Hr)	Closest Appr. Lat (°)	Closest Appr. Lon (°)	Phase at C/A (°)
Saturn Orbit Insertion/Probe Release											
T0	0	07/02/04	184	09:28:53	339123	I/B	Out	4.25	−64.9	332.4	66.9
TA	A	10/26/04	300	15:30:05	1174	I/B	In	10.64	38.9	88.7	91.0
TB	B	12/13/04	348	11:38:15	1192	I/B	In	10.52	59.2	84.7	101.5
TC	C	01/14/05	14	11:11:59	60007	I/B	In	10.58	−0.1	251.8	92.9
T3	3	02/15/05	46	06:57:53	1579	I/B	In	10.39	30.1	69.0	98.5
Occultations											
T4	5	03/31/05	90	20:05:16	2404	I/B	Out	5.32	33.1	118.6	66.4
T5	6	04/16/05	106	19:11:46	1027	I/B	Out	5.31	74.3	271.9	127.1
T6	13	08/22/05	234	08:53:38	3660	I/B	Out	5.00	−59.6	102.1	43.6
T7	14	09/07/05	250	08:11:58	1075	I/B	Out	5.00	−66.5	307.8	84.7
Petal Rotations/Magnetotail Passage											
T8	17	10/28/05	301	04:15:25	1353	I/B	In	9.39	1.0	246.2	104.8
T9	19	12/26/05	360	18:59:26	10411	I/B	Out	2.97	−0.4	110.4	67.1
T10	20	01/15/06	15	11:41:26	2043	I/B	In	8.56	−0.1	250.9	120.5
T11	21	02/27/06	58	08:25:18	1812	I/B	Out	0.98	−0.2	107.3	92.4
T12	22	03/19/06	78	00:05:55	1949	I/B	In	6.51	0.2	250.6	148.0
T13	23	04/30/06	120	20:58:14	1856	I/B	Out	22.93	0.0	106.3	120.7
T14	24	05/20/06	140	12:18:11	1879	O/B	In	4.44	0.6	249.9	163.0
T15	25	07/02/06	183	09:20:47	1906	I/B	Out	20.88	−0.4	105.5	147.8
T16	26	07/22/06	203	00:25:26	950	O/B	In	2.37	85.4	318.9	105.3
T17	28	09/07/06	250	20:16:51	1000	O/B	In	2.25	22.6	56.8	44.6
T18	29	09/23/06	266	18:58:48	960	O/B	In	2.21	70.9	358.0	89.8
T19	30	10/09/06	282	17:30:07	980	O/B	In	2.16	60.8	358.1	81.0
T20	31	10/25/06	298	15:58:07	1029	O/B	In	2.11	6.2	44.2	24.7

Table 4
(Continued)

Flyby	Orbit # (Rev)	Date	DOY	C/A Time	Alt (km)	Illum. Inb. or Outb.	Appr. dir. wrt. Saturn	Local Sol. Time (Dec-Hr)	Closest Appr. Lat (°)	Closest Appr. Lon (°)	Phase at C/A (°)
T21	35	12/12/06	346	11:41:31	1000	O/B	In	1.98	43.5	264.6	125.2
Pi-Transfer											
T22	36	12/28/06	362	10:05:21	1297	O/B	In	1.92	40.6	357.9	61.9
T23	37	01/13/07	13	08:38:31	1000	O/B	In	1.88	30.7	358.1	53.3
T24	38	01/29/07	29	07:15:55	2631	O/B	In	1.84	32.9	330.2	71.9
T25	39	02/22/07	53	03:12:24	1000	O/B	Out	13.66	30.4	16.1	161.3
T26	40	03/10/07	69	01:49:00	981	O/B	Out	13.61	31.7	357.7	149.5
T27	41	03/26/07	85	00:23:27	1010	O/B	Out	13.57	40.9	357.7	144.1
T28	42	04/10/07	100	22:58:00	991	O/B	Out	13.53	50.1	357.8	137.4
T29	43	04/26/07	116	21:32:58	981	O/B	Out	13.49	59.4	357.8	129.8
T30	44	05/12/07	132	20:09:58	959	O/B	Out	13.44	68.6	358.0	121.7
T31	45	05/28/07	148	18:51:55	2299	O/B	Out	13.41	76.6	358.7	114.4
T32	46	06/13/07	164	17:46:11	965	O/B	Out	13.39	84.4	358.3	107.0
T33	47	06/29/07	180	16:59:46	1933	O/B	Out	13.39	8.4	294.9	95.6
Icy Satellites											
T34	48	07/19/07	200	01:11:20	1332	O/B	In	18.46	1.4	244.7	34.4
T35	49	08/31/07	243	06:32:36	3324	O/B	Out	11.41	63.0	111.0	86.8
High Inclination											
T36	50	10/02/07	275	04:42:43	973	O/B	Out	11.39	−59.6	108.5	67.4
T37	52	11/19/07	323	00:47:25	999	O/B	Out	11.29	−21.2	117.3	51.3
T38	53	12/05/07	339	00:06:50	1298	O/B	Out	11.29	−79.1	173.6	69.8
T39	54	12/20/07	354	22:57:55	969	O/B	Out	11.27	−70.3	175.7	61.4
T40	55	01/05/08	5	21:30:19	1014	O/B	Out	11.23	−11.5	130.3	37.6
T41	59	02/22/08	53	17:32:07	1000	O/B	Out	11.12	−34.8	151.5	30.2
T42	62	03/25/08	85	14:27:48	999	O/B	Out	11.02	−27.2	156.3	21.4
T43	67	05/12/08	133	10:01:58	1001	O/B	Out	10.89	18.1	137.3	35.8
T44	69	05/28/08	149	08:24:32	1400	O/B	Out	10.84	10.4	150.3	21.0
High Inclination											
T45	78	07/31/08	213	02:13:11	1614	I/B	Out	10.64	−43.5	195.2	49.1
T46	91	11/03/08	308	17:35:23	1105	I/B	Out	10.39	−3.4	340.0	171.4
T47	93	11/19/08	324	15:56:28	1023	I/B	Out	10.34	−21.7	177.5	28.1
T48	95	12/05/08	340	14:25:45	961	I/B	Out	10.29	−10.4	178.7	25.0
T49	97	12/21/08	356	12:59:52	971	I/B	Out	10.25	−44.2	236.7	82.6
T50	102	02/07/09	38	08:50:52	967	I/B	Out	10.14	−33.9	306.4	136.1
T51	106	03/27/09	86	04:43:36	963	I/B	Out	10.03	−30.6	234.8	84.1
Saturn Equinox Viewing											
T52	108	04/04/09	94	01:47:46	4147	O/B	In	21.87	−2.7	176.3	151.5
T53	109	04/20/09	110	00:20:45	3599	O/B	In	21.83	−7.6	177.6	148.5
…	109	04/27/09	117	04:05:52	694947	Both	Out	8.50	28.3	69.6	64.0
T54	110	05/05/09	125	22:54:15	3242	O/B	In	21.79	−13.6	177.8	145.9
T55	111	05/21/09	141	21:26:41	966	O/B	In	21.75	−21.9	177.9	141.5
T56	112	06/06/09	157	20:00:00	968	O/B	In	21.71	−31.9	178.1	135.1
T57	113	06/22/09	173	18:32:35	955	O/B	In	21.67	−42.0	178.4	127.9
T58	114	07/08/09	189	17:04:03	966	O/B	In	21.62	−52.1	178.8	120.2
T59	115	07/24/09	205	15:34:03	956	O/B	In	21.58	−62.1	179.6	112.2
T60	116	08/09/09	221	14:03:53	971	O/B	In	21.53	−72.3	180.8	104.1
T61	117	08/25/09	237	12:51:37	961	O/B	In	21.51	−19.2	237.1	85.9
Icy Satellite Flybys and Ansa-to-Ansa Occultations											
T62	119	10/12/09	285	08:36:24	1299	O/B	In	21.39	−61.8	68.9	99.4
T63	122	12/12/09	346	01:03:14	4847	O/B	Out	16.61	33.4	114.6	124.4
T64	123	12/28/09	362	00:16:58	951	O/b	Out	16.61	82.1	172.4	85.9
T65	124	01/12/10	12	23:10:36	1074	O/B	Out	16.59	−82.2	359.1	95.2
T66	125	01/28/10	28	22:28:50	7486	O/b	Out	16.60	−53.0	296.7	68.6
T67	129	04/05/10	95	15:50:54	7438	O/B	In	20.89	0.4	240.4	73.0
High Northern Titan Ground tracks											
T68	131	05/20/10	140	03:24:20	1398	O/B	Out	15.75	−48.8	116.9	112.4
T69	132	06/05/10	156	02:26:27	2042	O/B	Out	15.74	87.0	6.0	87.2
T70	133	06/21/10	172	01:27:43	878	O/B	Out	15.73	83.8	172.9	82.3

Table 4
(Continued)

Flyby	Orbit # (Rev)	Date	DOY	C/A Time	Alt (km)	Illum. Inb. or Outb.	Appr. dir. wrt. Saturn	Local Sol. Time (Dec-Hr)	Closest Appr. Lat (°)	Closest Appr. Lon (°)	Phase at C/A (°)
Inclined—1											
T71	134	07/07/10	188	00:22:45	1004	O/B	Out	15.71	−56.5	303.3	82.3
T72	138	09/24/10	267	18:38:41	8178	O/B	Out	15.60	−14.9	290.4	59.8
T73	140	11/11/10	315	13:37:01	7926	O/B	Out	15.44	−35.3	108.4	120.9
Equatorial—1											
T74	145	02/18/11	49	16:04:11	3651	O/B	In	20.40	1.0	244.5	61.6
T75	147	04/19/11	109	05:00:39	10053	O/B	Out	13.69	0.4	106.9	101.3
T76	148	05/08/11	128	22:53:44	1873	O/B	In	19.58	0.3	247.6	46.7
T77	149	06/20/11	171	18:32:00	1359	O/B	Out	11.93	0.4	106.0	73.2
T78	153	09/12/11	255	02:50:06	5821	O/B	In	17.22	−0.4	60.2	159.1
T79	158	12/13/11	347	20:11:23	3583	O/b	Out	12.59	7.4	290.9	100.1
T80	159	01/02/12	2	15:13:38	29514	O/B	In	18.34	−59.5	246.9	75.8
T81	160	01/30/12	30	13:39:48	31130	O/B	Out	12.33	−59.7	105.1	96.3
T82	161	02/19/12	50	08:43:17	3803	O/B	In	18.08	9.5	61.4	142.6
T83	166	05/22/12	143	01:10:11	954	O/B	Out	13.40	72.7	127.7	71.2
Inclined—2											
T84	167	06/07/12	159	00:07:21	959	O/B	Out	13.38	38.8	282.7	74.6
T85	169	07/24/12	206	20:03:07	1012	O/B	Out	13.27	62.0	149.3	58.3
T86	172	09/26/12	270	14:35:38	956	O/B	Out	13.13	62.6	200.6	46.6
T87	174	11/13/12	318	10:22:08	974	O/B	Out	13.01	11.7	124.6	68.2
T88	175	11/29/12	334	08:56:59	1015	O/B	Out	12.97	25.9	147.9	44.1
T89	181	02/17/13	48	01:56:35	1978	O/B	Out	12.78	21.1	154.9	34.8
T90	185	04/05/13	95	21:43:30	1400	O/B	Out	12.66	−16.5	129.7	68.7
T91	190	05/23/13	143	17:32:55	970	O/B	Out	12.54	46.1	239.9	50.3
T92	194	07/10/13	191	13:21:47	964	O/B	Out	12.43	37.0	234.7	45.6
T93	195	07/26/13	207	11:56:22	1399	O/B	Out	12.39	28.1	249.2	58.0
T94	197	09/12/13	255	07:43:56	1397	I/B	Out	12.27	17.3	206.0	21.0
T95	198	10/14/13	287	04:56:27	961	I/B	Out	12.19	8.3	205.3	24.7
T96	199	12/01/13	335	00:41:19	1400	I/B	In	12.07	−13.6	143.4	50.4
T97	200	01/01/14	1	21:59:41	1400	I/B	In	12.00	−14.1	176.7	35.1
T98	201	02/02/14	33	19:12:38	1236	I/B	In	11.92	−22.6	176.8	43.9
T99	202	03/06/14	65	16:26:47	1500	I/B	In	11.84	−31.1	176.9	52.6
T100	203	04/07/14	97	13:41:14	963	I/B	In	11.76	−36.8	187.7	59.5
T101	204	05/17/14	137	16:12:15	2992	I/B	Out	0.04	−37.3	161.7	157.7
T102	205	06/18/14	169	13:28:25	3659	I/B	Out	23.97	−36.9	178.6	165.5
T103	206	07/20/14	201	10:40:58	5103	I/B	Out	23.89	−31.8	178.9	170.8
T104	207	8/21/14	233	08:09:09	964	I/B	Out	23.82	34.5	360.0	11.9
T105	208	9/22/14	265	05:23:19	1401	I/B	Out	23.75	43.8	0.5	21.0
T106	209	10/24/14	297	02:40:30	1013	I/B	Out	23.67	37.5	322.3	31.4
T107	210	12/10/14	344	22:26:35	980	I/B	Out	23.55	53.8	57.4	56.0
T108	211	1/11/15	11	19:48:35	970	I/B	Out	23.48	69.3	1.7	45.8
T109	212	2/12/15	43	17:08:04	1200	I/B	Out	23.40	78.7	4.3	55.0
T110	213	03/16/15	75	14:29:48	2275	I/B	Out	23.33	74.8	95.0	70.5
Equatorial—2											
T111	215	05/07/15	127	22:50:23	2722	I/B	In	6.00	−0.8	67.0	33.8
T112	218	07/07/15	188	08:09:50	10953	I/B	Out	0.77	0.8	293.9	78.5
T113	222	09/28/15	271	21:37:12	1035	I/B	In	6.35	−0.8	61.4	41.9
T114	225	11/13/15	317	05:46:31	11297	I/B	Out	2.49	−14.4	122.4	91.8
Inclined—3											
T115	230	01/16/16	16	02:20:24	3548	I/B	Out	2.46	−19.0	300.2	104.0
T116	231	02/01/16	32	01:00:05	1398	I/B	Out	2.42	−82.7	174.8	121.2
T117	232	02/16/16	47	23:49:41	1018	I/B	Out	2.40	−39.1	284.0	122.4
T118	234	04/04/16	95	19:42:42	990	I/B	Out	2.28	−62.8	243.5	138.5
T119	235	05/06/16	127	16:54:37	969	I/B	Out	2.20	−59.1	178.0	139.2
T120	236	06/07/16	159	14:06:17	974	I/B	Out	2.11	−35.8	146.8	124.6
T121	238	07/25/16	207	09:58:23	975	I/B	Out	1.99	−6.4	129.2	101.2
T122	239	08/10/16	223	08:30:53	1698	I/B	Out	1.95	12.3	123.6	88.4
T123	243	09/27/16	271	04:16:59	1775	I/B	Out	1.82	22.6	124.5	86.1
T124	248	11/13/16	318	23:55:56	1585	I/B	Out	1.69	37.3	120.9	78.4

Table 4
(Continued)

Flyby	Orbit # (Rev)	Date	DOY	C/A Time	Alt (km)	Illum. Inb. or Outb.	Appr. dir. wrt. Saturn	Local Sol. Time (Dec-Hr)	Closest Appr. Lat (°)	Closest Appr. Lon (°)	Phase at C/A (°)
T125	250	11/29/16	334	22:14:32	3159	I/B	Out	1.63	42.3	127.0	80.9
F Ring/Proximal Orbits											
⋯	253	12/15/16	350	21:52:44	342353	Both	In	1.75	67.9	96.0	58.4
⋯	255	12/31/16	366	12:19:04	679042	Both	In	1.00	45.2	44.6	29.1
⋯	259	02/01/17	32	19:52:54	219437	I/B	Out	2.00	−30.8	312.0	90.3
⋯	261	02/17/17	48	13:10:25	186791	Both	Out	1.25	56.6	128.3	77.6
⋯	264	03/05/17	64	11:53:50	489882	Both	In	1.25	60.0	57.4	42.4
T126	270	04/22/17	112	06:08:07	980	I/B	Out	1.03	65.5	100.5	63.8
⋯	273	05/07/17	127	20:32:16	496014	Both	In	0.75	38.1	41.2	30.7
⋯	275	05/24/17	144	00:18:54	117956	I/B	Out	0.50	−24.1	323.1	69.0
⋯	278	06/08/17	159	18:44:46	367299	Both	In	0.75	52.6	44.0	37.9
⋯	283	07/10/17	191	13:50:51	264317	Both	In	0.25	72.2	65.8	56.3
⋯	285	07/26/17	207	23:20:01	494283	Both	Out	0.75	−14.2	319.6	66.2
⋯	288	08/11/17	223	05:04:09	194991	O/B	In	0.00	70.9	131.9	77.4
⋯	292	09/11/17	254	19:04:48	119733	O/B	Out	23.50	63.3	132.7	85.6

(This table is available in machine-readable form.)

Appendix C
Catalog of Far-infrared Limb Observations

A complete listing of dates, times, durations, and latitudes targeted for CIRS far-infrared limb observations (five types) are given in Table 5. See Section 4 for details.

Table 5
CIRS Far-infrared Limb Observations

Flyby No.	Observation Name	Date	Year Day	Start Time	Duration (HR:MN)	Pointing (Latitudes)
T4	CIRS_005TI_FIRLMBT002_PRIME	04/01/05	090	20:05:16	0:45	80N, 70N
T4	CIRS_005TI_FIRLMBAER002_PRIME	04/01/05	090	20:50:16	0:30	85N, 75N
T4	CIRS_005TI_FIRLMBINT002_PRIME	04/01/05	090	21:20:16	0:45	85N
T6	CIRS_013TI_FIRLMBINT002_PRIME	08/23/05	234	06:38:37	1:00	55S
T6	CIRS_013TI_FIRLMBAER002_PRIME	08/23/05	234	07:38:37	0:30	50S
T6	CIRS_013TI_FIRLMBT002_PRIME	08/23/05	234	08:08:37	0:35	50S, 55S
T6	CIRS_013TI_FIRLMBT003_PRIME	08/23/05	234	09:03:37	0:35	45S, 40S
T6	CIRS_013TI_FIRLMBAER003_PRIME	08/23/05	234	09:38:37	0:30	40S
T6	CIRS_013TI_FIRLMBINT003_PRIME	08/23/05	234	10:08:37	1:00	45S
T10	CIRS_020TI_FIRLMBINT003_PRIME	01/16/06	015	12:41:27	1:00	55N
T14	CIRS_024TI_FIRLMBINT002_PRIME	05/21/06	140	09:48:11	1:25	50N
T14	CIRS_024TI_FIRLMBINT003_PRIME	05/21/06	140	13:45:11	0:48	50N
T15	CIRS_025TI_FIRLMBAER003_PRIME	07/03/06	183	09:50:47	1:00	62N
T15	CIRS_025TI_FIRLMBINT003_PRIME	07/03/06	183	10:50:47	1:00	62N
T16	CIRS_026TI_FIRLMBINT003_PRIME	07/23/06	203	01:40:26	1:00	45N
T17	CIRS_028TI_FIRLMBINT002_PRIME	09/08/06	250	17:52:51	1:00	15S
T17	CIRS_028TI_FIRLMBAER002_PRIME	09/08/06	250	18:52:51	0:39	15S
T17	CIRS_028TI_FIRLMBT002_PRIME	09/08/06	250	19:31:51	0:30	15S, 25S
T18	CIRS_029TI_FIRLMBINT003_PRIME	09/24/06	266	16:58:49	1:15	30N
T24	CIRS_038TI_FIRLMBINT001_PRIME	01/30/07	029	05:15:55	0:45	28N
T24	CIRS_038TI_FIRLMBT001_PRIME	01/30/07	029	06:00:55	0:52	28N
T26	CIRS_040TI_FIRLMBINT001_PRIME	03/10/07	068	23:34:00	0:51	10N
T26	CIRS_040TI_FIRLMBT002_PRIME	03/11/07	069	02:12:00	0:30	3N, 17N
T26	CIRS_040TI_FIRLMBAER002_PRIME	03/11/07	069	02:42:00	0:30	15N
T26	CIRS_040TI_FIRLMBINT002_PRIME	03/11/07	069	03:35:00	0:37	15N
T27	CIRS_041TI_FIRLMBINT002_PRIME	03/27/07	085	01:56:27	0:42	44N
T32	CIRS_046TI_FIRLMBINT903_PRIME	06/14/07	164	18:32:11	0:16	45N
T35	CIRS_049TI_FIRLMBINT001_PRIME	09/01/07	243	04:32:34	1:00	70N

Table 5
(Continued)

Flyby No.	Observation Name	Date	Year Day	Start Time	Duration (HR:MN)	Pointing (Latitudes)
T37	CIRS_052TI_FIRLMBINT001_PRIME	11/19/07	322	22:47:25	0:21	80S
T37	CIRS_052TI_FIRLMBAER001_PRIME	11/19/07	322	23:08:25	0:54	80S, 70S
T37	CIRS_052TI_FIRLMBT001_PRIME	11/20/07	323	00:02:25	0:30	65S, 75S
T38	CIRS_053TI_FIRLMBINT001_PRIME	12/05/07	338	21:36:50	1:15	0N
T38	CIRS_053TI_FIRLMBAER001_PRIME	12/05/07	338	22:51:50	0:25	0N
T38	CIRS_053TI_FIRLMBT001_PRIME	12/05/07	338	23:16:50	0:35	5S, 5N
T40	CIRS_055TI_FIRLMBINT001_PRIME	01/06/08	005	19:30:20	0:55	30S
T42	CIRS_062TI_FIRLMBINT003_PRIME	03/26/08	085	12:28:48	0:44	55S
T42	CIRS_062TI_FIRLMBAER001_PRIME	03/26/08	085	13:12:48	0:25	55S
T42	CIRS_062TI_FIRLMBT001_PRIME	03/26/08	085	13:37:48	0:29	52S, 62S
T46	CIRS_091TI_FIRLMBINT001_PRIME	11/04/08	308	15:45:24	0:22	no data
T47	CIRS_093TI_FIRLMBINT002_PRIME	11/20/08	324	16:58:28	1:13	45S
T48	CIRS_095TI_FIRLMBINT001_PRIME	12/06/08	340	11:25:45	1:00	35S
T48	CIRS_095TI_FIRLMBINT002_PRIME	12/06/08	340	15:20:45	1:20	25S
T49	CIRS_097TI_FIRLMBINT001_PRIME	12/22/08	356	09:59:52	1:00	10N
T53	CIRS_109TI_FIRLMBAER001_PRIME	04/20/09	109	22:45:45	0:37	8N
T53	CIRS_109TI_FIRLMBT001_PRIME	04/20/09	109	23:22:55	0:48	12S
T53	CIRS_109TI_FIRLMBAER002_PRIME	04/21/09	110	00:46:45	0:49	38S
T54	CIRS_110TI_FIRLMBINT001_PRIME	05/06/09	125	20:39:16	1:00	20N
T54	CIRS_110TI_FIRLMBAER001_PRIME	05/06/09	125	21:39:16	0:30	30N
T54	CIRS_110TI_FIRLMBT001_PRIME	05/06/09	125	22:09:16	0:35	10N, 5N
T57	CIRS_113TI_FIRLMBINT001_PRIME	06/23/09	173	16:17:35	1:05	10S
T59	CIRS_115TI_FIRLMBT002_PRIME	07/25/09	205	15:49:04	0:35	50S, 55S
T59	CIRS_115TI_FIRLMBAER002_PRIME	07/25/09	205	16:24:04	0:30	60S
T59	CIRS_115TI_FIRLMBINT002_PRIME	07/25/09	205	16:54:04	0:55	60S
T62	CIRS_119TI_FIRLMBT001_PRIME	10/13/09	285	07:45:25	0:30	75S
T62	CIRS_119TI_FIRLMBAER002_PRIME	10/13/09	285	09:01:25	0:50	70S
T62	CIRS_119TI_FIRLMBINT002_PRIME	10/13/09	285	09:51:25	1:00	75S
T64	CIRS_123TI_FIRLMBINT001_PRIME	12/28/09	361	22:01:59	0:59	45N
T64	CIRS_123TI_FIRLMBAER001_PRIME	12/28/09	361	23:01:59	0:37	50N
T66	CIRS_125TI_FIRLMBINT001_PRIME	01/29/10	028	19:58:49	1:08	30N
T66	CIRS_125TI_FIRLMBAER001_PRIME	01/29/10	028	21:06:49	0:34	20N
T66	CIRS_125TI_FIRLMBT001_PRIME	01/29/10	028	21:40:19	0:34	23N, 28N
T67	CIRS_129TI_FIRLMBCON001_PRIME	04/06/10	095	13:35:39	1:00	70N
T67	CIRS_129TI_FIRLMBAER001_PRIME	04/06/10	095	14:35:39	0:30	70N
T67	CIRS_129TI_FIRLMBT001_PRIME	04/06/10	095	15:05:39	0:30	70N
T70	CIRS_133TI_FIRLMBINT001_PRIME	06/21/10	171	23:12:18	1:02	55N
T72	CIRS_138TI_FIRLMBINT001_PRIME	09/25/10	267	16:23:41	1:00	87S
T72	CIRS_138TI_FIRLMBAER001_PRIME	09/25/10	267	17:23:41	0:30	87S
T72	CIRS_138TI_FIRLMBT001_PRIME	09/25/10	267	17:53:41	0:30	82S, 87S
T73	CIRS_140TI_FIRLMBT002_PRIME	11/12/10	315	13:12:01	1:10	Safing event
T73	CIRS_140TI_FIRLMBAER002_PRIME	11/12/10	315	14:22:01	0:30	Safing event
T73	CIRS_140TI_FIRLMBINT002_PRIME	11/12/10	315	14:52:01	1:00	Safing event
T76	CIRS_148TI_FIRLMBINT001_PRIME	05/09/11	128	20:23:45	1:00	50N
T76	CIRS_148TI_FIRLMBAER001_PRIME	05/09/11	128	21:23:45	0:45	50N
T76	CIRS_148TI_FIRLMBT001_PRIME	05/09/11	128	22:08:45	0:35	55N, 60N
T78	CIRS_153TI_FIRLMBINT001_PRIME	09/13/11	255	00:35:06	1:00	73S
T78	CIRS_153TI_FIRLMBAER001_PRIME	09/13/11	255	01:35:06	0:32	73S
T79	CIRS_158TI_FIRLMBINT501_PRIME	12/14/11	347	17:56:24	1:00	57S
T79	CIRS_158TI_FIRLMBAER501_PRIME	12/14/11	347	18:56:24	0:30	57S
T79	CIRS_158TI_FIRLMBT501_PRIME	12/14/11	347	19:26:24	0:45	37S
T82	CIRS_161TI_FIRLMBINT001_PRIME	02/20/12	050	06:28:17	1:00	75N
T82	CIRS_161TI_FIRLMBAER001_PRIME	02/20/12	050	07:28:17	0:30	75N
T82	CIRS_161TI_FIRLMBT001_PRIME	02/20/12	050	07:58:17	0:45	56S
T82	CIRS_161TI_FIRLMBT002_PRIME	02/20/12	050	08:43:17	0:45	56S, 51S
T82	CIRS_161TI_FIRLMBAER002_PRIME	02/20/12	050	09:28:17	0:30	56S
T82	CIRS_161TI_FIRLMBINT002_PRIME	02/20/12	050	09:58:17	1:00	56S
T85	CIRS_169TI_FIRLMBINT001_PRIME	07/25/12	206	17:33:08	1:15	37N
T85	CIRS_169TI_FIRLMBAER001_PRIME	07/25/12	206	18:48:08	0:30	37N
T85	CIRS_169TI_FIRLMBT001_PRIME	07/25/12	206	19:19:08	0:34	37N, 32N
T86	CIRS_172TI_FIRLMBINT001_PRIME	09/27/12	270	12:20:39	1:00	50N

Table 5
(Continued)

Flyby No.	Observation Name	Date	Year Day	Start Time	Duration (HR:MN)	Pointing (Latitudes)
T86	CIRS_172TI_FIRLMBAER001_PRIME	09/27/12	270	13:20:39	0:25	50N
T86	CIRS_172TI_FIRLMBT001_PRIME	09/27/12	270	13:46:39	0:31	50N, 45N
T86	CIRS_172TI_FIRLMBAER002_PRIME	09/27/12	270	15:10:39	0:40	49N
T86	CIRS_172TI_FIRLMBINT002_PRIME	09/27/12	270	16:12:39	0:38	49N
T88	CIRS_175TI_FIRLMBINT001_PRIME	11/30/12	334	06:41:59	1:00	2S
T88	CIRS_175TI_FIRLMBAER001_PRIME	11/30/12	334	07:41:59	0:30	2S
T88	CIRS_175TI_FIRLMBT001_PRIME	11/30/12	334	08:12:59	0:29	2S
T90	CIRS_185TI_FIRLMBINT001_PRIME	04/06/13	095	19:28:31	1:00	14N
T90	CIRS_185TI_FIRLMBAER001_PRIME	04/06/13	095	20:28:31	0:30	14N
T90	CIRS_185TI_FIRLMBT001_PRIME	04/06/13	095	20:58:31	0:30	14N
T94	CIRS_197TI_FIRLMBAER002_PRIME	09/13/13	255	08:23:56	0:35	19N
T94	CIRS_197TI_FIRLMBINT002_PRIME	09/13/13	255	08:58:56	1:00	18N
T96	CIRS_199TI_FIRLMBAER002_PRIME	12/02/13	335	01:11:19	0:45	10S
T96	CIRS_199TI_FIRLMBINT002_PRIME	12/02/13	335	01:56:19	1:00	10S
T97	CIRS_200TI_FIRLMBAER002_PRIME	01/02/14	001	22:29:41	0:45	24S
T97	CIRS_200TI_FIRLMBINT002_PRIME	01/02/14	001	23:14:41	1:00	24S
T100	CIRS_203TI_FIRLMBWTR001_PRIME	04/08/14	097	11:26:14	0:53	22S
T100	CIRS_203TI_FIRLMBAER002_PRIME	04/08/14	097	13:50:14	1:06	40S
T100	CIRS_203TI_FIRLMBINT002_PRIME	04/08/14	097	15:18:14	0:38	40S
T103	CIRS_206TI_FIRLMBINT005_PRIME	07/21/14	201	08:25:58	1:00	3S
T103	CIRS_206TI_FIRLMBAER001_PRIME	07/21/14	201	09:25:58	0:30	3S
T104	CIRS_208TI_FIRLMBAER001_PRIME	09/23/14	265	05:53:19	0:45	28N
T104	CIRS_208TI_FIRLMBINT002_PRIME	09/23/14	265	06:38:19	1:00	28N
T109	CIRS_212TI_FIRLMBAER001_PRIME	02/13/15	043	17:38:04	0:45	47N
T109	CIRS_212TI_FIRLMBINT002_PRIME	02/13/15	043	18:45:04	0:38	47N
T110	CIRS_213TI_FIRLMBAER002_PRIME	03/17/15	075	14:59:49	0:45	49N
T110	CIRS_213TI_FIRLMBINT002_PRIME	03/17/15	075	15:44:49	1:00	49N
T111	CIRS_215TI_FIRLMBT002_PRIME	05/08/15	127	23:00:24	0:35	60S, 55S
T111	CIRS_215TI_FIRLMBAER003_PRIME	05/08/15	127	23:35:24	0:30	60S
T111	CIRS_215TI_FIRLMBINT002_PRIME	05/09/15	128	00:05:24	1:00	60S
T112	CIRS_218TI_FIRLMBINT001_PRIME	07/08/15	188	05:54:51	1:00	80S
T112	CIRS_218TI_FIRLMBAER001_PRIME	07/08/15	188	06:54:51	0:30	80N
T112	CIRS_218TI_FIRLMBT001_PRIME	07/08/15	188	07:24:51	0:45	80N, 70N
T112	CIRS_218TI_FIRLMBT002_PRIME	07/08/15	188	08:09:51	0:45	65S, 75S
T112	CIRS_218TI_FIRLMBAER002_PRIME	07/08/15	188	08:54:51	0:30	79S
T112	CIRS_218TI_FIRLMBINT002_PRIME	07/08/15	188	09:24:51	1:00	79S
T113	CIRS_222TI_FIRLMBINT002_PRIME	09/29/15	271	23:14:12	0:53	36S
T114	CIRS_225TI_FIRLMBAER002_PRIME	11/14/15	317	06:01:31	1:10	80S, 85S
T114	CIRS_225TI_FIRLMBINT002_PRIME	11/14/15	317	07:11:31	0:50	85S
T115	CIRS_230TI_FIRLMBINT001_PRIME	01/17/16	016	00:05:24	1:00	65S
T115	CIRS_230TI_FIRLMBAER004_PRIME	01/17/16	016	01:05:24	0:30	65S
T115	CIRS_230TI_FIRLMBT001_PRIME	01/17/16	016	01:35:24	0:45	60S, 70S
T115	CIRS_230TI_FIRLMBT002_PRIME	01/17/16	016	02:20:24	0:45	70S, 75S
T115	CIRS_230TI_FIRLMBAER005_PRIME	01/17/16	016	03:05:24	0:30	75S
T115	CIRS_230TI_FIRLMBINT002_PRIME	01/17/16	016	03:35:24	1:00	75S
T116	CIRS_231TI_FIRLMBINT001_PRIME	02/01/16	031	22:30:05	1:18	57S
T118	CIRS_234TI_FIRLMBCON002_PRIME	04/05/16	095	20:47:42	1:10	66S
T119	CIRS_235TI_FIRLMBINT001_PRIME	05/07/16	127	14:37:37	1:02	54S
T119	CIRS_235TI_FIRLMBAER001_PRIME	05/07/16	127	15:39:37	0:30	54S
T119	CIRS_235TI_FIRLMBT001_PRIME	05/07/16	127	16:09:37	0:30	54S x2
T120	CIRS_236TI_FIRLMBINT001_PRIME	06/08/16	159	11:36:17	1:15	51S
T120	CIRS_236TI_FIRLMBAER002_PRIME	06/08/16	159	12:52:17	0:44	51S
T123	CIRS_243TI_FIRLMBT002_PRIME	09/28/16	271	04:31:59	0:30	40N, 50N
T123	CIRS_243TI_FIRLMBAER002_PRIME	09/28/16	271	05:01:59	0:30	50N
T123	CIRS_243TI_FIRLMBWTR001_PRIME	09/28/16	271	05:31:59	1:00	50N
T125	CIRS_250TI_FIRLMBT002_PRIME	11/30/16	334	22:29:32	0:30	10S
T125	CIRS_250TI_FIRLMBAER002_PRIME	11/30/16	334	22:59:32	0:30	10S
T125	CIRS_250TI_FIRLMBWTR001_PRIME	11/30/16	334	23:29:32	1:00	10S

(This table is available in machine-readable form.)

Appendix D
Catalog of Mid-infrared Limb Observations

A complete listing of dates, times, durations, and latitudes targeted for CIRS mid-infrared limb observations (MAPs, INTs, and PAIRs) are given in Table 6. See Section 5 for details.

Table 6
CIRS Mid-infrared Limb Observations

Flyby No.	Observation Name	Date	Year Day	Start Time	Duration (HR:MN)	Pointing (Latitudes)
TB	CIRS_00BTI_MIRLMBINT002_PRIME	12/14/04	348	16:38:13	2:00	10S
T3	CIRS_003TI_MIRLMBINT002_PRIME	02/15/05	045	19:57:53	4:00	80N
T4	CIRS_005TI_MIRLMBMAP002_PRIME	04/02/05	091	00:35:16	3:30	85N–0N
T6	CIRS_013TI_MIRLMBMAP002_PRIME	08/23/05	234	01:23:37	2:30	25N–35S
T6	CIRS_013TI_MIRLMBMAP003_PRIME	08/23/05	234	13:53:37	2:30	40S–80S
T8	CIRS_017TI_MIRLMBMAP003_PRIME	10/29/05	301	09:55:25	3:20	85M–10N
T10	CIRS_020TI_MIRLMBINT002_PRIME	01/16/06	015	02:41:27	4:00	55N
T13	CIRS_023TI_MIRLMBMAP004_PRIME	05/01/06	120	11:58:14	2:00	0N–40S
T13	CIRS_023TI_MIRLMBMAP006_PRIME	05/01/06	120	14:58:14	2:00	0N–40N
T14	CIRS_024TI_MIRLMBINT002_PRIME	05/21/06	140	03:18:11	1:30	32S
T14	CIRS_024TI_MIRLMBINT003_PRIME	05/21/06	140	17:18:11	5:00	50N
T15	CIRS_025TI_MIRLMBINT002_PRIME	07/03/06	183	01:20:47	2:40	55S
T16	CIRS_026TI_MIRLMBINT002_PRIME	07/22/06	202	15:25:26	2:00	45N
T16	CIRS_026TI_MIRLMBMAP003_PRIME	07/23/06	203	05:25:26	2:15	30N–75N
T19	CIRS_030TI_MIRLMBINT002_PRIME	10/10/06	282	08:30:07	3:40	60N
T19	CIRS_030TI_MIRLMBINT003_PRIME	10/10/06	282	22:50:07	2:40	30N
T20	CIRS_031TI_MIRLMBMAP004_PRIME	10/26/06	298	20:28:07	3:00	15S–50N
T21	CIRS_035TI_MIRLMBINT004_PRIME	12/13/06	346	02:41:31	1:30	15N
T21	CIRS_035TI_MIRLMBINT003_PRIME	12/13/06	346	18:41:31	2:00	15N
T23	CIRS_037TI_MIRLMBINT001_PRIME	01/13/07	012	23:38:31	4:00	5N
T24	CIRS_038TI_MIRLMBINT002_PRIME	01/30/07	029	12:15:55	4:00	30N
T25	CIRS_039TI_MIRLMBMAP001_PRIME	02/22/07	052	18:12:24	3:50	25N–30S
T26	CIRS_040TI_MIRLMBMAP001_PRIME	03/10/07	068	16:49:00	4:00	30N–30S
T27	CIRS_041TI_MIRLMBINT001_PRIME	03/26/07	084	15:23:27	4:00	20S
T28	CIRS_042TI_MIRLMBINT002_PRIME	04/12/07	101	02:58:00	1:00	30S
T32	CIRS_046TI_MIRLMBMAP001_PRIME	06/14/07	164	08:46:11	4:00	15N–80S
T35	CIRS_049TI_MIRLMBINT001_PRIME	08/31/07	242	21:32:34	4:00	70N
T37	CIRS_052TI_MIRLMBMAP001_PRIME	11/19/07	322	15:47:25	4:00	60S(R)–20S(L)
T39	CIRS_054TI_MIRLMBMAP001_PRIME	12/21/07	354	13:57:55	3:54	25S–75N
T39	CIRS_054TI_MIRLMBINT002_PRIME	12/22/07	355	04:02:55	3:55	45S
T42	CIRS_062TI_MIRLMBINT001_PRIME	03/26/08	085	05:27:48	4:00	55S
T42	CIRS_062TI_MIRLMBMAP002_PRIME	03/26/08	085	19:27:48	4:00	15S–55S
T43	CIRS_067TI_MIRLMBINT002_PRIME	05/13/08	133	15:01:58	4:00	40N
T45	CIRS_078TI_MIRLMBMAP002_PRIME	08/01/08	213	06:58:11	3:30	0N–45N
T47	CIRS_093TI_MIRLMBINT002_PRIME	11/21/08	325	20:56:28	4:00	19S
T49	CIRS_098TI_MIRLMBINT001_PRIME	12/22/08	356	18:29:52	3:30	15N
T50	CIRS_102TI_MIRLMBINT001_PRIME	02/07/09	037	23:20:51	4:00	BIU anomaly
T51	CIRS_107TI_MIRLMBINT002_PRIME	03/28/09	086	09:43:36	4:00	30S
T54	CIRS_110TI_MIRLMBMAP001_PRIME	05/06/09	125	13:54:16	3:50	30N–20S
T55	CIRS_111TI_MIRLMPAIR002_PRIME	05/23/09	142	02:26:41	4:00	25S
T59	CIRS_115TI_MIRLMBMAP001_PRIME	07/25/09	205	06:34:04	4:00	0N–60N
T59	CIRS_115TI_MIRLMBINT002_PRIME	07/25/09	205	20:34:04	2:00	65N
T61	CIRS_117TI_MIRLMBINT001_PRIME	08/26/09	237	03:51:38	3:50	60S
T63	CIRS_122TI_MIRLMBMAP001_PRIME	12/12/09	345	16:03:14	4:00	85N–0N
T64	CIRS_123TI_MIRLMPAIR001_PRIME	12/28/09	361	15:16:59	4:00	75N
T64	CIRS_123TI_MIRLMBINT002_PRIME	12/29/09	362	05:16:59	4:00	75N
T65	CIRS_124TI_MIRLMBINT001_PRIME	01/13/10	012	14:10:36	4:00	75S
T65	CIRS_124TI_MIRLMBMAP002_PRIME	01/14/10	013	04:10:36	4:00	85S–0N
T67	CIRS_129TI_MIRLMBINT001_PRIME	04/06/10	095	06:50:39	4:00	88N
T69	CIRS_132TI_MIRLMBMAP001_PRIME	06/05/10	155	17:08:27	4:18	85S–0N
T70	CIRS_133TI_MIRLMBMAP001_PRIME	06/21/10	171	16:27:43	4:00	5N–85N
T71	CIRS_134TI_MIRLMBINT001_PRIME	07/07/10	187	15:22:45	3:00	80S
T72	CIRS_138TI_MIRLMPAIR001_PRIME	09/25/10	267	09:38:41	4:00	76N

Table 6
(Continued)

Flyby No.	Observation Name	Date	Year Day	Start Time	Duration (HR:MN)	Pointing (Latitudes)
T73	CIRS_140TI_MIRMBMAP001_PRIME	11/12/10	315	04:37:01	4:00	Safing event
T76	CIRS_148TI_MIRLMBMAP001_PRIME	05/09/11	128	13:53:45	4:00	0N–85N
T77	CIRS_149TI_MIRLMBMAP002_PRIME	06/21/11	171	23:32:01	4:00	0N–85S
T78	CIRS_153TI_MIRLMBINT001_PRIME	09/12/11	254	17:50:06	4:00	85S
T79	CIRS_158TI_MIRLMBINT501_PRIME	12/14/11	347	11:11:24	4:00	80N
T80	CIRS_159TI_MIRLMBMAP001_PRIME	01/03/12	002	06:13:37	4:00	75N–10S
T82	CIRS_161TI_MIRLMBINT001_PRIME	02/19/12	049	23:43:17	4:00	45S
T82	CIRS_161TI_MIRLMBMAP002_PRIME	02/20/12	050	13:43:17	4:00	0N–80S
T83	CIRS_166TI_MIRLMBINT001_PRIME	05/22/12	142	16:10:11	4:00	0N
T84	CIRS_167TI_MIRLMBINT001_PRIME	06/07/12	158	15:07:21	4:00	45N
T85	CIRS_169TI_MIRLMBMAP002_PRIME	07/26/12	207	01:03:07	4:00	15S–65N
T88	CIRS_175TI_MIRLMBMAP001_PRIME	11/29/12	333	23:56:59	4:00	50S–30N
T90	CIRS_185TI_MIRLMBINT001_PRIME	04/06/13	095	12:43:31	4:00	25N
T91	CIRS_190TI_MIRLMBMAP001_PRIME	05/24/13	143	08:32:55	3:00	35N–15S
T92	CIRS_194TI_MIRLMBINT001_PRIME	07/11/13	191	04:21:47	3:00	20S
T93	CIRS_195TI_MIRLMBMAP002_PRIME	07/27/13	207	15:56:22	5:00	15N–15S
T95	CIRS_198TI_MIRLMPAIR001_PRIME	10/14/13	286	19:56:27	3:00	16N
T95	CIRS_198TI_MIRLMBINT001_PRIME	10/15/13	287	10:56:27	3:00	2S
T96	CIRS_199TI_MIRLMBINT002_PRIME	12/02/13	335	05:41:19	4:00	12N
T98	CIRS_201TI_MIRLMBMAP002_PRIME	02/04/14	034	01:12:38	3:00	20N–25N
T101	CIRS_204TI_MIRLMBINT002_PRIME	05/18/14	137	21:12:15	4:00	35S
T102	CIRS_205TI_MIRLMBINT001_PRIME	06/19/14	169	04:28:25	4:44	10N
T102	CIRS_205TI_MIRLMBMAP002_PRIME	06/19/14	169	18:28:25	4:00	40N–13S
T103	CIRS_206TI_MIRLMBINT002_PRIME	07/21/14	201	15:40:58	4:00	30N
T105	CIRS_208TI_MIRLMBINT001_PRIME	09/22/14	264	20:23:19	3:45	See MIDIRTMAP
T105	CIRS_208TI_MIRLMBMAP002_PRIME	09/23/14	265	12:38:19	2:00	40N–15N
T106	CIRS_209TI_MIRLMBINT001_PRIME	10/24/14	296	17:40:30	4:00	45S
T108	CIRS_211TI_MIRLMBMAP001_PRIME	01/12/15	011	10:48:35	4:00	30S (R)–55S (L)
T108	CIRS_211TI_MIRLMBINT002_PRIME	01/13/15	012	00:48:35	3:00	70N
T110	CIRS_213TI_MIRLMBMAP001_PRIME	03/17/15	075	05:29:49	4:00	80S (L)–85S –30S (R)
T110	CIRS_213TI_MIRLMBINT002_PRIME	03/17/15	075	19:29:49	4:00	80S
T111	CIRS_215TI_MIRLMBMAP002_PRIME	05/09/15	128	03:50:24	4:00	80N (L)–35N (L)
T113	CIRS_222TI_MIRLMBMAP001_PRIME	09/29/15	271	12:37:12	4:00	20S–85S
T113	CIRS_222TI_MIRLMBINT002_PRIME	09/30/15	272	02:37:12	4:00	85S
T114	CIRS_225TI_MIRLMBMAP001_PRIME	11/13/15	316	20:46:31	4:00	75N–5N
T115	CIRS_230TI_MIRLMBMAP002_PRIME	01/17/16	016	07:20:24	4:00	85S–25S
T116	CIRS_231TI_MIRLMBINT001_PRIME	02/01/16	031	16:00:05	4:00	85S
T116	CIRS_231TI_MIRLMBMAP002_PRIME	02/02/16	032	06:00:05	4:00	80N–20N
T117	CIRS_232TI_MIRLMBINT001_PRIME	02/17/16	047	14:49:41	4:00	80S
T117	CIRS_232TI_MIRLMBMAP002_PRIME	02/18/16	048	04:49:41	4:00	75N–10N
T119	CIRS_235TI_MIRLMBMAP001_PRIME	05/07/16	127	07:54:37	4:00	50S–15N
T120	CIRS_236TI_MIRLMBINT001_PRIME	06/08/16	159	05:06:17	4:00	50S
T120	CIRS_236TI_MIRLMBMAP002_PRIME	06/08/16	159	19:06:17	4:00	50N–15S
T121	CIRS_238TI_MIRLMBINT002_PRIME	07/26/16	207	00:15:43	4:43	0N
T124	CIRS_248TI_MIRLMBMAP002_PRIME	11/15/16	319	04:55:56	4:00	10S–50N
T125	CIRS_250TI_MIRLMBINT002_PRIME	12/01/16	335	03:14:32	4:00	50N
N/A	CIRS_259TI_MIRLMBMAP002_PRIME	02/02/17	032	20:21:00	5:15	60S–15N
N/A	CIRS_261TI_MIRLMBMAP001_PRIME	02/18/17	048	08:41:00	4:00	15N–35S
N/A	CIRS_261TI_MIRLMBINT001_PRIME	02/18/17	048	13:41:00	3:00	10S
N/A	CIRS_275TI_MIRLMBINT001_PRIME	05/24/17	143	16:44:00	6:34	50S
N/A	CIRS_275TI_MIRLMBMAP002_PRIME	05/25/17	144	06:33:00	4:00	80S–20S

(This table is available in machine-readable form.)

Appendix E
Catalog of Far-infrared Nadir Maps

A complete listing of dates, times, durations, and map centroids for CIRS far-infrared nadir maps and CIRS riders on UVIS EUVFUV maps are given in Table 7. See Section 6.1 for details.

Table 7
CIRS Far-infrared Nadir Maps and UVIS EUVFUV

Flyby No.	Observation Name	Date	Year Day	Start Time	Duration (HR:MN)	Pointing (Center Lat., Lon.)
TB	CIRS_00BTI_FIRNADMAP001_UVIS	12/14/04	348	03:38:13	4:00	6S 159W
TB	CIRS_00BTI_FIRNADMAP002_UVIS	12/14/04	348	14:08:13	2:30	10N 347W
T3	CIRS_003TI_FIRNADMAP003_UVIS	02/16/05	046	08:30:53	3:27	2N 340W
T5	CIRS_006TI_FIRNADMAP003_UVIS	04/17/05	106	11:11:46	5:00	8N 27W
T6	CIRS_013TI_FIRNADMAP002_PRIME	08/23/05	234	03:53:37	2:45	3N 32W
T6	CIRS_013TI_FIRNADMAP003_PRIME	08/23/05	234	11:08:37	2:45	15S 208W
T9	CIRS_019TI_FIRNADMAP005_UVIS	12/27/05	360	21:29:30	6:24	0N 28W
T11	CIRS_021TI_FIRNADMAP003_UVIS	02/28/06	058	13:25:19	3:30	0N 344W
T13	CIRS_023TI_FIRNADMAP003_UVIS	05/02/06	121	02:18:14	5:10	0N 10W
T14	CIRS_024TI_FIRNADMAP002_UVIS	05/21/06	140	04:48:11	5:00	0N 158W
T14	CIRS_024TI_FIRNADMAP003_PRIME	05/21/06	140	14:33:11	2:45	0N 155W
T15	CIRS_025TI_FIRNADMAP003_UVIS	07/03/06	183	11:50:47	5:30	0N 200W
T16	CIRS_026TI_FIRNADMAP003_PRIME	07/23/06	203	02:40:26	2:45	6S 339W
T17	CIRS_028TI_FIRNADMAP002_UVIS	09/08/06	250	12:46:51	4:45	10N 149W
T18	CIRS_029TI_FIRNADMAP002_UVIS	09/24/06	266	11:28:49	4:30	14N 141W
T21	CIRS_035TI_EUVFUV001_UVIS	12/13/06	346	04:11:31	5:00	32N 129W
T22	CIRS_036TI_FIRNADMAP002_PRIME	12/29/06	362	04:35:22	3:00	41N 133W
T22	CIRS_036TI_FIRNADMAP003_PRIME	12/29/06	362	13:35:22	2:00	42S 319W
T24	CIRS_038TI_EUVFUV001_UVIS	01/29/07	028	22:15:55	6:00	59N 116W
T24	CIRS_038TI_FIRNADMAP002_PRIME	01/30/07	029	11:15:55	1:00	53S 307W
T26	CIRS_040TI_FIRNADMAP001_PRIME	03/10/07	068	20:49:00	2:45	47S 43W
T26	CIRS_040TI_FIRNADMAP002_PRIME	03/11/07	069	06:04:00	0:45	46N 228W
T26	CIRS_040TI_EUVFUV002_UVIS	03/11/07	069	06:49:00	3:00	…
T27	CIRS_041TI_EUVFUV001_UVIS	03/26/07	084	20:49:27	2:23	36S 35W
T27	CIRS_041TI_FIRNADMAP002_PRIME	03/27/07	085	02:38:27	0:45	32N 218W
T27	CIRS_041TI_EUVFUV002_UVIS	03/27/07	085	03:23:27	5:00	39N 223W
T29	CIRS_043TI_FIRNADMAP001_PRIME	04/27/07	116	16:32:58	2:50	27S 28W
T30	CIRS_044TI_EUVFUV001_UVIS	05/13/07	132	11:09:58	3:50	…
T31	CIRS_045TI_EUVFUV001_UVIS	05/29/07	148	09:51:55	6:00	11S 24W
T31	CIRS_045TI_FIRNADMAP004_PRIME	05/29/07	148	22:51:55	1:00	13N 212W
T32	CIRS_046TI_FIRNADMAP002_UVIS	06/14/07	164	12:46:11	2:00	7S 24W
T32	CIRS_046TI_FIRNADMAP901_UVIS	06/14/07	164	16:12:11	0:51	…
T32	CIRS_046TI_FIRNADMAP902_PRIME	06/14/07	164	20:04:11	2:42	4N 212W
T33	CIRS_047TI_EUVFUV001_UVIS	06/30/07	180	11:59:46	3:00	…
T33	CIRS_047TI_FIRNADMAP002_PRIME	06/30/07	180	20:59:46	1:15	0N 209W
T34	CIRS_048TI_EUVFUV001_UVIS	07/19/07	199	16:11:20	6:00	…
T34	CIRS_048TI_FIRNADMAP002_PRIME	07/20/07	200	05:11:20	1:00	0N 339W
T35	CIRS_049TI_FIRNADMAP001_PRIME	09/01/07	243	01:32:34	3:00	6S 159W
T35	CIRS_049TI_FIRNADMAP004_PRIME	09/01/07	243	10:32:34	1:00	10N 347W
T36	CIRS_050TI_EUVFUV001_UVIS	10/02/07	274	19:42:43	3:49	…
T37	CIRS_052TI_FIRNADMAP001_PRIME	11/19/07	322	19:47:25	3:00	4S 22W
T37	CIRS_052TI_FIRNADMAP002_PRIME	11/20/07	323	04:47:25	1:00	1N 205W
T38	CIRS_053TI_FIRNADMAP001_PRIME	12/05/07	338	18:36:50	3:00	8N 27W
T38	CIRS_053TI_FIRNADMAP002_PRIME	12/06/07	339	04:06:50	1:00	10N 215W
T40	CIRS_055TI_EUVFUV001_UVIS	01/06/08	005	12:30:20	4:00	21S 32W
T40	CIRS_055TI_EUVFUV501_UVIS	01/06/08	005	16:30:20	2:00	…
T40	CIRS_055TI_FIRNADMAP002_PRIME	01/07/08	006	01:30:20	1:00	5S 211W
T41	CIRS_059TI_EUVFUV002_UVIS	02/23/08	053	20:02:07	2:30	25N 227W
T42	CIRS_062TI_FIRNADMAP001_PRIME	03/26/08	085	09:27:48	3:00	0N 28W
T42	CIRS_062TI_FIRNADMAP002_PRIME	03/26/08	085	18:27:48	1:00	0N 189W
T43	CIRS_067TI_FIRNADMAP002_PRIME	05/13/08	133	12:11:58	2:50	0N 344W
T44	CIRS_069TI_EUVFUV001_UVIS	05/28/08	148	23:24:32	6:00	BIU anomaly
T46	CIRS_091TI_FIRNADMAP001_PRIME	11/04/08	308	14:06:23	2:01	BIU anomaly

Table 7
(Continued)

Flyby No.	Observation Name	Date	Year Day	Start Time	Duration (HR:MN)	Pointing (Center Lat., Lon.)
T46	CIRS_091TI_EUVFUV002_UVIS	11/04/08	308	19:27:23	7:08	
T47	CIRS_093TI_FIRNADMAP002_PRIME	11/20/08	324	18:11:28	2:45	34N 253W
T48	CIRS_095TI_EUVFUV001_UVIS	12/06/08	340	16:40:45	6:45	…
T50	CIRS_102TI_EUVFUV001_UVIS	02/08/09	038	14:50:51	3:00	BIU anomaly
T51	CIRS_107TI_FIRNADMAP002_PRIME	03/28/09	086	06:32:45	3:11	54N 266W
T52	CIRS_108TI_FIRNADMAP002_PRIME	04/05/09	094	03:37:47	1:40	58S 257W
T54	CIRS_110TI_FIRNADMAP001_PRIME	05/06/09	125	18:04:16	2:35	55N 82W*
T54	CIRS_110TI_EUVFUV001_UVIS	05/07/09	126	00:54:16	7:00	…
T55	CIRS_111TI_EUVFUV001_UVIS	05/22/09	141	12:26:41	6:30	…
T55	CIRS_111TI_FIRNADMAP002_PRIME	05/22/09	141	23:56:41	2:30	55S 270W*
T56	CIRS_112TI_EUVFUV001_UVIS	06/07/09	157	21:41:01	7:19	…
T57	CIRS_113TI_EUVFUV001_UVIS	06/23/09	173	09:32:35	6:45	…
T57	CIRS_113TI_EUVFUV002_UVIS	06/24/09	174	00:02:35	3:00	…
T58	CIRS_114TI_EUVFUV001_UVIS	07/09/09	189	08:04:03	6:40	…
T58	CIRS_114TI_FIRNADMAP002_PRIME	07/09/09	189	19:04:03	1:30	24S 294W*
T59	CIRS_115TI_FIRNADMAP002_PRIME	07/25/09	205	18:10:09	2:23	23S 326W
T60	CIRS_116TI_EUVFUV001_UVIS	08/10/09	221	05:03:53	3:50	Downlink
T62	CIRS_119TI_EUVFUV001_UVIS	10/12/09	284	23:36:25	6:51	…
T62	CIRS_119TI_EUVFUV002_UVIS	10/13/09	285	11:12:30	6:24	…
T63	CIRS_122TI_FIRNADMAP002_PRIME	12/13/09	346	03:48:14	1:00	0N 200W
T64	CIRS_123TI_FIRNADMAP001_PRIME	12/28/09	361	19:16:59	2:45	4N 121W
T65	CIRS_124TI_FIRNADMAP001_PRIME	01/13/10	012	18:10:37	2:45	Angled track
T65	CIRS_124TI_FIRNADMAP002_PRIME	01/14/10	013	01:10:37	3:00	Angled track
T66	CIRS_125TI_EUVFUV001_UVIS	01/29/10	028	13:28:49	6:30	…
T66	CIRS_125TI_EUVFUV002_UVIS	01/30/10	029	00:28:49	7:00	…
T67	CIRS_129TI_FIRNADMAP001_PRIME	04/06/10	095	10:50:39	2:45	25S 130W*
T67	CIRS_129TI_FIRNADMAP002_PRIME	04/06/10	095	19:50:39	1:00	10N 310W*
T69	CIRS_132TI_EUVFUV001_UVIS	06/06/10	156	04:26:27	7:00	…
T70	CIRS_133TI_FIRNADMAP001_PRIME	06/21/10	171	20:27:43	2:45	0N 9W
T72	CIRS_138TI_FIRNADMAP001_PRIME	09/25/10	267	13:38:41	2:45	5S 50W*
T72	CIRS_138TI_EUVFUV002_UVIS	09/25/10	267	20:53:41	6:45	…
T73	CIRS_140TI_FIRNADMAP001_PRIME	11/12/10	315	08:37:01	2:45	Safing event
T75	CIRS_147TI_EUVFUV001_UVIS	04/20/11	109	07:30:39	6:30	…
T76	CIRS_148TI_FIRNADMAP001_PRIME	05/09/11	128	17:53:45	2:45	0N 20W*
T76	CIRS_148TI_EUVFUV001_UVIS	05/10/11	129	01:53:45	6:00	…
T77	CIRS_149TI_EUVFUV001_UVIS	06/21/11	171	06:37:00	9:25	…
T77	CIRS_149TI_FIRNADMAP002_PRIME	06/21/11	171	21:02:01	2:30	0N 217W
T78	CIRS_153TI_FIRNADMAP001_PRIME	09/12/11	254	21:50:06	2:45	0N 118W*
T79	CIRS_158TI_FIRNADMAP501_PRIME	12/14/11	347	15:11:24	2:45	0N 15W
T80	CIRS_159TI_FIRNADMAP001_PRIME	01/03/12	002	10:13:38	2:45	25S 138W
T81	CIRS_160TI_EUVFUV001_UVIS	01/31/12	030	04:39:47	6:45	…
T81	CIRS_160TI_EUVFUV002_UVIS	01/31/12	030	16:39:47	6:00	…
T82	CIRS_161TI_FIRNADMAP001_PRIME	02/20/12	050	03:43:17	2:45	0N 148W
T82	CIRS_161TI_FIRNADMAP002_PRIME	02/20/12	050	10:58:17	2:45	0N 330W*
T83	CIRS_166TI_FIRNADMAP001_PRIME	05/22/12	142	20:10:11	2:33	0N 20W
T84	CIRS_167TI_FIRNADMAP001_PRIME	06/07/12	158	19:07:21	2:45	22N 18W
T84	CIRS_167TI_EUVFUV002_UVIS	06/08/12	159	02:22:21	6:45	…
T85	CIRS_169TI_FIRNADMAP002_PRIME	07/25/12	206	22:18:08	2:45	18S 202W
T86	CIRS_172TI_EUVFUV001_UVIS	09/27/12	270	05:35:38	6:45	…
T86	CIRS_172TI_EUVFUV002_UVIS	09/27/12	270	16:50:38	6:45	…
T88	CIRS_175TI_FIRNADMAP001_PRIME	11/30/12	334	03:56:59	2:45	35N 30W
T90	CIRS_185TI_FIRNADMAP001_PRIME	04/06/13	095	16:43:31	2:45	42N 48W
T93	CIRS_195TI_EUVFUV001_UVIS	07/27/13	207	02:56:19	6:45	…
T94	CIRS_197TI_EUVFUV001_UVIS	09/13/13	255	09:58:56	6:45	…
T96	CIRS_199TI_FIRNADMAP002_PRIME	12/02/13	335	02:56:19	2:45	90S 0W*
T97	CIRS_200TI_EUVFUV001_UVIS	01/02/14	001	12:59:41	6:45	…
T97	CIRS_200TI_EUVFUV002_UVIS	01/03/14	002	00:14:41	6:45	…
T100	CIRS_203TI_EUVFUV001_UVIS	04/08/14	097	15:56:14	6:45	…
T101	CIRS_204TI_EUVFUV001_UVIS	05/18/14	137	02:12:15	5:15	…
T101	CIRS_204TI_FIRNADMAP002_PRIME	05/18/14	137	18:57:15	2:15	78N 240W, 72N 313W

Table 7
(Continued)

Flyby No.	Observation Name	Date	Year Day	Start Time	Duration (HR:MN)	Pointing (Center Lat., Lon.)
T102	CIRS_205TI_FIRNADMAP002_PRIME	06/19/14	169	16:31:25	1:57	65N 195W*
T103	CIRS_206TI_FIRNADMAP002_PRIME	07/21/14	201	13:40:58	2:00	78N 240W
T105	CIRS_208TI_EUVFUV001_UVIS	09/23/14	265	02:23:19	0:45	…
T105	CIRS_208TI_EUVFUV002_UVIS	09/23/14	265	11:08:19	1:30	…
T105	CIRS_208TI_FIRNADMAP002_PRIME	09/23/14	265	07:38:19	3:30	57N 200W*
T109	CIRS_212TI_EUVFUV001_UVIS	02/13/15	043	08:08:04	6:45	…
T109	CIRS_212TI_EUVFUV002_UVIS	02/13/15	043	19:23:04	6:45	…
T110	CIRS_213TI_FIRNADMAP002_PRIME	03/17/15	075	16:44:49	2:45	6S 200W
T111	CIRS_215TI_FIRNADMAP002_PRIME	05/09/15	128	01:05:24	2:45	10S 340W
T112	CIRS_218TI_FIRNADMAP002_PRIME	07/08/15	188	10:24:51	2:45	6N 220W
T113	CIRS_222TI_FIRNADMAP001_PRIME	09/29/15	271	16:37:12	3:00	0N 150W
T113	CIRS_222TI_FIRNADMAP002_PRIME	09/30/15	272	00:07:12	2:30	0N 335W
T114	CIRS_225TI_EUVFUV002_UVIS	11/14/15	317	08:01:31	6:45	…
T115	CIRS_230TI_EUVFUV001_UVIS	01/16/16	015	17:20:24	6:45	…
T115	CIRS_230TI_FIRNADMAP002_PRIME	01/17/16	016	04:35:24	2:45	0N 218W
T116	CIRS_231TI_EUVFUV001_UVIS	02/02/16	032	04:20:05	1:40	…
T116	CIRS_231TI_FIRNADMAP001_PRIME	02/01/16	031	20:00:05	2:30	5S 24W
T117	CIRS_232TI_FIRNADMAP002_PRIME	02/18/16	048	02:28:41	2:21	13N 207W
T118	CIRS_234TI_EUVFUV001_UVIS	04/05/16	095	10:42:42	6:45	…
T118	CIRS_234TI_EUVFUV002_UVIS	04/05/16	095	21:57:42	6:45	…
T119	CIRS_235TI_FIRNADMAP001_PRIME	05/07/16	127	11:54:37	2:42	25S 30W*
T120	CIRS_236TI_FIRNADMAP001_PRIME	06/08/16	159	09:06:17	2:30	36S 20W
T120	CIRS_236TI_FIRNADMAP002_PRIME	06/08/16	159	16:21:17	2:45	38N 207W
T121	CIRS_238TI_FIRNADMAP001_PRIME	07/26/16	207	04:58:23	2:45	41S 26W
T123	CIRS_243TI_EUVFUV001_UVIS	09/27/16	270	19:16:59	6:45	…
T123	CIRS_243TI_EUVFUV002_UVIS	09/28/16	271	06:31:59	6:45	…
T124	CIRS_248TI_FIRNADMAP002_PRIME	11/15/16	319	02:27:56	2:28	33N 244W
T125	CIRS_250TI_FIRNADMAP002_PRIME	12/01/16	335	00:29:32	2:45	31N 246W
N/A	CIRS_275TI_FIRNADMAP002_PRIME	05/25/17	144	01:18:00	4:15	20S 305W*
N/A	CIRS_292TI_FIRNADMAP001_PRIME	09/12/17	254	23:46:00	3:00	N Pole mosaic

(This table is available in machine-readable form.)

Appendix F
Catalog of Far-infrared Nadir Integrations

A complete listing of dates, times, durations, and pointing positions for CIRS far-infrared nadir integrations are given in Table 8. See Section 6.3 for details.

Table 8
CIRS Far-infrared Nadir Integrations

Flyby No.	Observation Name	Date	DOY	Start Time	Duration (HR:MN)	Pointing (Center Lat., Lon.)
T0	CIRS_000TI_FIRNADCMP017_PRIME	07/04/04	185	01:00:00	2:15	visible center
T0	CIRS_000TI_FIRNADCMP001_PRIME	07/04/04	185	04:00:00	6:00	visible center
TA	CIRS_00ATI_FIRNADCMP001_PRIME	10/27/04	300	00:00:09	4:00	30S 200W
TB	CIRS_00BTI_FIRNADCMP001_PRIME	12/13/04	347	23:38:13	4:00	10N 120W
T3	CIRS_003TI_FIRNADCMP002_PRIME	02/16/05	046	14:57:53	4:00	18S 35W
T4	CIRS_005TI_FIRNADCMP002_PRIME	04/01/05	090	07:35:16	4:00	40S 15W
T4	CIRS_005TI_FIRNADCMP003_PRIME	04/02/05	091	04:05:16	4:00	47N 210W
T5	CIRS_006TI_FIRNADCMP002_PRIME	04/17/05	106	07:16:46	3:25	55N 15W
T6	CIRS_013TI_FIRNADCMP003_PRIME	08/22/05	233	22:05:37	3:18	30N 330W
T6	CIRS_013TI_FIRNADCMP004_PRIME	08/23/05	234	16:23:37	4:30	60S 220W
T8	CIRS_017TI_FIRNADCMP003_PRIME	10/29/05	301	13:15:25	3:00	20N 35W
T9	CIRS_019TI_FIRNADCMP002_PRIME	12/27/05	360	07:49:30	2:10	0N 62W
T10	CIRS_020TI_FIRNADCMP002_PRIME	01/15/06	014	23:41:27	2:00	20N 190W
T11	CIRS_021TI_FIRNADCMP002_PRIME	02/28/06	058	16:55:19	4:40	30S 170W
T12	CIRS_022TI_FIRNADCMP003_PRIME	03/19/06	077	10:05:57	7:00	0N 190W

Table 8
(Continued)

Flyby No.	Observation Name	Date	DOY	Start Time	Duration (HR:MN)	Pointing (Center Lat., Lon.)
T12	CIRS_022TI_FIRNADCMP008_PRIME	03/20/06	078	12:25:57	1:41	25N 315W
T13	CIRS_023TI_FIRNADCMP003_PRIME	05/01/06	120	05:34:14	6:24	25S 320W
T13	CIRS_023TI_FIRNADCMP002_PRIME	05/02/06	121	07:28:14	4:07	35S 210W
T14	CIRS_024TI_FIRNADCMP003_PRIME	05/20/06	139	20:48:11	6:30	15S 125W
T15	CIRS_025TI_FIRNADCMP003_PRIME	07/02/06	182	19:50:47	3:30	15N 230W
T15	CIRS_025TI_FIRNADCMP002_PRIME	07/03/06	183	18:20:47	5:30	40N 20W
T17	CIRS_028TI_FIRNADCMP003_PRIME	09/08/06	250	06:16:51	6:00	30N 145W
T18	CIRS_029TI_FIRNADCMP003_PRIME	09/24/06	266	04:58:49	5:30	10N 95W
T19	CIRS_030TI_FIRNADCMP003_PRIME	10/10/06	282	03:30:07	5:00	60S 300W
T19	CIRS_030TI_FIRNADCMP002_PRIME	10/11/06	283	03:30:07	5:51	35N 115W
T21	CIRS_035TI_FIRNADCMP003_PRIME	12/12/06	345	21:11:31	5:30	65N 130W
T21	CIRS_035TI_FIRNADCMP023_PRIME	12/13/06	346	22:09:31	3:00	80S 300W
T22	CIRS_036TI_FIRNADCMP003_PRIME	12/28/06	361	20:05:22	5:30	80N 160W
T22	CIRS_036TI_FIRNADCMP002_PRIME	12/29/06	362	18:35:22	2:30	90S 320W
T23	CIRS_037TI_FIRNADCMP001_PRIME	01/13/07	012	19:38:31	3:00	75N 210W
T23	CIRS_037TI_FIRNADCMP002_PRIME	01/14/07	013	17:38:31	2:00	70S 210W
T24	CIRS_038TI_FIRNADCMP001_PRIME	01/29/07	028	16:15:55	5:00	85N 290W
T24	CIRS_038TI_FIRNADCMP002_PRIME	01/30/07	029	16:15:55	5:00	40S 280W
T25	CIRS_039TI_FIRNADCMP001_PRIME	02/22/07	052	14:12:24	3:00	30S 90W
T25	CIRS_039TI_FIRNADCMP002_PRIME	02/23/07	053	12:12:24	2:00	70N 350W
T26	CIRS_040TI_FIRNADCMP001_PRIME	03/10/07	068	12:49:00	3:00	50S 80W
T26	CIRS_040TI_FIRNADCMP002_PRIME	03/11/07	069	10:49:00	2:00	90N 60W
T27	CIRS_041TI_FIRNADCMP001_PRIME	03/26/07	084	11:23:27	3:00	70S 20W
T27	CIRS_041TI_FIRNADCMP002_PRIME	03/27/07	085	09:23:27	2:00	60N 150W
T28	CIRS_042TI_FIRNADCMP001_PRIME	04/11/07	100	07:58:00	2:00	60S 30W
T28	CIRS_042TI_FIRNADCMP002_PRIME	04/12/07	101	07:58:00	5:00	70N 180W
T29	CIRS_043TI_FIRNADCMP001_PRIME	04/27/07	116	06:46:58	4:46	50S 30W
T29	CIRS_043TI_FIRNADCMP002_PRIME	04/28/07	117	06:32:58	2:00	75N 220W
T30	CIRS_044TI_FIRNADCMP002_PRIME	05/14/07	133	05:09:58	2:00	0N 260W
T31	CIRS_045TI_FIRNADCMP001_PRIME	05/29/07	148	04:42:55	4:09	20S 330W
T31	CIRS_045TI_FIRNADCMP002_PRIME	05/30/07	149	03:51:55	6:14	50N 230W
T32	CIRS_046TI_FIRNADCMP001_PRIME	06/14/07	164	03:39:11	1:07	20N 50W
T32	CIRS_046TI_FIRNADCMP002_PRIME	06/15/07	165	02:46:11	2:00	20S 257W
T33	CIRS_047TI_FIRNADCMP001_PRIME	06/30/07	180	02:44:46	4:15	10N 330W
T33	CIRS_047TI_FIRNADCMP002_PRIME	07/01/07	181	02:14:46	4:45	20N 170W
T34	CIRS_048TI_FIRNADCMP001_PRIME	07/19/07	199	10:11:20	2:00	35S 125W
T34	CIRS_048TI_FIRNADCMP002_PRIME	07/20/07	200	10:11:20	4:49	50N 345W
T35	CIRS_049TI_FIRNADCMP001_PRIME	08/31/07	242	18:17:34	2:15	10S 40W
T35	CIRS_049TI_FIRNADCMP002_PRIME	09/01/07	243	15:32:34	6:00	37S 240W
T36	CIRS_050TI_FIRNADCMP001_PRIME	10/02/07	274	13:30:43	5:12	10S 320W
T36	CIRS_050TI_FIRNADCMP002_PRIME	10/03/07	275	13:42:43	2:00	30N 255W
T37	CIRS_052TI_FIRNADCMP002_PRIME	11/20/07	323	09:47:25	5:00	40N 185W
T38	CIRS_053TI_FIRNADCMP001_PRIME	12/05/07	338	09:59:50	4:07	40S 340W
T38	CIRS_053TI_FIRNADCMP002_PRIME	12/06/07	339	09:06:50	2:00	60N 215W
T39	CIRS_054TI_FIRNADCMP002_PRIME	12/22/07	355	07:57:55	2:00	60N 270W
T40	CIRS_055TI_FIRNADCMP001_PRIME	01/06/08	005	08:07:20	3:23	20N 355W
T40	CIRS_055TI_FIRNADCMP002_PRIME	01/07/08	006	06:30:20	5:00	45N 280W
T41	CIRS_059TI_FIRNADCMP001_PRIME	02/23/08	053	04:29:07	3:03	25S 65W
T41	CIRS_059TI_FIRNADCMP002_PRIME	02/24/08	054	02:32:07	2:00	15N 285W
T42	CIRS_062TI_FIRNADCMP002_PRIME	03/26/08	085	23:27:48	2:00	60N 310W
T43	CIRS_067TI_FIRNADCMP001_PRIME	05/12/08	132	23:07:58	0:54	60S 60W
T43	CIRS_067TI_FIRNADCMP002_PRIME	05/13/08	133	19:01:58	5:00	30N 300W
T44	CIRS_069TI_FIRNADCMP001_PRIME	05/28/08	148	17:24:32	2:00	45S 50W
T44	CIRS_069TI_FIRNADCMP002_PRIME	05/29/08	149	17:24:32	2:00	10N 300W
T46	CIRS_091TI_FIRNADCMP001_PRIME	11/04/08	308	02:35:24	6:00	BIU anomay
T46	CIRS_091TI_FIRNADCMP002_PRIME	11/05/08	309	03:35:24	4:38	
T47	CIRS_093TI_FIRNADCMP002_PRIME	11/21/08	325	01:56:28	3:00	45N 255W
T48	CIRS_095TI_FIRNADCMP001_PRIME	12/06/08	340	01:25:45	4:00	15S 70W
T49	CIRS_097TI_FIRNADCMP001_PRIME	12/21/08	355	23:59:52	4:00	10S 110W
T50	CIRS_102TI_FIRNADCMP001_PRIME	02/07/09	037	19:50:51	3:30	BIU anomaly
T51	CIRS_106TI_FIRNADCMP001_PRIME	03/27/09	085	16:43:36	3:00	60S 150W

Table 8
(Continued)

Flyby No.	Observation Name	Date	DOY	Start Time	Duration (HR:MN)	Pointing (Center Lat., Lon.)
T51	CIRS_107TI_FIRNADCMP002_PRIME	03/28/09	086	14:43:36	3:00	35N 215W
T52	CIRS_108TI_FIRNADCMP002_PRIME	04/05/09	094	10:47:47	3:00	70S 75W
T53	CIRS_109TI_FIRNADCMP001_PRIME	04/20/09	109	09:13:42	5:07	Downlink
T54	CIRS_110I_FIRNADCMP001_PRIME	05/07/09	126	07:54:16	5:00	70S 190W
T55	CIRS_111TI_FIRNADCMP002_PRIME	05/23/09	142	06:26:41	3:00	25S 5W
T56	CIRS_112TI_FIRNADCMP001_PRIME	06/07/09	157	06:07:49	3:52	50N 60W
T56	CIRS_112TI_FIRNADCMP002_PRIME	06/08/09	158	05:00:01	5:00	60S 255W
T57	CIRS_113TI_FIRNADCMP001_PRIME	06/23/09	173	05:05:48	3:27	15N 75W
T58	CIRS_114TI_FIRNADCMP001_PRIME	07/10/09	190	02:04:03	3:00	70S 340W
T59	CIRS_115TI_FIRNADCMP001_PRIME	07/25/09	205	02:34:04	3:00	50N 100W
T60	CIRS_116TI_FIRNADCMP001_PRIME	08/10/09	221	02:01:49	2:02	Downlink
T62	CIRS_119TI_FIRNADCMP001_PRIME	10/12/09	284	19:36:25	3:00	25S 105W
T62	CIRS_119TI_FIRNADCMP002_PRIME	10/13/09	285	17:36:25	3:00	0N 20W
T63	CIRS_122TI_FIRNADCMP001_PRIME	12/12/09	345	11:05:56	3:57	40N 0W
T64	CIRS_123TI_FIRNADCMP002_PRIME	12/29/09	362	09:16:59	3:00	45S 190W
T65	CIRS_124TI_FIRNADCMP002_PRIME	01/14/10	013	08:10:37	5:00	0N 170W
T66	CIRS_125TI_FIRNADCMP001_PRIME	01/29/10	028	08:07:18	4:22	40N 40W
T66	CIRS_125TI_FIRNADCMP002_PRIME	01/30/10	029	07:28:49	5:00	45S 225W
T67	CIRS_129TI_FIRNADCMP001_PRIME	04/06/10	095	03:44:18	2:06	45S 110W
T68	CIRS_131TI_FIRNADCMP001_PRIME	05/20/10	139	14:24:20	3:00	30S 30W
T68	CIRS_131TI_FIRNADCMP002_PRIME	05/21/10	140	12:24:20	4:00	20S 230W
T69	CIRS_132TI_FIRNADCMP002_PRIME	06/06/10	156	11:26:27	3:00	50N 195W
T70	CIRS_133TI_FIRNADCMP001_PRIME	06/21/10	171	12:06:01	3:21	50S 0W
T71	CIRS_134TI_FIRNADCMP001_PRIME	07/07/10	187	11:07:45	4:15	10S 60W
T72	CIRS_138TI_FIRNADCMP001_PRIME	09/25/10	267	06:12:41	3:26	30S 40W
T73	CIRS_140TI_FIRNADCMP001_PRIME	11/12/10	315	00:37:01	4:00	Safing event
T76	CIRS_148TI_FIRNADCMP001_PRIME	05/09/11	128	09:42:00	4:12	10S 115W
T78	CIRS_153TI_FIRNADCMP001_PRIME	09/12/11	254	13:50:06	4:00	10N 110W
T79	CIRS_158TI_FIRNADCMP501_PRIME	12/14/11	347	04:20:00	6:52	30S 330W
T80	CIRS_159TI_FIRNADCMP001_PRIME	01/03/12	002	01:16:59	4:57	40S 150W
T81	CIRS_160TI_FIRNADCMP001_PRIME	01/30/12	029	23:36:01	5:04	40S 330W
T81	CIRS_160TI_FIRNADCMP002_PRIME	01/31/12	030	22:39:48	5:36	0N 240W
T82	CIRS_161TI_FIRNADCMP001_PRIME	02/19/12	049	20:43:17	2:00	10N 150W
T82	CIRS_161TI_FIRNADCMP002_PRIME	02/20/12	050	17:43:17	2:06	15S 290W
T83	CIRS_166TI_FIRNADCMP001_PRIME	05/23/12	143	10:10:11	5:36	15S 170W
T84	CIRS_167TI_FIRNADCMP002_PRIME	06/08/12	159	09:07:21	5:00	45S 255W
T85	CIRS_169TI_FIRNADCMP001_PRIME	07/25/12	206	07:03:07	4:00	10S 345W
T86	CIRS_172TI_FIRNADCMP001_PRIME	09/27/12	270	01:10:59	4:25	45N 315W
T86	CIRS_172TI_FIRNADCMP002_PRIME	09/27/12	270	23:35:38	5:00	70S 240W
T87	CIRS_174TI_FIRNADCMP002_PRIME	11/14/12	318	19:22:08	5:00	72S 185W
T88	CIRS_175TI_FIRNADCMP001_PRIME	11/29/12	333	21:26:59	2:30	15N 60W
T88	CIRS_175TI_FIRNADCMP002_PRIME	11/30/12	334	17:56:59	5:00	60S 165W
T90	CIRS_185TI_FIRNADCMP001_PRIME	04/06/13	095	08:43:31	4:00	15N 70W
T90	CIRS_185TI_FIRNADCMP002_PRIME	04/07/13	096	06:43:31	5:00	89S 245W
T91	CIRS_190TI_FIRNADCMP001_PRIME	05/24/13	143	04:32:55	4:00	0N 50W
T91	CIRS_190TI_FIRNADCMP002_PRIME	05/25/13	144	02:32:55	5:00	45S 300W
T92	CIRS_194TI_FIRNADCMP001_PRIME	07/11/13	191	01:21:47	3:00	30N 90W
T93	CIRS_195TI_FIRNADCMP001_PRIME	07/26/13	206	23:56:22	3:00	20N 15W
T94	CIRS_197TI_FIRNADCMP001_PRIME	09/12/13	254	17:43:56	5:00	60N 110W
T95	CIRS_198TI_FIRNADCMP001_PRIME	10/14/13	286	16:56:27	3:00	89N 30W
T95	CIRS_198TI_FIRNADCMP002_PRIME	10/15/13	287	13:56:27	4:53	70S 100W
T96	CIRS_199TI_FIRNADCMP001_PRIME	12/01/13	334	10:41:19	5:00	90N (FPB)
T97	CIRS_200TI_FIRNADCMP001_PRIME	01/02/14	001	09:59:41	3:00	50N 165W
T97	CIRS_200TI_FIRNADCMP002_PRIME	01/03/14	002	07:21:41	4:00	60S 45W
T98	CIRS_201TI_FIRNADCMP001_PRIME	02/03/14	033	05:12:39	5:00	20N 135W
T98	CIRS_201TI_FIRNADCMP002_PRIME	02/04/14	034	04:12:39	4:00	40S 20W
T100	CIRS_203TI_FIRNADCMP001_PRIME	04/08/14	097	01:41:14	3:00	75N 90W
T100	CIRS_203TI_FIRNADCMP002_PRIME	04/08/14	097	22:41:14	4:00	0N 0W
T101	CIRS_204TI_FIRNADCMP002_PRIME	05/19/14	138	01:12:15	4:00	0N 210W
T102	CIRS_205TI_FIRNADCMP001_PRIME	06/19/14	169	01:28:25	3:00	45S 300W

Table 8
(Continued)

Flyby No.	Observation Name	Date	DOY	Start Time	Duration (HR:MN)	Pointing (Center Lat., Lon.)
T102	CIRS_205TI_FIRNADCMP002_PRIME	06/19/14	169	22:28:25	3:00	30N 180W
T103	CIRS_206TI_FIRNADCMP001_PRIME	07/20/14	200	22:40:58	3:00	50S 320W
T103	CIRS_206TI_FIRNADCMP002_PRIME	07/21/14	201	19:40:58	3:00	30N 240W
T104	CIRS_207TI_FIRNADCMP001_PRIME	08/21/14	232	20:09:09	3:00	70S 110W
T104	CIRS_207TI_FIRNADCMP002_PRIME	08/22/14	233	17:09:09	3:00	80N 150W
T105	CIRS_208TI_FIRNADCMP001_PRIME	09/22/14	264	15:23:19	5:00	80S 300W
T105	CIRS_208TI_FIRNADCMP002_PRIME	09/23/14	265	14:38:19	2:45	60N 270W
T106	CIRS_209TI_FIRNADCMP001_PRIME	10/24/14	296	14:40:30	3:00	35S 320W
T106	CIRS_209TI_FIRNADCMP002_PRIME	10/25/14	297	11:40:30	4:00	50N 255W
T107	CIRS_210TI_FIRNADCMP001_PRIME	12/11/14	344	08:26:35	5:00	70S 0W
T107	CIRS_210TI_FIRNADCMP002_PRIME	12/12/14	345	07:26:35	4:00	20S 195W
T108	CIRS_211TI_FIRNADCMP001_PRIME	01/12/15	011	07:15:35	3:33	20N 20W
T108	CIRS_211TI_FIRNADCMP002_PRIME	01/13/15	012	04:48:35	4:00	40N 160W
T109	CIRS_212TI_FIRNADCMP002_PRIME	02/14/15	044	02:08:04	4:00	40S 200W
T110	CIRS_213TI_FIRNADCMP001_PRIME	03/17/15	075	02:29:49	3:00	30S 345W
T110	CIRS_213TI_FIRNADCMP002_PRIME	03/17/15	075	23:29:49	4:00	25N 205W
T111	CIRS_215TI_FIRNADCMP001_PRIME	05/08/15	127	09:50:24	4:00	50S 140W
T111	CIRS_215TI_FIRNADCMP002_PRIME	05/09/15	128	07:50:24	4:00	30S 310W
T112	CIRS_218TI_FIRNADCMP001_PRIME	07/07/15	187	19:09:51	4:00	20S 40W
T112	CIRS_218TI_FIRNADCMP002_PRIME	07/08/15	188	17:09:51	4:00	40S 250W
T113	CIRS_222TI_FIRNADCMP001_PRIME	09/29/15	271	09:27:12	2:10	30N 110W
T113	CIRS_222TI_FIRNADCMP002_PRIME	09/30/15	272	06:37:12	4:00	0N 310W
T115	CIRS_230TI_FIRNADCMP001_PRIME	01/16/16	015	12:55:31	4:24	15S 345W
T116	CIRS_231TI_FIRNADCMP001_PRIME	02/01/16	031	11:56:59	4:03	15N 345W
T116	CIRS_231TI_FIRNADCMP002_PRIME	02/02/16	032	10:00:05	4:05	0N 260W
T117	CIRS_232TI_FIRNADCMP001_PRIME	02/17/16	047	10:56:37	3:53	50S 20W
T117	CIRS_232TI_FIRNADCMP002_PRIME	02/18/16	048	08:49:41	2:00	20S 240W
T118	CIRS_234TI_FIRNADCMP001_PRIME	04/05/16	095	05:42:42	5:00	20N 0W
T119	CIRS_235TI_FIRNADCMP001_PRIME	05/07/16	127	04:54:37	3:00	60S 320W
T119	CIRS_235TI_FIRNADCMP002_PRIME	05/08/16	128	01:54:37	4:00	15N 255W
T120	CIRS_236TI_FIRNADCMP001_PRIME	06/08/16	159	03:33:39	1:33	70S 10W
T120	CIRS_236TI_FIRNADCMP002_PRIME	06/08/16	159	23:06:17	4:00	60N 220W
T121	CIRS_238TI_FIRNADCMP002_PRIME	07/26/16	207	18:58:23	3:30	15N 260W
T124	CIRS_248TI_FIRNADCMP001_PRIME	11/14/16	318	11:55:56	3:00	89S 50W
T124	CIRS_248TI_FIRNADCMP002_PRIME	11/15/16	319	08:55:56	3:00	30N 280W
T125	CIRS_250TI_FIRNADCMP002_PRIME	12/01/16	335	07:14:32	4:00	20S 260W
T126	CIRS_270TI_FIRNADCMP001_PRIME	04/22/17	111	18:08:07	3:00	75S 55W

(This table is available in machine-readable form.)

Appendix G
Catalog of Mid-infrared Nadir Maps

A complete listing of dates, times, and durations for CIRS mid-infrared nadir maps ARE given in Table 9. See Section 7.1 for details.

Table 9
CIRS Mid-infrared Nadir Maps

Flyby #	Observation Name	Date	DOY	Start Time	Duration (HR:MN)
T0	CIRS_000TI_TEMPMAP101_PRIME	07/03/04	184	03:30:21	1:22
T0	CIRS_000TI_TEMPMAP102_PRIME	07/03/04	184	05:16:21	1:24
T0	CIRS_000TI_TEMPMAP103_PRIME	07/03/04	184	07:04:21	1:26
T0	CIRS_000TI_TEMPMAP104_PRIME	07/03/04	184	10:30:21	4:00
T0	CIRS_000TI_TEMPMAP105_PRIME	07/03/04	184	15:15:21	1:45
TA	CIRS_00ATI_MIDIRTMAP001_PRIME	10/26/04	299	17:30:09	5:15

Table 9
(Continued)

Flyby #	Observation Name	Date	DOY	Start Time	Duration (HR:MN)
TB	CIRS_00BTI_MIDIRTMAP001_PRIME	12/13/04	347	15:13:13	8:25
T3	CIRS_003TI_MIDIRTMAP002_PRIME	02/15/05	045	09:57:53	9:00
T3	CIRS_003TI_MIDIRTMAP003_PRIME	02/16/05	046	18:57:53	4:20
T4	CIRS_005TI_MIDIRTMAP003_PRIME	04/02/05	091	08:05:16	6:30
T6	CIRS_013TI_MIDIRTMAP007_PRIME	08/23/05	234	20:53:37	7:03
T7	CIRS_014TI_MIDIRTMAP006_PRIME	09/07/05	249	06:00:00	5:00
T7	CIRS_014TI_MIDIRTMAP005_PRIME	09/08/05	250	20:11:57	6:11
T8	CIRS_017TI_MIDIRTMAP008_PRIME	10/28/05	300	01:24:00	7:00
T8	CIRS_017TI_MIDIRTMAP005_PRIME	10/29/05	301	16:15:25	7:48
T9	CIRS_019TI_MIDIRTMAP009_PRIME	12/28/05	361	14:04:00	13:33
T10	CIRS_020TI_MIDIRTMAP010_PRIME	01/15/06	014	14:23:27	9:18
T14	CIRS_024TI_MIDIRTMAP001_PRIME	05/22/06	141	01:18:11	2:00
T14	CIRS_024TI_MIDIRTMAP002_PRIME	05/22/06	141	06:18:11	2:58
T15	CIRS_025TI_MIDIRTMAP002_PRIME	07/03/06	183	23:50:47	7:54
T17	CIRS_028TI_MIDIRTMAP006_PRIME	09/07/06	249	21:56:51	7:20
T18	CIRS_029TI_TEMPMAP009_PRIME	09/23/06	265	03:30:00	7:00
T18	CIRS_029TI_MIDIRTMAP004_PRIME	09/23/06	265	20:58:49	7:00
T19	CIRS_030TI_MIDIRTMAP006_PRIME	10/09/06	281	20:16:07	6:14
T20	CIRS_031TI_TEMPMAP022_PRIME	10/25/06	297	01:26:00	7:30
T21	CIRS_035TI_MIDIRTMAP006_PRIME	12/12/06	345	16:08:31	4:03
T22	CIRS_036TI_MIDIRTMAP006_PRIME	12/28/06	361	15:04:22	5:01
T23	CIRS_037TI_MIDIRTMAP001_PRIME	01/13/07	012	14:23:31	2:15
T23	CIRS_037TI_MIDIRTMAP002_PRIME	01/13/07	012	17:38:31	2:00
T23	CIRS_037TI_MIDIRTMAP003_PRIME	01/14/07	013	22:38:31	3:25
T24	CIRS_038TI_MIDIRTMAP001_PRIME	01/29/07	028	13:00:55	2:15
T24	CIRS_038TI_MIDIRTMAP002_PRIME	01/30/07	029	21:15:55	5:14
T24	CIRS_038TI_TEMPMAP011_PRIME	01/31/07	030	16:37:00	6:00
T25	CIRS_039TI_MIDIRTMAP001_PRIME	02/22/07	052	12:12:24	2:00
T25	CIRS_039TI_MIDIRTMAP002_PRIME	02/23/07	053	17:12:24	7:15
T26	CIRS_040TI_MIDIRTMAP001_PRIME	03/10/07	068	11:08:00	1:41
T27	CIRS_041TI_MIDIRTMAP001_PRIME	03/26/07	084	09:07:27	2:16
T28	CIRS_042TI_MIDIRTMAP002_PRIME	04/12/07	101	12:58:00	7:14
T29	CIRS_043TI_TEMPMAP029_PRIME	04/29/07	118	00:15:00	3:00
T30	CIRS_044TI_MIDIRTMAP001_PRIME	05/13/07	132	05:45:58	1:24
T30	CIRS_044TI_MIDIRTMAP002_PRIME	05/14/07	133	10:09:58	1:19
T30	CIRS_044TI_TEMPMAP030_PRIME	05/14/07	133	21:43:00	3:30
T32	CIRS_046TI_MIDIRTMAP002_PRIME	06/15/07	165	07:46:11	2:15
T34	CIRS_048TI_TEMPMAP013_PRIME	07/18/07	198	07:40:00	3:00
T34	CIRS_048TI_MIDIRTMAP001_PRIME	07/19/07	199	01:48:20	7:23
T35	CIRS_049TI_MIDIRTMAP002_PRIME	09/01/07	243	21:32:34	6:00
T36	CIRS_050TI_MIDIRTMAP002_PRIME	10/03/07	275	18:42:43	8:46
T36	CIRS_050TI_TEMPMAP031_PRIME	10/04/07	276	17:30:00	6:22
N/A	CIRS_051TI_TEMPMAP014_PRIME	10/22/07	294	20:53:00	6:10
T37	CIRS_052TI_TEMPMAP016_PRIME	11/18/07	321	20:40:00	4:00
T37	CIRS_052TI_MIDIRTMAP002_PRIME	11/20/07	323	14:47:25	7:00
T38	CIRS_053TI_MIDIRTMAP002_PRIME	12/06/07	339	14:06:50	9:37
T40	CIRS_055TI_TEMPMAP034_PRIME	01/05/08	004	16:48:00	6:23
T40	CIRS_055TI_MIDIRTMAP002_PRIME	01/07/08	006	11:30:20	7:00
T41	CIRS_059TI_MIDIRTMAP002_PRIME	02/24/08	054	12:32:07	2:53
T41	CIRS_059TI_TEMPMAP037_PRIME	02/24/08	054	17:55:07	3:25
T41	CIRS_059TI_TEMPMAP038_PRIME	02/24/08	054	23:35:07	1:52
T43	CIRS_067TI_MIDIRTMAP002_PRIME	05/14/08	134	02:46:58	6:30
T44	CIRS_069TI_MIDIRTMAP001_PRIME	05/28/08	148	10:24:32	6:00
N/A	CIRS_072TI_TEMPMAP018_PRIME	06/14/08	165	05:40:00	4:00
T45	CIRS_078TI_MIDIRTMAP001_PRIME	07/31/08	212	08:05:21	4:07
T46	CIRS_091TI_MIDIRTMAP001_PRIME	11/03/08	307	20:17:34	BIU anomaly
T46	CIRS_091TI_MIDIRTMAP002_PRIME	11/05/08	309	07:35:24	omitted
T47	CIRS_093TI_MIDIRTMAP002_PRIME	11/21/08	325	05:56:28	2:00

Table 9
(Continued)

Flyby #	Observation Name	Date	DOY	Start Time	Duration (HR:MN)
T48	CIRS_096TI_MIDIRTMAP001_PRIME	12/07/08	341	04:25:45	3:06
T49	CIRS_097TI_MIDIRTMAP001_PRIME	12/21/08	355	17:24:32	6:35
T49	CIRS_098TI_MIDIRTMAP002_PRIME	12/23/08	357	02:29:52	3:30
T50	CIRS_102TI_MIDIRTMAP002_PRIME	02/08/09	038	18:50:51	BIU anomaly
T50	CIRS_102TI_MIDIRTMAP003_PRIME	02/08/09	038	22:20:51	
T51	CIRS_106TI_MIDIRTMAP001_PRIME	03/27/09	085	11:00:31	3:43
T51	CIRS_107TI_MIDIRTMAP002_PRIME	03/28/09	086	18:13:36	5:12
T52	CIRS_107TI_MIDIRTMAP001_PRIME	04/04/09	093	10:29:34	1:48
T52	CIRS_108TI_MIDIRTMAP002_PRIME	04/05/09	094	15:47:47	7:37
T53	CIRS_109TI_MIDIRTMAP002_PRIME	04/21/09	110	14:20:45	Downlink
T54	CIRS_110TI_MIDIRTMAP001_PRIME	05/06/09	125	08:11:47	4:42
T55	CIRS_111TI_MIDIRTMAP001_PRIME	05/22/09	141	07:09:49	1:17
T55	CIRS_111TI_MIDIRTMAP002_PRIME	05/23/09	142	11:26:41	8:00
T57	CIRS_113TI_MIDIRTMAP002_PRIME	06/24/09	174	08:32:35	8:00
T59	CIRS_115TI_MIDIRTMAP001_PRIME	07/24/09	204	23:34:04	3:00
T62	CIRS_119TI_MIDIRTMAP001_PRIME	10/12/09	284	14:45:21	4:21
T63	CIRS_122TI_MIDIRTMAP002_PRIME	12/13/09	346	15:03:14	5:00
T64	CIRS_123TI_MIDIRTMAP001_PRIME	12/28/09	361	10:07:24	4:10
T65	CIRS_124TI_MIDIRTMAP002_PRIME	01/14/10	013	13:10:37	5:21
T68	CIRS_131TI_MIDIRTMAP001_PRIME	05/20/10	139	08:10:04	5:44
T68	CIRS_131TI_MIDIRTMAP002_PRIME	05/21/10	140	16:24:20	4:40
T73	CIRS_140TI_MIDIRTMAP001_PRIME	11/11/10	314	21:14:00	Safing event
T74	CIRS_145TI_MIDIRTMAP001_PRIME	02/18/11	048	21:26:11	6:38
T74	CIRS_145TI_MIDIRTMAP002_PRIME	02/20/11	050	04:04:11	6:31
T76	CIRS_148TI_MIDIRTMAP002_PRIME	05/10/11	129	12:53:45	8:13
T77	CIRS_149TI_MIDIRTMAP002_PRIME	06/22/11	172	08:32:01	9:45
T78	CIRS_153TI_MIDIRTMAP001_PRIME	09/12/11	254	07:42:00	6:08
T79	CIRS_158TI_MIDIRTMAP002_PRIME	12/15/11	348	10:11:24	2:29
T82	CIRS_161TI_MIDIRTMAP001_PRIME	02/19/12	049	15:54:00	4:49
T84	CIRS_167TI_MIDIRTMAP001_PRIME	06/07/12	158	08:24:00	2:43
T84	CIRS_167TI_MIDIRTMAP002_PRIME	06/08/12	159	14:07:21	7:12
T85	CIRS_169TI_MIDIRTMAP001_PRIME	07/24/12	205	21:32:59	9:30
T86	CIRS_172TI_MIDIRTMAP002_PRIME	09/28/12	271	04:35:39	14:45
T87	CIRS_174TI_MIDIRTMAP001_PRIME	11/13/12	317	14:55:59	6:26
T87	CIRS_174TI_MIDIRTMAP002_PRIME	11/15/12	319	00:22:08	5:14
T88	CIRS_175TI_MIDIRTMAP002_PRIME	11/30/12	334	22:56:59	11:43
T89	CIRS_181TI_MIDIRTMAP001_PRIME	02/17/13	047	09:20:59	2:30
T89	CIRS_181TI_MIDIRTMAP002_PRIME	02/18/13	048	13:56:36	8:19
T90	CIRS_185TI_MIDIRTMAP001_PRIME	04/06/13	095	05:56:00	2:48
T90	CIRS_185TI_MIDIRTMAP002_PRIME	04/07/13	096	11:43:31	5:52
T91	CIRS_190TI_MIDIRTMAP001_PRIME	05/24/13	143	02:41:00	1:52
T91	CIRS_190TI_MIDIRTMAP002_PRIME	05/25/13	144	07:32:55	8:03
T93	CIRS_195TI_MIDIRTMAP001_PRIME	07/26/13	206	13:33:59	8:22
T94	CIRS_197TI_MIDIRTMAP001_PRIME	09/12/13	254	08:57:59	8:46
T95	CIRS_198TI_MIDIRTMAP001_PRIME	10/14/13	286	07:09:59	7:46
T96	CIRS_199TI_MIDIRTMAP001_PRIME	12/01/13	334	04:40:00	6:01
T97	CIRS_200TI_MIDIRTMAP001_PRIME	01/02/14	001	02:42:59	5:17
T97	CIRS_200TI_MIDIRTMAP002_PRIME	01/03/14	002	10:59:41	3:23
T98	CIRS_201TI_MIDIRTMAP001_PRIME	02/03/14	033	00:46:59	4:26
T98	CIRS_201TI_MIDIRTMAP002_PRIME	02/04/14	034	08:12:39	5:59
T99	CIRS_202TI_MIDIRTMAP002_PRIME	03/08/14	066	04:26:47	7:19
T100	CIRS_203TI_MIDIRTMAP001_PRIME	04/07/14	096	20:39:59	3:01
T100	CIRS_203TI_MIDIRTMAP002_PRIME	04/09/14	098	02:41:14	8:24
T101	CIRS_204TI_MIDIRTMAP001_PRIME	05/17/14	136	17:55:59	3:46
T101	CIRS_204TI_MIDIRTMAP002_PRIME	05/19/14	138	05:12:15	2:54
T102	CIRS_205TI_MIDIRTMAP001_PRIME	06/18/14	168	15:39:00	7:49
T102	CIRS_205TI_MIDIRTMAP002_PRIME	06/20/14	170	01:28:25	3:06
T103	CIRS_206TI_MIDIRTMAP001_PRIME	07/20/14	200	13:20:59	7:20

Table 9
(Continued)

Flyby #	Observation Name	Date	DOY	Start Time	Duration (HR:MN)
T104	CIRS_207TI_MIDIRTMAP001_PRIME	08/21/14	232	11:15:59	6:53
T104	CIRS_207TI_MIDIRTMAP002_PRIME	08/22/14	233	22:09:09	2:17
T105	CIRS_208TI_MIDIRTMAP001_PRIME	09/22/14	264	09:11:59	6:11
T105	CIRS_208TI_MIDIRTMAP002_PRIME	09/23/14	265	17:23:19	2:44
T106	CIRS_209TI_MIDIRTMAP001_PRIME	10/24/14	296	07:10:00	5:31
T106	CIRS_209TI_MIDIRTMAP002_PRIME	10/25/14	297	15:40:30	3:10
T107	CIRS_210TI_MIDIRTMAP001_PRIME	12/11/14	344	04:25:00	4:02
T107	CIRS_210TI_MIDIRTMAP002_PRIME	12/12/14	345	11:26:35	4:38
T108	CIRS_211TI_MIDIRTMAP001_PRIME	01/13/15	012	08:48:35	6:03
T109	CIRS_212TI_MIDIRTMAP002_PRIME	02/14/15	044	06:08:04	8:17
T110	CIRS_213TI_MIDIRTMAP001_PRIME	03/16/15	074	22:50:00	3:39
T110	CIRS_213TI_MIDIRTMAP002_PRIME	03/18/15	076	03:29:49	8:31
T111	CIRS_215TI_MIDIRTMAP001_PRIME	05/08/15	127	05:09:59	4:41
T111	CIRS_215TI_MIDIRTMAP002_PRIME	05/09/15	128	11:50:24	5:29
T112	CIRS_218TI_MIDIRTMAP001_PRIME	07/07/15	187	12:27:00	6:42
T112	CIRS_218TI_MIDIRTMAP002_PRIME	07/08/15	188	21:09:51	3:54
T113	CIRS_222TI_MIDIRTMAP002_PRIME	09/30/15	272	10:37:12	5:45
T114	CIRS_225TI_MIDIRTMAP001_PRIME	11/13/15	316	06:53:59	8:53
T117	CIRS_232TI_MIDIRTMAP002_PRIME	02/18/16	048	10:49:41	4:00
T118	CIRS_234TI_MIDIRTMAP001_PRIME	04/04/16	094	19:59:00	9:44
T119	CIRS_235TI_MIDIRTMAP001_PRIME	05/06/16	126	20:09:00	6:46
T119	CIRS_235TI_MIDIRTMAP002_PRIME	05/08/16	128	05:54:37	3:24
T120	CIRS_236TI_MIDIRTMAP002_PRIME	06/09/16	160	03:06:17	3:52
T121	CIRS_238TI_MIDIRTMAP002_PRIME	07/26/16	207	22:28:23	5:04
T123	CIRS_243TI_MIDIRTMAP001_PRIME	09/27/16	270	10:07:58	4:09
T124	CIRS_248TI_MIDIRTMAP001_PRIME	11/14/16	318	07:24:00	2:32
T124	CIRS_248TI_MIDIRTMAP002_PRIME	11/15/16	319	13:55:56	4:53
T125	CIRS_250TI_MIDIRTMAP002_PRIME	12/01/16	335	11:14:32	6:33
N/A	CIRS_253TI_MIDIRTMAP001_PRIME	12/16/16	350	10:16:00	6:05
N/A	CIRS_253TI_MIDIRTMAP002_PRIME	12/16/16	350	22:21:00	4:00
N/A	CIRS_253TI_MIDIRTMAP003_PRIME	12/17/16	351	05:51:00	1:30
N/A	CIRS_253TI_MIDIRTMAP004_PRIME	12/17/16	351	08:21:00	2:12
N/A	CIRS_259TI_MIDIRTMAP001_PRIME	02/02/17	032	09:19:00	3:47
N/A	CIRS_259TI_MIDIRTMAP002_PRIME	02/03/17	033	02:36:00	7:00
N/A	CIRS_261TI_MIDIRTMAP001_PRIME	02/18/17	048	02:31:00	5:10
N/A	CIRS_270TI_MIDIRTMAP001_PRIME	04/22/17	111	13:24:58	2:43
N/A	CIRS_270TI_MIDIRTMAP002_PRIME	04/23/17	112	19:08:07	9:53
N/A	CIRS_273TI_MIDIRTMAP001_PRIME	05/08/17	127	19:02:00	3:00
N/A	CIRS_275TI_MIDIRTMAP002_PRIME	05/25/17	144	11:33:00	4:00
N/A	CIRS_278TI_MIDIRTMAP001_PRIME	06/09/17	159	12:26:00	3:00
N/A	CIRS_278TI_MIDIRTMAP002_PRIME	06/09/17	159	16:26:00	3:00
N/A	CIRS_278TI_MIDIRTMAP003_PRIME	06/09/17	159	20:26:00	2:00
N/A	CIRS_278TI_MIDIRTMAP004_PRIME	06/09/17	159	23:26:00	3:00
N/A	CIRS_278TI_MIDIRTMAP005_PRIME	06/10/17	160	03:26:00	3:00
N/A	CIRS_278TI_MIDIRTMAP006_PRIME	06/10/17	160	07:26:00	2:54
N/A	CIRS_283TI_MIDIRTMAP001_PRIME	07/11/17	191	09:06:00	4:15
N/A	CIRS_283TI_MIDIRTMAP002_PRIME	07/11/17	191	14:21:00	4:45
N/A	CIRS_283TI_MIDIRTMAP003_PRIME	07/11/17	191	20:36:00	3:00
N/A	CIRS_287TI_MIDIRTMAP001_PRIME	08/11/17	222	16:51:00	6:40
N/A	CIRS_292TI_MIDIRTMAP001_PRIME	09/12/17	254	06:22:00	2:54
N/A	CIRS_292TI_MIDIRTMAP002_PRIME	09/13/17	255	07:46:00	5:00
N/A	CIRS_293TI_MIDIRTMAP003_PRIME	09/13/17	255	13:46:00	4:30

(This table is available in machine-readable form.)

Appendix H
Catalog of Distant Titan Observations

A complete listing of dates, times, and durations for distant observations of Titan by CIRS are given in Table 10. See Section 7.3 for details.

Table 10
CIRS Distant Titan Observations

Observation Name	Date	DOY	Time	Duration (HR:MN)
CIRS_009TI_COMPMAP002_PRIME	06/07/05	157	09:30:00	06:30:00
CIRS_010TI_COMPMAP003_PRIME	06/23/05	173	03:00:00	11:00:00
CIRS_015TI_COMPMAP005_PRIME	09/25/05	267	19:50:00	08:15:00
CIRS_016TI_COMPMAP006_PRIME	10/10/05	282	20:27:00	11:00:00
CIRS_022TI_COMPMAP002_PRIME	03/18/06	076	08:20:00	13:59:00
CIRS_030TI_COMPMAP007_PRIME	10/11/06	283	19:30:00	03:50:00
CIRS_031TI_COMPMAP008_PRIME	10/24/06	296	11:26:00	14:00:00
CIRS_033TI_COMPMAP009_PRIME	11/25/06	328	18:15:00	10:45:00
CIRS_035TI_COMPMAP010_PRIME	12/11/06	344	19:17:00	10:30:00
CIRS_036TI_COMPMAP024_PRIME	12/27/06	360	19:49:00	09:00:00
CIRS_037TI_COMPMAP026_PRIME	01/12/07	011	16:13:00	09:51:00
CIRS_037TI_COMPMAP012_PRIME	01/15/07	014	14:04:00	02:00:00
CIRS_038TI_COMPMAP013_PRIME	01/27/07	026	17:51:00	09:00:00
CIRS_040TI_COMPMAP026_PRIME	03/09/07	067	19:51:00	04:00:00
CIRS_041TI_COMPMAP028_PRIME	03/25/07	083	16:50:00	04:00:00
CIRS_041TI_COMPMAP029_PRIME	03/28/07	086	07:42:00	15:22:00
CIRS_041TI_COMPMAP030_PRIME	03/29/07	087	08:45:00	05:30:00
CIRS_043TI_COMPMAP002_PRIME	04/28/07	117	11:32:58	00:42:00
CIRS_044TI_COMPMAP015_PRIME	05/15/07	134	02:43:00	08:00:00
CIRS_048TI_COMPMAP013_PRIME	07/18/07	198	10:40:00	04:00:00
CIRS_051TI_COMPMAP016_PRIME	10/20/07	292	20:53:00	11:00:00
CIRS_051TI_COMPMAP017_PRIME	10/21/07	293	20:23:00	03:07:00
CIRS_051TI_COMPMAP018_PRIME	10/22/07	294	02:00:00	06:23:00
CIRS_052TI_COMPMAP016_PRIME	11/20/07	323	21:47:25	02:19:09
CIRS_052TI_COMPMAP015_PRIME	11/21/07	324	10:27:00	07:00:00
CIRS_055TI_COMPMAP001_PRIME	01/07/08	006	18:30:20	03:14:00
CIRS_057TI_COMPMAP018_PRIME	01/23/08	022	14:11:00	07:54:00
CIRS_059TI_COMPMAP001_PRIME	02/22/08	052	12:06:00	06:15:00
CIRS_062TI_COMPMAP019_PRIME	03/28/08	087	01:50:00	21:30:00
CIRS_066TI_COMPMAP021_PRIME	04/28/08	118	07:17:00	07:00:00
CIRS_067TI_COMPMAP001_PRIME	05/14/08	134	09:16:58	03:04:00
CIRS_069TI_COMPMAP001_PRIME	05/28/08	148	08:19:32	02:05:00
CIRS_072TI_COMPMAP021_PRIME	06/14/08	165	09:40:00	08:00:00
CIRS_083TI_COMPMAP001_PRIME	09/01/08	244	17:04:00	07:46:00
CIRS_103TI_COMPMAP001_PRIME	02/14/09	044	13:13:00	08:17:00
CIRS_122TI_COMPMAP002_PRIME	12/13/09	346	20:03:14	04:00:00
CIRS_123TI_COMPMAP001_PRIME	12/30/09	363	15:32:00	08:00:00
CIRS_124TI_COMPMAP002_PRIME	01/14/10	013	18:31:36	03:39:00
CIRS_128TI_COMPMAP001_PRIME	03/20/10	078	03:49:00	07:15:00
CIRS_131TI_COMPMAP001_PRIME	05/22/10	141	09:40:00	08:00:00
CIRS_134TI_COMPMAP001_PRIME	07/09/10	189	12:49:00	10:10:00
CIRS_139TI_COMPMAP001_PRIME	10/15/10	287	04:52:00	13:30:00
CIRS_140TI_COMPMAP001_PRIME	11/13/10	316	22:00:00	08:00:00
CIRS_140TI_COMPMAP002_PRIME	11/16/10	319	09:19:00	08:00:00
CIRS_143TI_COMPMAP001_PRIME	01/15/11	014	17:05:00	10:10:00
CIRS_149TI_TEA001_PRIME	06/23/11	173	09:00:00	07:30:00
CIRS_149TI_TEA002_PRIME	06/24/11	174	05:42:00	21:00:00
CIRS_149TI_TEA003_PRIME	06/25/11	175	11:42:00	15:00:00
CIRS_149TI_TEA004_PRIME	06/26/11	176	11:42:00	37:29:00
CIRS_154TI_COMPMAP001_PRIME	09/27/11	269	22:50:00	06:00:00
CIRS_155TI_TEA003_PRIME	10/25/11	297	05:00:00	19:00:00
CIRS_155TI_TEA004_PRIME	10/26/11	298	14:32:00	13:15:00
CIRS_155TI_TEA005_PRIME	10/27/11	299	14:17:00	13:30:00
CIRS_156TI_TEA003_PRIME	10/31/11	303	14:02:00	13:30:00

Table 10
(Continued)

Observation Name	Date	DOY	Time	Duration (HR:MN)
CIRS_156TI_TEA004_PRIME	11/01/11	304	14:02:00	13:30:00
CIRS_156TI_TEA005_PRIME	11/02/11	305	14:02:00	28:45:00
CIRS_156TI_TEA006_PRIME	11/04/11	307	03:47:00	15:00:00
CIRS_157TI_COMPMAP001_PRIME	11/28/11	331	18:00:00	15:34:00
CIRS_158TI_TEA001_PRIME	12/17/11	350	11:20:00	15:00:00
CIRS_160TI_TEA002_PRIME	02/02/12	032	15:57:00	31:30:00
CIRS_160TI_TEA003_PRIME	02/04/12	034	08:27:00	15:00:00
CIRS_160TI_TEA004_PRIME	02/05/12	035	08:27:00	20:45:00
CIRS_160TI_TEA005_PRIME	02/08/12	038	17:22:00	11:10:00
CIRS_161TI_TEA001_PRIME	02/12/12	042	17:08:00	11:10:00
CIRS_181TI_TEA001_PRIME	02/19/13	049	09:46:00	25:41:00
CIRS_181TI_TEA002_PRIME	02/20/13	050	21:57:00	23:30:00
CIRS_182TI_TEA001_PRIME	02/22/13	052	07:57:00	21:00:00
CIRS_182TI_TEA002_PRIME	02/23/13	053	15:52:00	11:10:00
CIRS_185TI_TEA001_PRIME	04/08/13	097	07:36:00	10:55:00
CIRS_186TI_TEA001_PRIME	04/09/13	098	05:01:00	14:45:00
CIRS_186TI_TEA002_PRIME	04/10/13	099	04:46:00	15:00:00
CIRS_202TI_TEA001_PRIME	03/03/14	061	21:56:00	15:00:00
CIRS_202TI_TEA002_PRIME	03/04/14	062	21:56:00	15:00:00
CIRS_202TI_TEA003_PRIME	03/05/14	063	21:56:00	13:30:00
CIRS_206TI_TEAFP1001_PRIME	07/11/14	191	00:00:00	13:00:00
CIRS_206TI_TEA002_PRIME	07/11/14	191	13:00:00	13:27:00
CIRS_206TI_TEA003_PRIME	07/12/14	192	12:57:00	37:15:00
CIRS_219TI_TEA001_PRIME	07/24/15	204	13:06:00	13:20:00
CIRS_219TI_TEA002_PRIME	07/25/15	205	12:56:00	13:30:00
CIRS_233TI_TEA001_PRIME	03/07/16	066	16:00:00	08:00:00
CIRS_241TI_TEA002_PRIME	08/28/16	240	11:23:00	35:20:00
CIRS_252TI_COMPMAP001_PRIME	12/16/16	350	06:16:00	04:00:00
CIRS_253TI_COMPMAP001_PRIME	12/16/16	350	17:21:00	04:00:00
CIRS_253TI_COMPMAP002_PRIME	12/17/16	351	03:21:00	01:30:00
CIRS_259TI_COMPMAP001_PIE	02/02/17	032	14:06:00	05:15:00
CIRS_259TI_COMPMAP002_PRIME	02/03/17	033	09:36:00	05:45:00
CIRS_268TI_COMPMAP001_PIE	04/08/17	097	02:36:00	05:47:00
CIRS_268TI_COMPMAP002_PIE	04/08/17	097	09:23:00	05:16:00
CIRS_271TI_COMPMAP001_PRIME	04/24/17	113	23:36:00	11:36:00
CIRS_278TI_COMPMAP001_PRIME	06/09/17	159	08:26:00	03:00:00
CIRS_280TI_COMPMAP001_PIE	06/26/17	176	00:28:00	04:24:00
CIRS_283TI_COMPMAP001_PRIME	07/11/17	191	04:20:00	03:46:00
CIRS_283TI_COMPMAP002_PRIME	07/12/17	192	00:36:00	03:42:00
CIRS_283TI_COMPMAP003_PRIME	07/12/17	192	08:04:00	01:51:00
CIRS_285TI_COMPMAP001_PRIME	07/27/17	207	21:51:00	01:30:00
CIRS_287TI_COMPMAP001_PIE	08/12/17	223	00:31:00	05:00:00
CIRS_288TI_COMPMAP001_PIE	08/12/17	223	06:31:00	05:00:00
CIRS_288TI_COMPMAP002_PIE	08/12/17	223	12:31:00	04:30:00
CIRS_288TI_COMPMAP003_PIE	08/12/17	223	18:01:00	06:15:00
CIRS_290TI_COMPMAP001_PIE	08/29/17	240	00:19:00	04:16:00
CIRS_292TI_COMPMAP001_PRIME	09/13/17	255	03:46:00	03:00:00
CIRS_293TI_COMPMAP002_PRIME	09/13/17	255	18:46:00	02:20:00

(This table is available in machine-readable form.)

ORCID iDs

Conor A. Nixon https://orcid.org/0000-0001-9540-9121
Nicholas A. Lombardo https://orcid.org/0000-0002-0301-4614
Gordon L. Bjoraker https://orcid.org/0000-0002-9679-4153
Richard K. Achterberg https://orcid.org/0000-0002-7643-7626
Andrew M. Annex https://orcid.org/0000-0002-0253-2313
Malena Rice https://orcid.org/0000-0002-7670-670X
Athena Coustenis https://orcid.org/0000-0003-3414-3491
Bruno Bézard https://orcid.org/0000-0002-5433-5661
Emmanuel Lellouch https://orcid.org/0000-0001-7168-1577
Nicholas A. Teanby https://orcid.org/0000-0003-3108-5775
Valeria Cottini https://orcid.org/0000-0003-0839-5855
F. Michael Flasar https://orcid.org/0000-0001-7186-5181

References

Achterberg, R. K., Conrath, B. J., Gierasch, P. J., Flasar, F. M., & Nixon, C. A. 2008a, Icar, 197, 549
Achterberg, R. K., Conrath, B. J., Gierasch, P. J., Flasar, F. M., & Nixon, C. A. 2008b, Icar, 194, 263
Achterberg, R. K., Gierasch, P. J., Conrath, B. J., Michael Flasar, F., & Nixon, C. A. 2011, Icar, 211, 686
Anderson, C. M., Samuelson, R., Achterberg, R., Barnes, J., & Flasar, F. 2014, Icar, 243, 129
Anderson, C. M., & Samuelson, R. E. 2011, Icar, 212, 762
Anderson, C. M., Samuelson, R. E., Bjoraker, G. L., & Achterberg, R. K. 2010, Icar, 207, 914
Anderson, C. M., Samuelson, R. E., & Nna-Mvondo, D. 2018, SSRv, 214, 125
Anderson, C. M., Samuelson, R. E., Yung, Y. L., & McLain, J. L. 2016, GeoRL, 43, 3088
Bampasidis, G., Coustenis, A., Achterberg, R. K., et al. 2012, ApJ, 760, 144
Bauduin, S., Irwin, P., Lellouch, E., et al. 2018, Icar, 311, 288
Bézard, B., Nixon, C. A., Kleiner, I., & Jennings, D. E. 2007, Icar, 191, 397
Bézard, B., & Vinatier, S. 2019, Icar, in press (doi:10.1016/j.icarus.2019.03.038)
Bird, M. K., Allison, M., Asmar, S. W., et al. 2005, Natur, 438, 800
Brown, R. H., Baines, K. H., Bellucci, G., et al. 2004, SSRv, 115, 111
Cottini, V., Nixon, C. A., Jennings, D. E., et al. 2012a, P&SS, 60, 62
Cottini, V., Nixon, C. A., Jennings, D. E., et al. 2012b, Icar, 220, 855
Courtin, R., Sim, C. K., Kim, S. J., & Gautier, D. 2012, P&SS, 69, 89
Coustenis, A., Achterberg, R. K., Conrath, B. J., et al. 2007, Icar, 189, 35
Coustenis, A., Atreya, S. K., Balint, T., et al. 2009, ExA, 23, 893
Coustenis, A., Bampasidis, G., Achterberg, R. K., et al. 2013, ApJ, 779, 177
Coustenis, A., Bezard, B., Gautier, D., & Marten, A. 1991, Icar, 89, 152
Coustenis, A., Jennings, D. E., Achterberg, R. K., et al. 2016, Icar, 270, 409
Coustenis, A., Jennings, D. E., Achterberg, R. K., et al. 2018, ApJL, 854, L30
Coustenis, A., Jennings, D. E., Jolly, A., et al. 2008, Icar, 197, 539
Coustenis, A., Jennings, D. E., Nixon, C. A., et al. 2010, Icar, 207, 461
Coustenis, A., Salama, A., Lellouch, E., et al. 1998, A&A, 336, L85
de Kok, R., Irwin, P., & Teanby, N. 2010, Icar, 209, 854
de Kok, R., Irwin, P. G. J., Teanby, N. A., et al. 2007a, Icar, 191, 223
de Kok, R., Irwin, P. G. J., Teanby, N. A., et al. 2007b, Icar, 186, 354
de Kok, R., Irwin, P. G. J., & Teanby, N. A. 2008, Icar, 197, 572
de Kok, R., Irwin, P. G. J., Teanby, N. A., et al. 2010, Icar, 207, 485
Esposito, L. W., Barth, C. A., Colwell, J. E., et al. 2004, SSRv, 115, 299
Flasar, F. M., Achterberg, R. K., Conrath, B. J., et al. 2005, Sci, 308, 975
Flasar, F. M., Kunde, V. G., Abbas, M. M., et al. 2004, SSRv, 115, 169
Fulchignoni, M., Ferri, F., Angrilli, F., et al. 2005, Natur, 438, 785
Hanel, R., Crosby, D., Herath, L., et al. 1980, ApOpt, 19, 1391
Israël, G., Szopa, C., Raulin, F., et al. 2005, Natur, 438, 796
Jennings, D. E., Achterberg, R. K., Cottini, V., et al. 2015, ApJL, 804, L34
Jennings, D. E., Anderson, C. M., Samuelson, R. E., et al. 2012a, ApJL, 761, L15
Jennings, D. E., Anderson, C. M., Samuelson, R. E., et al. 2012b, ApJL, 754, L3
Jennings, D. E., Cottini, V., Nixon, C. A., et al. 2011, ApJL, 737, L15
Jennings, D. E., Cottini, V., Nixon, C. A., et al. 2016, ApJL, 816, L17
Jennings, D. E., Flasar, F. M., Kunde, V. G., et al. 2009, ApJL, 691, L103
Jennings, D. E., Flasar, F. M., Kunde, V. G., et al. 2017, ApOpt, 56, 5274
Jennings, D. E., Nixon, C. A., Jolly, A., et al. 2008, ApJL, 681, L109
Jolly, A., Cottini, V., Fayt, A., et al. 2015, Icar, 248, 340
Jolly, A., Fayt, A., Benilan, Y., et al. 2010, ApJ, 714, 852
Kuiper, G. P. 1944, ApJ, 100, 378
Kunde, V. G., Ade, P. A., Barney, R. D., et al. 1996, Proc. SPIE, 2803, 162
Lebonnois, S., Burgalat, J., Rannou, P., & Charnay, B. 2012, Icar, 218, 707
Lebonnois, S., Rannou, P., & Hourdin, F. 2009, RSPTA, 367, 665
Lebreton, J.-P., Witasse, O., Sollazzo, C., et al. 2005, Natur, 438, 758
Lellouch, E., Bézard, B., Flasar, F. M., et al. 2014, Icar, 231, 323
Li, L. 2015, NatSR, 5, 8239
Li, L., Nixon, C. A., Achterberg, R. K., et al. 2011, GeoRL, 38, 23201
Lockwood, G., & Thompson, D. 2009, Icar, 200, 616
Lombardo, N. A., Nixon, C. A., Achterberg, R. K., et al. 2019a, Icar, 317, 454
Lombardo, N. A., Nixon, C. A., Sylvestre, M., et al. 2019b, AJ, 157, 160
Lorenz, R. D., & Waite, J. H., Jr. 2008, Titan Explorer Flagship Mission Study, Tech. Rep., Baltimore, MD: Johns Hopkins Univ. Appl. Phys. Lab.
Matson, D. L. 2002, SSRv, 104, 1
McMahon, S. K. 1996, P&SS, 44, 3
Moreno, R., Lellouch, E., Lara, L. M., et al. 2012, Icar, 221, 753
Niemann, H. B., Atreya, S. K., Bauer, S. J., et al. 2005, Natur, 438, 779
Nixon, C., Lorenz, R., Achterberg, R., et al. 2018, P&SS, 155, 50
Nixon, C. A., Achterberg, R. K., & Flasar, F. M. 2010a, in Proc. IEEE Aerospace Conf., ed. K. Profet, D. Woerner, & R. Mattingly (Piscataway, NJ: IEEE), 1174
Nixon, C. A., Achterberg, R. K., Teanby, N. A., et al. 2010b, FaDi, 147, 65
Nixon, C. A., Achterberg, R. K., Vinatier, S., et al. 2008a, Icar, 195, 778
Nixon, C. A., Ansty, T. M., Flasar, F. M., & Achterberg, R. K. 2012a, in Proc. IEEE Aerospace Conf., ed. K. Profet, D. Woerner, & R. Mattingly (Piscataway, NJ: IEEE), 1633
Nixon, C. A., Jennings, D. E., Bézard, B., et al. 2008b, ApJL, 681, L101
Nixon, C. A., Jennings, D. E., Bézard, B., et al. 2013a, ApJL, 776, L14
Nixon, C. A., Jennings, D. E., Flaud, J.-M., et al. 2009a, P&SS, 57, 1573
Nixon, C. A., Teanby, N. A., Calcutt, S. B., et al. 2009b, ApOpt, 48, 1912
Nixon, C. A., Teanby, N. A., Irwin, P., & Hörst, S. M. 2013b, Icar, 224, 253
Nixon, C. A., Temelso, B., Vinatier, S., et al. 2012b, ApJ, 749, 159
Porco, C. C., West, R. A., Squyres, S., et al. 2004, SSRv, 115, 363
Samuelson, R. E., Smith, M. D., Achterberg, R. K., & Pearl, J. C. 2007, Icar, 189, 63
Smith, B. A., Soderblom, L., Beebe, R., et al. 1981, Sci, 212, 163
Steadman, K., Pitesky, J., Ray, T., Burton, M., & Alonge, N. 2010, Cassini Titan Science Integration: Getting a "Jumpstart" on the Process (Reston, VA: AIAA)
Stoehr, F., Lacy, M., Leon, S., et al. 2014, Proc. SPIE, 9149, 914902
Stone, E. C., & Miner, E. D. 1981, Sci, 212, 159
Sylvestre, M., Teanby, N. A., Vinatier, S., Lebonnois, S., & Irwin, P. G. J. 2018, A&A, 609, A64
Teanby, N. A., Bézard, B., Vinatier, S., et al. 2017, NatCo, 8, 1586
Teanby, N. A., de Kok, R., Irwin, P. G. J., et al. 2008a, JGRE, 113, E12003
Teanby, N. A., de Kok, R., & Irwin, P. G. J. 2009a, Icar, 204, 645
Teanby, N. A., Irwin, P. G., de Kok, R., et al. 2006, Icar, 181, 243
Teanby, N. A., Irwin, P. G. J., de Kok, R., et al. 2007, Icar, 186, 364
Teanby, N. A., Irwin, P. G. J., de Kok, R., et al. 2008b, Icar, 193, 595
Teanby, N. A., Irwin, P. G. J., de Kok, R., et al. 2009b, Icar, 202, 620
Teanby, N. A., Irwin, P. G. J., de Kok, R., & Nixon, C. A. 2009c, RSPTA, 367, 697
Teanby, N. A., Irwin, P. G. J., de Kok, R., & Nixon, C. A. 2010a, FaDi, 147, 51
Teanby, N. A., Irwin, P. G. J., de Kok, R., & Nixon, C. A. 2010b, ApJL, 724, L84
Teanby, N. A., Irwin, P. G. J., & de Kok, R. J. 2010c, P&SS, 58, 792
Teanby, N. A., Irwin, P. G. J., Nixon, C. A., et al. 2012, Natur, 491, 732
Teanby, N. A., Sylvestre, M., Sharkey, J., et al. 2019, GeoRL, 46, 3079
Tobie, G., Teanby, N., Coustenis, A., et al. 2014, P&SS, 104, 59
Tomasko, M. G., Archinal, B., Becker, T., et al. 2005, Natur, 438, 765
Tyler, G. L., Eshleman, V. R., Anderson, J. D., et al. 1981, Sci, 212, 201
Vinatier, S., Bézard, B., de Kok, R., et al. 2010a, Icar, 210, 852
Vinatier, S., Bézard, B., Fouchet, T., et al. 2007a, Icar, 188, 120
Vinatier, S., Bézard, B., Lebonnois, S., et al. 2015, Icar, 250, 95
Vinatier, S., Bézard, B., & Nixon, C. A. 2007b, Icar, 191, 712
Vinatier, S., Bézard, B., Nixon, C. A., et al. 2010b, Icar, 205, 559
Vinatier, S., Rannou, P., Anderson, C. M., et al. 2012, Icar, 219, 5
Vinatier, S., Schmitt, B., Bézard, B., et al. 2018, Icar, 310, 89
Vuitton, V., Yelle, R. V., Klippenstein, S. J., Hörst, S. M., & Lavvas, P. 2019, Icar, 324, 120
Yelle, R. V., Cui, J., & Müller-Wodarg, I. C. F. 2008, JGRE, 113, E10003
Zarnecki, J. C., Leese, M. R., Hathi, B., et al. 2005, Natur, 438, 792